ZEBRAFISH XENOTRANSPLANTATION AS A PRECLINICAL THERAPEUTIC PLATFORM FOR T-CELL ACUTE LYMPHOBLASTIC LEUKEMIA

by

Victoria L. Bentley

Submitted in partial fulfilment of the requirements
for the degree of Master of Science

at

Dalhousie University
Halifax, Nova Scotia
August 2014

TABLE OF CONTENTS

LIST OF FIGURES

ABSTRACT

Pediatric T-cell Acute Lymphoblastic leukemia (T-ALL) is a high-risk disease. There is a need for targeted therapies for T-ALL, and techniques to rapidly screen drug candidates and personalize patient therapy. I developed a zebrafish xenotransplantation (XT) model to screen novel agents for efficacy and toxicity. I demonstrated that T-ALL cell lines recapitulate *in vitro* responses to targeted therapies *in vivo.* Importantly, patient-derived lymphoblasts engraft in zebrafish and specific drug responses can be quantitatively determined. I identified a mutation sensitive to γ-secretase inhibition in a xenograft from a child with T-cell acute lymphoblastic leukemia, confirmed by Sanger sequencing and validated as a gain-of-function *NOTCH1* mutation. Furthermore, I employed the zebrafish XT assay to determine the efficacy of two novel compounds to protect against doxorubicin-induced cardiac damage. The zebrafish XT platform provides a novel cost-effective means of screening novel agents, and tailoring leukemia therapy in real-time to maximize efficacy and minimize toxicity.

LIST OF ABBREVIATIONS USED

ABCB8	ATP-binding cassette protein-B8
ADAM10	A disintegrin and metalloproteinase 10
AKT	Protein kinase B (PKB)
ALL	Acute lymphoblastic leukemia
AML	Acute myeloid leukemia
ANK	Ankyrin-like repeats
APH1	Anterior pharynx-defective 1 homolog
APH1	Anterior pharynx-defective 1 homolog
ARF	Alternate reading frame product of the p16INK41 protein
BFM	Berlin-Frankfurt-Münster
bHLH	Basic helix-loop-helix
BM	Bone marrow
CBP/p300	CREB-binding protein
CK2	Casein kinase 2
CNS	Central nervous system
Co-R	Co-repressor
COG	Children's oncology group
CR	Complete remission
CR domain	LNR/cysteine-rich domain
CREB	cAMP response element-binding protein
CSF	Cerebral spinal fluid
CSL	CBF1, suppressor of hairless, Lag-1
CtBP1	C-terminal binding protein 1
DEPTOR	DEP domain-containing mTOR-interacting protein
DFO	Deferoxamine
Dll	Delta-like
DMEM	Dulbecco's Modified Eagle Medium
DMSO	Dimethyl sulfoxide
DPU	Diphenylurea

DR	Dietary restriction
DSL	Delta-Serrate-Lag2
Dxz	Dexrazoxane
EDTA	Ethylenediaminetetraacetic acid
EFS	Event free survival
EGF	Epidermal growth factor
ERK	Extracellular-regulated kinase
FBS	Fetal bovine serum
FBXW7	F-box/WD repeat-containing protein 7
FDA	US Food and drug administration
FOXO3A	Forkhead box transcription factor 3A
GAB	GRB2-associated binding protein
GAP	GTP-ase activating protein
GI	Gastrointestinal
GRB2	Growth factor receptor-bound protein 2
GSI	γ-secretase inhibitor
GSK3	Glycogen synthase kinase 3
HD	Heterodimerization domain
HES	Hairy enhancer of split
hpf	Hours post fertilization
hpi	Hours post injection
hpt	Hours post treatment
HSCs	Hematopoietic stem cells
IR	Insulin receptor
IRS	Insulin receptor substrate
IT	Intrathecal
IV	Intravenous
Jag	Jagged
LICs	Leukemia initiating cells
LSCs	Leukemic stem cells
MAML1	Mastermind-like protein

MAPK	Ras-mitogen-activated protein kinase
Mdm2	Murine double minute 2
Mfrn-2	Mitoderrin-2
miRNA	Micro-ribonucleic acids (RNAs)
MLL	Lysine methyltransferase mixed lineage leukemia gene
mLST8	Mammalian lethal with SEC13 protein 8
MRD	Minimal residual disease
mSIN1	Stress-activated MAP kinase-interacting protein 1 (or MAPKAP1)
MTD	Maximum tolerated dose
mTOR	Mammalian target of rapamycin
mTORC1	Mammalian target of rapamycin complex 1
mTORC2	Mammalian target of rapamycin complex 2
MuLV	Murine leukemia virus
MYB	Myeloblastosis viral oncogene homolog
MYC	Myelocytomatosis viral oncogene homolog
NcoR	Nuclear receptor co-repressor 2 (or SMRT)
NCSTN	Nicastrin
ND	Not determined
N^{EC}	N-terminal extracellular domain of NOTCH
NICD	Notch intracellular domain
NLS	Nuclear localization signal
NOD/SCID	Non-obese diabetic/severe combined immunodeficient
NRR	Negative regulatory region
NSCLCs	Non-small cell lung carcinomas
N^{TM}	C-terminal transmembrane-intracellular domain of NOTCH
OPA	Optic atrophy 1
PB	Peripheral blood
PBD	Phosphatifylinositol-4,5-bisphosphate (PtdIns(4,5)P_2)-binding domain
PBS	Phosphate Buffered Saline

PCR	Polymerase chain reaction
PDK1	3-phosphoinositide-dependent kinase 1
PEN2	Presenilin enhancer 2 homolog
PEN2	Presenilin enhancer 2 homolog
PEST	Proline (P), glutamic acid (E), serine (S) and threonine (T) rich domain
PI3K	Phosphatidylinositol 3-kinase
PICS	PTEN loss-induced cellular senescence
PIP_2	Phosphatidylinositol (4,5) bisphosphate
PIP_3	Phosphatidylinositol (3,4,5) triphosphate
PML	Promyelocytic leukemia
Precursor-B-ALL	Precursor-B-cell acute lymphoblastic leukemia
PRR5	Pro-rich protein 5 (or PROTOR)
PSEN1	Presenilin
PTEN	Phosphatase with tensin homology tumour suppressor
RAM	RBP-associated molecule
RBPJ	Recombination signal binding protein for immunoglobulin kappa J
RHEB	RAS-related small GTPase RAS homologue enriched in brain
RICTOR	Rapamycin insensitive companion of mTOR
ROS	Reactive oxygen species
SCF	SKP1-CUL1-F-box protein
SHARP	SMRT/HDAC-1-associated repressor protein
SMRT	Silencing mediator for retinoid or thyroid-hormone receptors (or NCOR)

ACKNOWLEDGMENTS

I would like to thank my co-supervisors Dr. Graham Dellaire and Dr. Jason Berman for welcoming me into their labs. Thank you for your patience and encouragement, and for enthusiastically asking all the hard questions. I would also like to extend my gratitude to the members of my committee, Dr. Paola Marcato and Dr. Conrad Fernandez for our helpful discussions. A huge thank you to Eileen Kaiser for keeping me in line, and reminding me of everything I inevitably forgot to do. Thank you to all the members of the Dellaire and Berman laboratories – you have made the past two years fun!

Most importantly, thank you to my supportive family and friends. Even though my research probably seemed nonsensical most of the time, I appreciate that you listened and nodded along as though you were interested.

CHAPTER 1: INTRODUCTION

1.1: PREAMBLE

Acute lymphoblastic leukemia (ALL) is a malignant disease characterized by the uncontrolled proliferation of lymphoblasts committed to the B-cell lineage (precursor-B-ALL) or the T-cell lineage (T-ALL). ALL is the most common pediatric malignancy, with an incidence of 3.5 per 100,000 children under the age of 19 years (Hutchcroft, Clarke, & Mao, 1995). T -ALL is an aggressive hematologic malignancy caused by the arrested development and differentiation of thymocyte progenitors. While the overall prognosis for T-ALL patients has improved with the use intensified chemotherapy protocols, T-ALL is often associated with primary non-responsive, high minimal residual disease (MRD) and a high rate of relapse (Vlierberghe & Ferrando, 2012; Vrooman & Silverman, 2009; Weng et al., 2004; J. Zhang et al., 2012). For patients with primary relapsed or resistant disease, additional intensification of standard chemotherapy agents leads to unacceptable toxicities, highlighting a desperate need for molecularly-targeted agents for T-ALL and improved animal models for preclinical testing of novel agents (Grabher, von Boehmer, & Look, 2006; Vlierberghe & Ferrando, 2012).

This study aims to establish xenotransplantation (XT) of human leukemia in zebrafish as a relevant animal model of pediatric T-ALL. This platform will be used to evaluate toxicities of existing treatment paradigms and to screen novel targeted agents (Corkery, Dellaire, & Berman, 2011; Liu et al., 2014; Smithen et al., 2013). Furthermore, since patient-derived T-ALL can be successfully engrafted in zebrafish and specific drug

responses can be quantitatively determined, the zebrafish XT platform provides a novel cost-effective means of tailoring leukemia therapy in real-time (Bentley et al., 2013).

1.2: CLINICAL PRESENTATION OF T-ALL

T-cell acute lymphoblastic leukemia (T-ALL) is an aggressive hematologic malignancy that accounts for 10-15% of pediatric and 25% of adult ALL cases. This study focuses on the clinical and molecular hallmarks of pediatric T-ALL, and the development of a preclinical therapeutic platform for pediatric T-ALL. ALL is diagnosed through a complete blood count, bone marrow (BM) aspiration and biopsy, lumbar puncture, and cytogenetic analysis of leukemic blasts. BM examined by light microscopy can reveal different degrees of leukemia involvement, and patients are scored into three classes: M1, M2, and M3. M1 is defined as BM with fewer than 5% of lymphoblasts, while M2 is 5% to 25%, and M3 is greater than 25%. Most ALL patients will present with M3 stage marrow involvement (National Cancer Institute, 2014).

ALL is characterized by the uncontrolled expansion of immature lymphoid cells, termed lymphoblasts. T-ALL results from the multistep oncogenic transformation of thymocyte progenitors, altering their cell growth, proliferation, survival and differentiation, and is characterized by the presence of lymphoblasts bearing immature T-lineage immunophenotypic markers in the BM and in the peripheral blood (PB). T-ALL patients often present with high white blood cell counts, masses in the mediastinum with pleural effusions, organomegaly and infiltration of the central nervous system (CNS). In childhood ALL the most common cause of treatment failure is relapse, which occurs in 15 to 20% of all pediatric patients (Locatelli, Schrappe, Bernardo, & Rutella, 2012). Treatment failure is a particular challenge when treating childhood T-ALL, as T-ALL

patients have rapid disease progression, and have higher rates of induction failure, induction death, relapse (in addition to shorter time to relapse), and CNS relapse than those with precursor-B-ALL (Demarest, Ratti, & Capobianco, 2008; Goldberg et al., 2003). Furthermore, T-ALL lymphoblasts are intrinsically more resistant to standard chemotherapy agents, necessitating the use of intensified treatment strategies, which increases the risk of treatment-related toxicity (Pieters et al., 1993, 1998). The epidemiology of T-ALL follows a pattern seen with other types of leukemia. T-ALL is more common in whites than other races, and males are more likely to be affected than females (Vlierberghe & Ferrando, 2012).

1.3: THE GENETIC BASIS OF T-ALL

1.3.1: OVERVIEW

While T-ALL can be subdivided into distinct molecular groups, several signalling pathways are commonly dysregulated in T-ALL. One such pathway commonly dysregulated is the Notch pathway (Vlierberghe & Ferrando, 2012). Activating mutations of *NOTCH1* have been found in approximately 60% of all T-ALL cases, and across all defined subtypes, suggesting that Notch pathway activation is a necessary step in T-ALL leukemogenesis (Demarest et al., 2008). The *NOTCH1* gene encodes the Notch receptor, which is important for both normal thymocyte development and plays a central role in the malignant transformation of thymocytes by regulating cell-cycle progression and apoptosis. The pro-tumourigenic effects of Notch signalling are considered to be central to the development of T-ALL, and Notch effects on T-cells can be produced directly through mutations in *NOTCH1* or through mutations in other pathways that recapitulate Notch effects on neoplastic cells. Indeed, inactivating mutations in the phosphatase with tensin homology tumour suppressor (PTEN) and hyperactivation of the phosphatidylinositol 3-kinase (PI3K)-AKT-mammalian target of rapamycin (mTOR) signalling axis is characteristic of T-ALL (**Figure 1.3.1**) (Demarest et al., 2008; Vlierberghe & Ferrando, 2012).

The Notch pathway will be discussed in detail, and it's central role in normal thymocyte development and in thymocyte transformation and T-ALL disease will be highlighted, followed by a discussion of Notch1 as a therapeutic target in T-ALL.

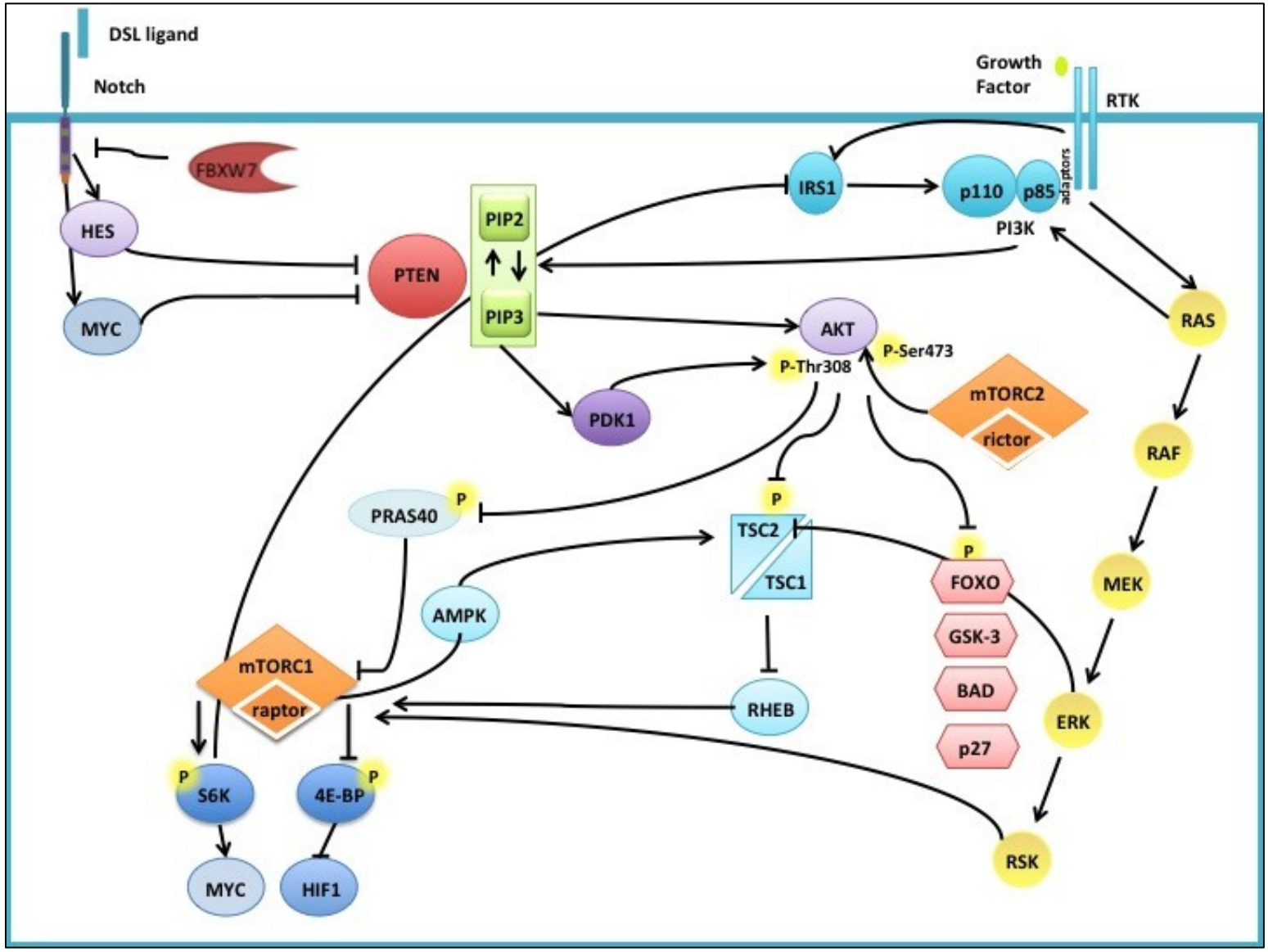
DSL ligand
Notch
Growth Factor
RTK
FBXW7
HES
MYC
PTEN
PIP2
PIP3
IRS1
p110
p85
adaptors
PI3K
RAS
AKT
P-Thr308
P-Ser473
PDK1
mTORC2
rictor
RAF
PRAS40
P
TSC2
TSC1
FOXO
GSK-3
BAD
p27
MEK
AMPK
mTORC1
raptor
RHEB
ERK
S6K
4E-BP
MYC
HIF1
RSK

Figure 1.3.1: The PTEN/PI3K/AKT/mTOR signalling network. The tumour suppressor phosphatase with tensin homology (PTEN) opposes the function of phosphoinositide 3-kinase (PI3K). PI3K is composed of a regulator subunit (p85) that can directly interact with receptors, or interacts through adaptor proteins such as growth factor receptor-bound protein 10 (GRB10). Upon ligand activation of receptor tyrosine kinases (RTK), PI3K is activated, and promotes the conversion of phosphatidylinositol (4,5) bisphosphate (PIP_2) to phosphatidylinositol (3,4,5) triphosphate (PIP_3). PIP_3 accumulation at the plasma membrane recruits AKT and 3-phosphoinositide-dependent kinase 1 (PDK1) through interaction with their pleckstrin homology (PH) domains. AKT is activated by phosphorylation at Thr308 by PDK1, and at Ser 473 by mammalian target of rapamycin complex 2. Activated AKT phosphorylates downstream targets, resulting in cell survival and proliferation. AKT activates mTORC1, through inhibition of tuberous sclerosis protein 2 (TSC2), blocking the formation of the GTP-ase activating TSC2-TSC1 complex. AKT also activates mTORC1 by phosphorylating and inactivating the mTORC1 inhibitor proline-rich AKT substrate 40kDa (PRAS40). This results in the mTORC1 activation of ribosomal protein S6 kinase (S6K) and eukaryotic translation-initiation factor 4E (eIF4E)-binding protein 1 (4E-BP1), resulting in protein synthesis. The TSC2-TSC1 is a common node of Ras signalling, AMP-activated protein kinase (AMPK) signalling, and the PI3K pathway. AKT also phosphorylates and inhibits forkhead box transcription factor (FOXO), glycogen synthase kinase 3 (GSK-3), the cell cycle inhibitor p27, and the pro-apoptotic BCL-2 associated death promoter (BAD). The Notch pathway regulates the PI3K signalling axis through the activation of the transcriptional factors hairy enhancer of split (HES) and myelocytomatosis viral oncogene homolog (Myc), which both suppress transcription of PTEN. Inactivation or inhibition of mTORC1 can promote AKT signalling by blocking the S6K mediated phosphorylation and inhibition of insulin receptor substrate 1 (IRS1). IRS1 promotes PI3K activation and downstream signalling. (Cully, You, Levine, & Mak, 2006; Demarest et al., 2008; Song, Salmena, & Pandolfi, 2012; Vlierberghe & Ferrando, 2012; Yuan & Cantley, 2008)

1.3.2: THE NOTCH SIGNALLING PATHWAY IN T-ALL

1.3.2.1 Overview of the Notch signalling pathway

There are four paralogues of Notch receptors in mammals, termed NOTCH1-4. Notch receptors are class I single-pass transmembrane glycoproteins that function as ligand-activated transcription factors. The Notch pathway is a highly evolutionarily conserved and transduces cell-to-cell signals at the cell surface into gene expression changes. Notch signalling is important for self-renewal and differentiation in numerous tissue types, and is involved in normal and malignant hematopoietic processes. Thomas Hunt Morgan first described the Notch protein in 1917, while studying a strain of *Drosophila* with notched wings (Morgan et al., 1917). In the 1980s the Notch receptor was cloned and sequenced independently by Artavanis-Tsakonas and Young (Wharton et al., 1985 and Kidd et al., 1986).

Notch receptors are plasma membrane-spanning receptors, noncovalently bound as heterodimers of the N-terminal extracellular (N^{EC}) and C-terminal transmembrane-intracellular (N^{TM}) subunits through their heterodimerization domain (HD) (**Figure 1.3.2.1**). All paralogues of Notch are activated through the interaction of their extracellular domain with ligands of the Delta-Serrate-Lag2 (DSL) family (transmembrane proteins with large epidermal growth factor (EGF)-like repeats) located on the surface of neighbouring cells. There are five ligands encoded by the DSL family in mammals: Delta-like 1 (Dll1), 3 (Dll3), 4 (Dll4) and Jagged 1 (Jag1), 2 (Jag2). The extracellular domain of Notch receptors is comprised of a variable number of EGF-like repeats (Notch1 and Notch2 have 36 EGF-like repeats; Notch3, 34; Notch4, 29) that interact with the DSL ligands (Lobry, Oh, Mansour, Look, & Aifantis, 2014; Rebay et al.,

1991). Signal transduction between cells requires cell-to-cell contact since the receptor and ligand are membrane-bound. The E3 ligases Neuralized and Mindbomb can regulate Notch signalling through the ubiquitination of Notch ligands (Pitsouli & Delidakis, 2005).

As stated above, Notch signalling is activated through the interaction of a DSL ligand on a neighbouring cell with the EGF repeats on the N^{EC} domain of Notch. Upon activation, the negative regulatory region (NRR, discussed below) undergoes a conformational change, allowing a disintegrin and metalloproteinase 10 (ADAM10) to access the S2 proteolytic site in the juxtamembrane region of the extracellular domain. This cleavage event produces a truncated Notch, and is necessary for the secondary cleavage of Notch at the S3 site of the transmembrane domain by the γ-secretase complex (comprised of presenilin (PSEN1), anterior pharynx-defective 1 homolog (APH1), presenilin enhancer 2 homolog (PEN2) and Nicastrin (NCSTN)), leading to the release of the soluble Notch intracellular domain (NICD) (Bray, 2006).

Once released, the NICD rapidly translocates to the nucleus through the nuclear localization signal domain (NLS). In the nucleus, NICD associates with the DNA-binding protein recombination signal binding protein for immunoglobulin kappa J (RBPJ or RBP-Jκ; from the CSL family of DNA-bound transcription factors) through its RBP-associated molecule (RAM) and CDC10/ANK (composed of seven ankyrin-like repeats; ANK) domain. RBPJ acts as a transcriptional repressor when not bound to NICD, and an activator when bound to NICD. Additional co-repressors include silencing mediator for retinoid or thyroid-hormone receptors (SMRT, also called nuclear receptor co-repressor 2 (NcoR)) and spen family transcriptional repressor (SHARP), and the general repressors

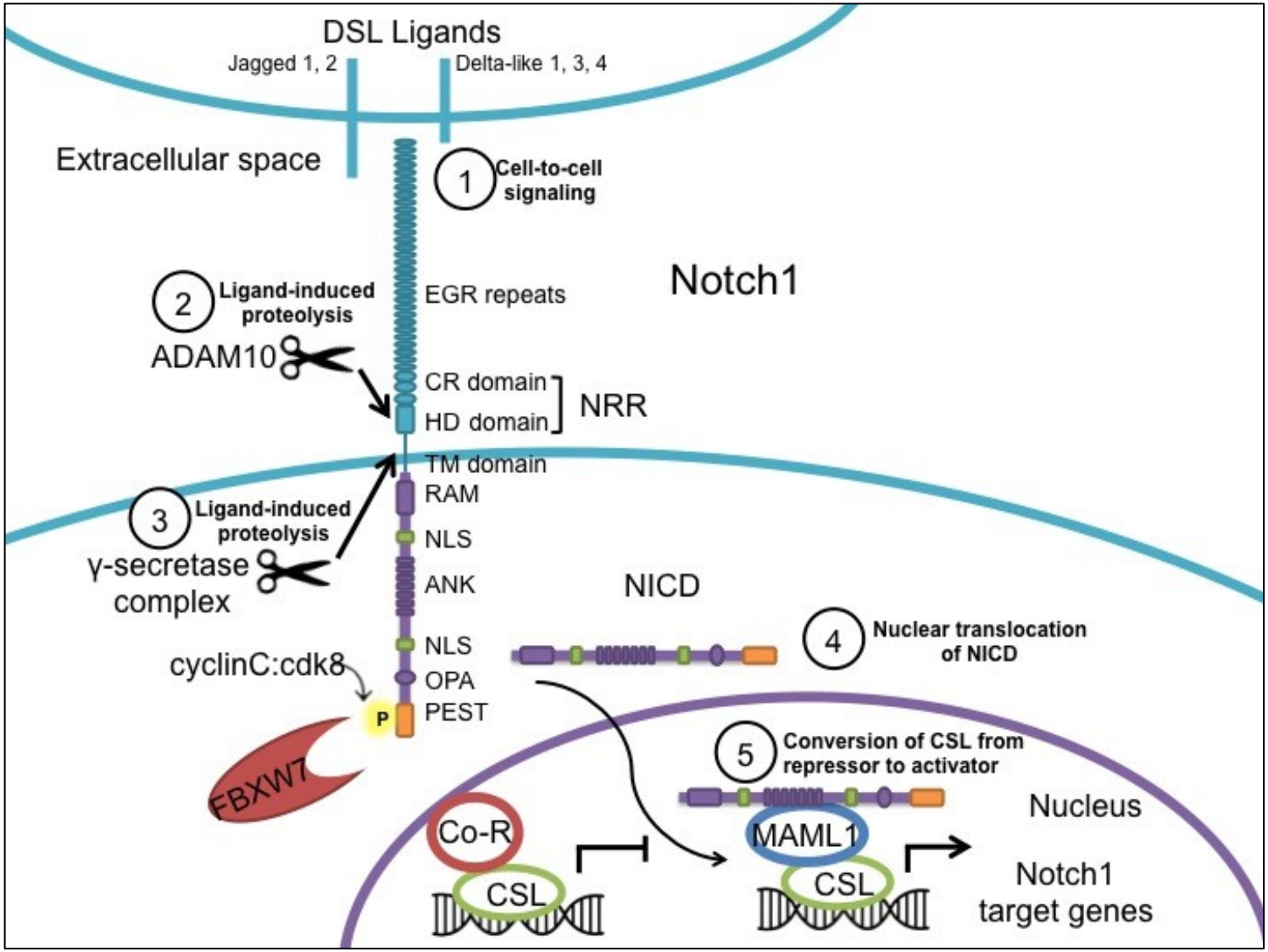
DSL Ligands
Jagged 1, 2
Delta-like 1, 3, 4
Extracellular space
1
Cell-to-cell signaling
Notch1
2
Ligand-induced proteolysis
EGR repeats
ADAM10
CR domain
HD domain
NRR
TM domain
RAM
3
Ligand-induced proteolysis
NLS
γ-secretase complex
ANK
NICD
NLS
4
Nuclear translocation of NICD
cyclinC:cdk8
OPA
P
PEST
FBXW7
5
Conversion of CSL from repressor to activator
Nucleus
Co-R
MAML1
CSL
CSL
Notch1 target genes

Figure 1.3.2.1: Notch1 signalling in T-ALL. Delta-Serrate-Lag2 (DSL) ligands on neighbouring cells interact with Notch1, causing a conformational change of the negative regulatory region (NRR), exposing the S2 and S3 cleavage sites. This allows two proteolytic cleavage events to occur. First a disintegrin and metalloproteinase 10 (ADAM10) cleaves at the S2 site in the heterodimerization (HD) domain, and second the γ-secretase complex (GSI) cleaves at the S3 site in the transmembrane (TM) domain. The intracellular domain of NOTCH (NICD) is released from the membrane, travels to the nucleus, and converts CBF1, suppressor of hairless, Lag-1 (CSL) DNA-binding protein from a repressor to an activator, through the release of co-repressors (co-R) and the recruitment of co-activators (such as mastermind-like protein (MAML1)). In T-ALL the most important CSL protein is Recombination signal binding protein for immunoglobulin kappa J (RBPJ). This permits the transcription of Notch1 target genes. F-box/WD repeat-containing protein 7 (FBXW7) is an E3 ubiquitin ligase that recognized the phosphorylated PEST (Proline (P), glutamic acid (E), serine (S) and threonine (T) rich) domain of Notch1, and targets it for degradation, thus terminating the transcription of Notch1 target genes. (Demarest et al., 2008; A. A. Ferrando, 2009; Vlierberghe & Ferrando, 2012; Weng et al., 2004)

c-terminal binding protein 1 (CtBP1) and sirtuin 1(SIRT1; which recruit histone deacetylases and histone demethylases) (Kao et al., 1998; Mulligan et al., 2011; Nagel et al., 2005; Yatim et al., 2012). The interaction of NICD with RBPJ displaces co-repressors and recruits additional co-activators of gene transcription, such as the mastermind-like protein (MAML1) and cAMP response element-binding protein (CREB)-binding protein (CBP/p300). This results in the short-term transcriptional activation of Notch target genes. Numerous genes can be regulated by Notch, and gene targets may be cell-type specific. In the context of T-ALL, important transcriptional targets of Notch-RBPJ include the hairy enhancer of split (*HES*) and myelocytomatosis viral oncogene homolog (*c-MYC*) (Palomero et al., 2006; Weng et al., 2006; Gladys W Wong, Knowles, Mak, Ferrando, & Zu, 2012).

Ligand-independent activation of the Notch pathway is prevented by the LNR/cysteine-rich (CR) domain (Sanchez-Irizarry et al., 2004). The CR domain is made of three CR Lin-12 repeats. Together, the HD and CR domains act as a negative regulatory region (NRR), which conformationally inhibits metalloproteinase cleavage when there is no receptor-ligand interaction, due to close association of the HD and CR (effectively shielding the HD domain). Additional negative regulation of Notch signalling is accomplished through the phosphorylation of the c-terminal PEST domain by cyclinC:cdk8, which facilitates binding of the F-box/WD repeat-containing protein 7 (FBXW7) (Fryer, White, & Jones, 2004), which terminates the transcriptional activation of Notch. The PEST (proline [P], glutamic acid [E], serine [S] and threonine [T] rich) domain can also be ubiquitinated by SCF^{FBW7}, leading to proteosomal degradation (Gupta-Rossi et al., 2004). All together, the PEST domain is important in regulating

Notch protein turnover, and deletion or mutation of the PEST domain (denoted ΔPEST) can result in increased NICD stability, and therefore increased Notch signalling.

1.3.2.2: Notch signalling in T-cell development

Notch signalling has been described as playing essential roles in the development, maintenance and self-renewal of hematopoietic stem cells (HSC) (Bigas, Guiu, & Gama-Norton, 2013). This role is well conserved in zebrafish (*danio rerio*), where Notch signalling is required for the specification of HSCs (Clements et al., 2011). However, there has been a great deal of controversy regarding the role of Notch signalling in embryonic development of HSCs, as compared to adult HSCs, as adult HSCs do not seem to require Notch activation (Bigas & Espinosa, 2012; Dzierzak & Speck, 2008; Kumano et al., 2003). Recently, it has been demonstrated that human cord blood progenitor cells can proliferate in response to Notch signalling (Delaney et al., 2010). In this study, CD34+ human cord blood progenitor cells were expanded *ex vivo* through exposure to the Notch ligand Dll1, and these expanded cells had enhanced and rapid engraftment when clinically transplanted following myeloablative irradiation (Delaney et al., 2010). Indeed, active Notch signalling in stem cells themselves as well as in stromal and niche cells appears to be important for the repopulation of HSCs (Butler et al., 2010).

Notch1 is essential to commitment of lymphoid cells to the T-lineage. In a conditional mouse knock-out model of *NOTCH1*, mice have a severe deficiency in thymocyte development. *Notch1*-deficient mice completely lack lymphoblasts with any T-lineage markers, indicating that Notch1 is necessary for early T-cell development. Bone marrow from mice with wild-type (WT) *Notch1* is able to repopulate all cell lineages in lethally irradiated recipient mice (Radtke et al., 1999). Conditional deletion of

Rbp-jκ (encoding the DNA-bound transcriptional factor RBPJ, a co-activator of NICD) leads to a block of T-cell development, reinforcing an essential role for Notch1 for the commitment of lymphoid cells to the T-lineage. Furthermore, *Rbp-jκ*-deficient mice also showed an expansion of B cells in the thymus. RBPJ and NOTCH1 together commit lymphoid cells to the T-lineage at the expense of B-cell development and expansion (Han et al., 2002).

1.3.2.3: Activating *NOTCH1* mutations in T-ALL

T-ALL is a heterogeneous disease with a unique repertoire of genetic lesions. Genetic abnormalities that hold prognostic relevance specific to T-ALL have emerged, such as those associated with *NOTCH1* (Vlierberghe & Ferrando, 2012). The *NOTCH1* gene was originally identified as a possible oncogene in 1991 through the isolation of the t(7;9)(q34;q34.3) chromosomal translocation in a T-ALL patient sample (Ellisen et al., 1991). This chromosomal abnormality fuses the 3' region of *NOTCH1* into the *TCRβ* locus and leads to the expression of a truncated and constitutively active form of Notch1 (Vlierberghe & Ferrando, 2012). While this particular chromosomal translocation is very rare in T-ALL patients, aberrant activation of Notch signalling (caused through various genetic mechanisms to be discussed below) is seen in approximately 60% of all T-ALL cases (Sanda et al., 2010; Weng et al., 2004).

Numerous mutations in the *NOTCH1* gene can lead to its unchecked activation; however there are two mutational hotspots, and mutations are commonly found in the HD resulting in ligand-independent activation of Notch, and in the C-terminal PEST domain resulting in increased stability of the NICD, and increased transcriptional activation of Notch1-responsive genes. Additionally, mutations in *FBXW7*, an E3 ubiquitin gene

encoding F-box/WD repeat-containing protein 7 (FBXW7), decrease the ability of the E3 to degrade its target proteins. FBXW7 is an ubiquitin ligase that controls the rate of Notch protein turnover. As mentioned above, cyclinC:cdk8 phosphorylates the PEST region of Notch, leading to the binding of FBXW7 and subsequent ubiquitination by the SKP1-cullin-F-box (SCF) complex, which targets Notch for proteosomal degradation. Therefore, mutations in *FBXW7* lead to increased protein stability of both Notch and c-MYC (Demarest et al., 2008; Vlierberghe & Ferrando, 2012). Together these events lead to inappropriate Notch signalling. Mutations in the HD occur alone in 20% of all cases, or in *cis* with mutations in the PEST domain or in *FBXW7* in another 20% of cases. Mutations in the PEST domain alone occur at a prevalence of 5%, and mutations in *FBXW7* alone occur in 5% of T-ALL cases (see **Figure 1.3.2.3**) (Vlierberghe & Ferrando, 2012).

Activation of Notch signalling appears to be characteristic of T-cell malignancy, since no B cell malignancies with *NOTCH1* mutations have been described and myeloid leukemias with *NOTCH1* mutations are very rare (Lobry et al., 2014; Vlierberghe & Ferrando, 2012). However, mutations in all members of the Notch family have been reported in other human malignancies such as in breast, prostate, colorectal, pancreatic, melanoma and medulloblastoma, and also in neurodegenerative diseases such as Alzheimer's disease (Koch and Radtke 2007, Roy et al., 2007). In these contexts Notch signalling is implicated in driving disease progression; however, in other cellular contexts, Notch can act as a tumour suppressor (Lobry et al., 2014).

Notch signalling is altered in one third of all non-small cell lung carcinomas (NSCLCs), and in different contexts Notch has been implicated as a tumour suppressor (due to the

presence loss of function mutations in patient samples) or as an oncogenic driver (supported by the presence of gain of function mutations). In squamous cell carcinoma loss of function mutations in *NOTCH1* and/or *NOTCH2* have been identified in 12.5% of small cell carcinoma of all cases examined, while in 10% of cases activating mutations have been described (Westhoff et al., 2009). Furthermore, in acute myeloid leukemia (AML) the Notch pathway can have either a pro-leukemic or a tumour suppressor role (Lobry et al., 2013, 2014). This is in a context dependent manner that likely depends on a patient's particular genetic landscape. However, there is an increasing body of evidence that suggests that Notch may indeed act primarily as a tumour suppressor in AML, and therefore loss or inactivation of Notch may be an important step in leukemogenesis for AML (Lobry et al., 2014).

There is still controversy over the prognostic significance of Notch mutations and clinical outcome for patients. Overall, there is a favourable effect of mutations in *NOTCH1* on initial response to early treatment, and in particular with prednisone response, but this advantage is not seen when mutations in *NOTCH1* are correlated with long-term survival outcomes (Vlierberghe & Ferrando, 2012). Similarly, mutations in the negative regulator of Notch, *FBXW7*, have been correlated with an increased response to early treatment and lower MRD levels (Clappier et al., 2010). However, the overall impact of mutations in *NOTCH1* and *FBXW7* on long-term survival of patients may depend on differences in therapeutic strategies used in each trial, further confounding the analysis of the prognostic significance of a patient's *NOTCH1* mutational status (A. Ferrando, 2010; Tzoneva & Ferrando, 2012).

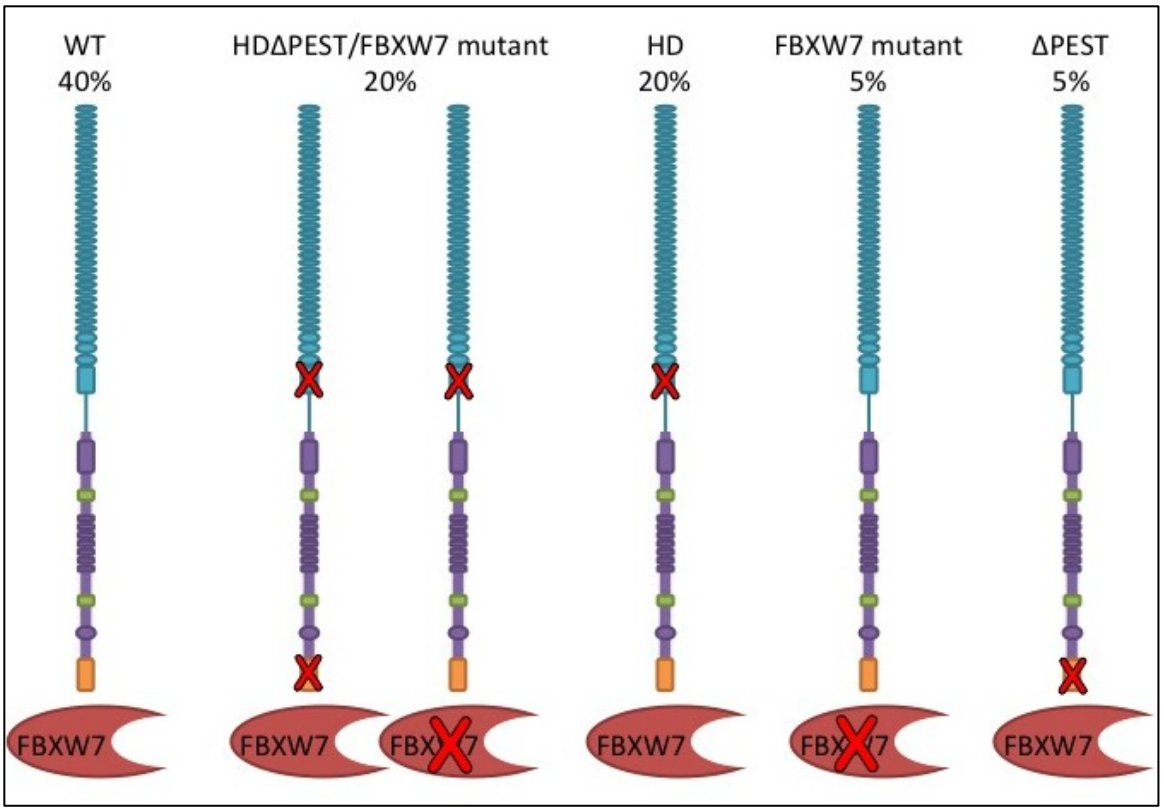

Figure 1.3.2.3: Prevalence and mechanisms of aberrant NOTCH1 signalling in T-ALL. Mutations in the *NOTCH1* gene can lead to its unchecked activation and are clustered around two mutational hotspots: in the heterodimerization domain (HD) resulting in ligand-independent activation of Notch, and in the C-terminal PEST domain resulting in increased stability of the notch intracellular domain (NICD), and increased transcriptional activation of Notch1-responsive genes. Additionally, mutations in F-box/WD repeat-containing protein 7 (*FBXW7*) decrease the ability of FBXW7 to degrade target proteins, lead to increased protein stability of Notch and c-MYC, and result in inappropriate Notch signalling. *NOTCH1* is unmutated (WT) is approximately 40% of cases. Mutations in the HD occur alone in 20% of all cases, or in *cis* with mutations in the PEST domain or in *FBXW7* in another 20% of cases. Mutations in the PEST domain alone occur at a prevalence of 5%, and mutations in *FBXW7* alone occur in 5% of patient cases. (Demarest et al., 2008; A. A. Ferrando, 2009; Vlierberghe & Ferrando, 2012; Weng et al., 2004)

1.3.2.3.1: Notch1 in T-cell transformation

In T-ALL, *NOTCH1* is a critical promoter of leukemogenesis through the transcriptional upregulation of genes involved in ribosome synthesis, protein translation, and nucleotide and amino acid biosynthesis. Moreover, Notch indirectly controls leukemogenesis by promoting the expression of the oncogenes *c-MYC* and *HES1*, which promote cell growth and metabolism (Palomero et al., 2006; Weng et al., 2006; Gladys W Wong et al., 2012). Notch activation of c-MYC, HES1 will be discussed below, in addition to the role of Notch in inhibiting p53-depending apoptosis, and the activation PI3K-AKT-mTOR signalling axis.

1.3.2.3.2 Notch1 promotes expression of c-MYC

In Notch-dependent T-ALL cell lines, c-MYC is a direct target of NOTCH1 (Weng et al., 2006). Using an integrative systems biology, it was determined that NOTCH1 controls a positively-regulated transcriptional program which ultimately promotes cell survival and growth (Palomero et al., 2006). Using gene expression array analysis and chromatin immunoprecipitation, it was determined by Dr. Adolfo Ferrando's group that NOTCH1 directly promotes c-MYC gene expression (through binding to the *c-MYC* promoter), and that NOTCH1 and c-MYC together enhance transcription of common target genes that promote the growth of human T-ALL cells. Furthermore, in a T-ALL cell line (DND-41) treatment with anti-Notch therapy slowed cell growth and resulted in a decrease in cell size. However, overexpression of *c-MYC* in Notch-inhibited cells provided a mechanism of resistance to Notch inhibition. These results suggest that c-MYC is an essential mediator of NOTCH1 leukemogenesis (Palomero et al., 2006).

1.3.2.3.3: Notch1 inhibits tumour suppressor p53

In T-ALL, Notch signalling is able to suppress the effects of the tumour suppressor p53 by promoting its proteolytic degradation. One current model proposes that Notch inhibits the alternate reading frame product of the p16INK41 protein (ARF), leading to constitutive murine double minute 2 (Mdm2)-regulated proteosomal degradation of p53 (Beverly, Felsher, & Capobianco, 2005). In a murine model of T-ALL, it was found that p53 mRNA levels were normal, but the protein levels of p53 were greatly reduced and ARF levels were undetectable. Normally, ARF binds to the E3 ubiquitin ligase Mdm2, preventing Mdm2 from ubiquitinating p53 and targeting it for degradation. ARF therefore allows p53 to accumulate in the cell, leading to cell-cycle arrest or apoptosis (Demarest et al., 2008). Notch-mediated suppression of apoptosis is posited to be a central aspect of T-ALL leukemogenesis (Demarest et al., 2008) and activating mutations in the Notch pathway and loss of p53 activity appear to be mutually exclusive events (Uren et al., 2008). Uren *et al*, compared lymphomas generated by murine leukemia virus (MuLV) insertional mutagenesis of p53 wild type and *TP53*$^{-/-}$ mice, and found that Notch1 is more frequently mutated in wild-type mice than in the *TP53*$^{-/-}$ mice (Uren et al., 2008). This suggests that either activation of Notch or loss of p53 can lead to leukemogenesis.

1.3.2.3.4: Notch1 activates the PI3K-AKT-mTOR signalling axis

Notch1 also regulates cell growth by activating the phosphatidylinositol 3-kinase (PI3K)-AKT-mammalian target of rapamycin (mTOR) pathways. Notch signalling regulates cell size, glucose uptake and glycolytic metabolism through the activation of the PI3K and AKT signalling axis (Ciofani & Zúñiga-Pflücker, 2005). This is

accomplished in part through the transcription of *HES1* (a Notch1 responsive target gene), which acts to inhibit the phosphatase with tensin homology tumour suppressor (PTEN), a potent inhibitor of the PI3K-AKT-mTOR signalling pathway (Palomero et al., 2007). The involvement of the PI3K-AKT-mTOR axis in T-ALL will be discussed below in **1.3.8 The role of PI3K and AKT signalling in T-ALL**, and the role of *HES1* in T-ALL will be discussed in **1.3.7.4 Regulation of PTEN in T-ALL**.

1.3.3: PHOSPHATASE WITH TENSIN HOMOLOGY TUMOUR SUPPRESSOR IN T-ALL

In T-ALL, Notch-induced transcription of *HES1* can inhibit the tumour suppressor PTEN, which allows leukemic cell proliferation and survival. However, in the context of T-ALL treated with Notch inhibitors, loss of PTEN is proposed as a potential resistance mechanism. Therefore, because PTEN links both the Notch signalling pathway and the PI3K-AKT-mTOR signalling axis (**Figure 1.3.1**), an understanding of this tumour suppressor is central to the molecular mechanism of T-ALL pathogenesis. In this section the structure and molecular mechanisms of PTEN signalling will be discussed, as well as the regulation of this tumour suppressor. Furthermore, the role of PTEN in malignant contexts will be explored.

1.3.3.1 Overview of PTEN signalling

PTEN is a lipid phosphatase, which converts phosphatidylinositol (3,4,5) triphosphate (PIP_3) to phosphatidylinositol (4,5) bisphosphate (PIP_2), acting as the primary negative regulator of the class I phosphatidylinositol 3-kinase (PI3K) pathway. The lipid secondary messenger PIP_3 acts as a potent activator of 3-phosphoinositide-dependent kinase 1 (PDK1) and AKT (also known as protein kinase B – PKB). PI3K

converts PIP_2 to PIP_3, and if PTEN expression is downregulated or lost, PIP_3 accumulates at the plasma membrane and recruits proteins containing pleckstrin homology (PH) domains, including PDK1 and AKT. PDK1 activates AKT through phosphorylation at the Thr308 residue, and mammalian target of rapamycin complex 2 (mTORC2) activates AKT through phosphorylation at Ser473. Three active isoforms of AKT (AKT1, AKT2, and AKT3) activate downstream targets through their serine-threonine kinase activity. The net result of AKT signalling is cell survival and proliferation, driving T-ALL leukemogenesis (Cully et al., 2006).

PTEN acts as a phosphatase on both polypeptide and phosphoinositide substrates, and has a wide range of roles in a variety of biological processes. PTEN, as a negative regulator of AKT, is involved in regulating cellular metabolism, cellular senescence (via PTEN loss-induced cellular senescence – PICS), cell mobility and polarity, and leukemic stem cells. While PTEN acts primarily as a negative regulator of the PI3K/AKT pathways, it also has AKT-independent functions.

PTEN has five functional domains, all of which appear to be physiologically relevant to the role of PTEN in tumourigenesis, because diverse tumour-associated mutations have been found in all domains (Song et al., 2012). The five functional domains are: a phosphatidylinositol-4,5-bisphosphate (PtdIns(4,5)P_2)-binding domain (PBD), a phosphatase domain, a C2 domain, a carboxy-terminal tail and a PDZ-binding domain. Mutation or loss of PTEN results in hyperactivation of the PI3K/AKT pathways, driving tumourigenesis, as well as contributing to chemotherapeutic resistance (Hildebrandt et al., 2009; W.-C. Huang & Hung, 2009). In some tissues PTEN acts as a haploinsufficient tumour suppressor, and downregulation of PTEN protein levels

correlate with tumourigenesis and progression. Taken together, these findings indicate that there is a continuum of functional consequences of reduced PTEN expression or activity, and highlights the important role of PTEN regulation in cancer (Song et al., 2012).

1.3.3.2 Cellular regulation of PTEN

PTEN is regulated by a spectrum of cellular processes. Epigenetic silencing (Hollander, Blumenthal, & Dennis, 2011; Lu et al., 2009), transcriptional regulation (Escrivà et al., 2008), microRNAs (miRNAs) (Bartel, 2009), post-translational modification, as well as genetic mutations (Eng, 2003; Trotman et al., 2007) can alter the levels of functional PTEN in tissues. Below is a discussion of the most prominent regulatory mechanisms of PTEN in T-ALL.

In T-ALL, the HES1 transcriptional factor has emerged as a primary negative regulator of *PTEN* transcription. HES1 is a direct transcriptional target of Notch, and is a member of the basic helix-loop-helix family of oncogenic transcription factors. HES1 plays a critical role in normal thymocyte development and fate specification, amongst other processes, and $Hes1^{-/-}$ is embryonically lethal in murine models (Pear, 2010; Wendorff et al., 2010). Through HES1, in addition to NOTCH mediated c-MYC transcription, Notch signalling promotes PI3K pathway activation (G. W. Wong, Knowles, Mak, Ferrando, & Zuniga-Pflucker, 2012). In Hes1-deficient mice expressing an oncogenic Notch1 allele, mice did not develop T-ALL, indicating that Hes1 may be required for efficient induction of leukemogenesis (Wendorff et al., 2010). Hes1 appears to be necessary for the development of murine Notch1-induced T-ALL, and plays an important role in T-ALL maintenance.

In T-ALL, the casein kinase 2 (CK2) is another important regulator of PTEN. In T-ALL cell lines, the serine and threonine residues in the C-terminal tail of PTEN are frequently phosphorylated by CK2, resulting in increased protein stabilization and, paradoxically, PTEN functional inactivation. This correlates with the finding that T-ALL patient samples can have high levels of PTEN protein, but constitutively activated PI3K and AKT signalling (Silva et al., 2010).

The PI3K pathway can also increase its activation through a positive feedback interaction with PTEN. The p85 regulatory subunit of PI3K binds PTEN and decreases the phosphatase activity of the tumour suppressor, resulting in activation of AKT/PI3K (Song et al., 2012). As described above, p53 is a transcriptional activator of the *PTEN* gene.

1.3.3.3 Loss of PTEN is a mechanism of resistance to Notch-inhibition

As stated above, resistance to GSIs is a common problem in T-ALL both *in vitro* and *in vivo*, highlighted by the lack of objective outcome in the Dana-Farber Cancer Institute 04-390 phase I clinical trial of MK-0752 (DeAngelo et al., 2006). Loss of the tumour suppressor PTEN appears to mediate resistance of Notch-mutated T-ALL cell lines to GSIs (Bailis & Pear, 2012; Palomero et al., 2007; Tzoneva & Ferrando, 2012). The Ferrando group found that in an *in vitro* model of $PTEN^{-/-}$ GSI-resistant T-ALL, treatment with a GSI inhibited Notch signalling, but produced limited cytostatic and apoptotic effects (Palomero et al., 2007). They hypothesized that in the absence of PTEN, unchecked AKT signalling can compensate for Notch inhibition, leading to suppression of apoptosis. These cells were no longer dependent on Notch signalling to drive neoplastic proliferation, but were 'addicted' to AKT signalling. Indeed, AKT is a serine-

threonine kinase that phosphorylates and activates Mdm2, leading to increased degradation of p53. Despite GSI inhibition of Notch-mediated p53 suppression, T-ALL cell lines can adapt *in vitro* through aberrant AKT activation that once again suppresses p53 in the context of PTEN loss (Ogawara et al., 2002).

These results compliment the clinical finding that deletion mutations in *PTEN* occur frequently in T-ALL. One group reported deletion mutations in *PTEN* in 5%-10% of primary samples, but approximately 17% of primary adult T-ALL samples lacked functional PTEN protein expression (Vlierberghe & Ferrando, 2012). Of these patient samples with mutations in *PTEN*, only a small proportion (approximately 10%) had activating *NOTCH1* mutations. These results provide evidence that *PTEN* mutations may be sufficient to mimic Notch activation in T-ALL, and in particular, PTEN loss can mimic Notch-mediated suppression of p53-mediated apoptosis (Demarest et al., 2008; Palomero et al., 2007). In pediatric T-ALL, approximately 18% of cases have mutations in *PTEN*, but these mutations are absent or rare in pediatric B-cell ALL (Jotta et al., 2010). Elsewhere, it has been reported that loss of PTEN occurs in up to 40% of primary pediatric T-ALL samples (Gutierrez et al., 2011).

The importance of PTEN loss in T-ALL disease progression suggests that treating T-ALL with Notch inhibitors could stress T-lymphoblasts to become dependent on alternative signalling pathways to drive their expansion and survival. This could provide a selective pressure to acquire *PTEN* and *TP53* inactivating mutations, ultimately leading to GSI resistance. Of interest, human T-ALL relapse tumours have a higher frequency of *TP53* mutations than do their primary tumour counterparts (Demarest et al., 2008). Furthermore, *PTEN* mutations and deletions are frequent in T-ALL cell lines created

from relapsed patient samples and late-stage disease patient samples (Jotta et al., 2010; Ogawara et al., 2002).

While Notch signalling remains a focal point of T-ALL research, the disappointment of GSIs in both *in vitro* assays and clinical trials has stressed the need for new molecular targets for this haematological malignancy, especially for use in combination with existing cytotoxic and molecularly-targeted agents. The PTEN and phosphatidylinositol 3-kinase (PI3K) signalling transduction pathways have emerged as novel therapeutic targets, as have T-ALL specific transcription factor oncogenes.

1.3.3.4 PTEN modulates cellular metabolism

The PTEN/PI3K/AKT/mTOR pathway has a central role in cellular metabolism. PI3K and AKT signalling promoted by the loss or downregulation of PTEN has the following effects on glucose and lipid metabolism. PI3K and AKT are positioned downstream of insulin receptor tyrosine kinases, and promote insulin-mediated glucose uptake and inhibit gluconeogenesis. PI3K and AKT, through their inhibition of glycogen synthase kinase 3 (GSK3), promote lipogenesis. Hyperactivation of the PI3K and AKT pathway in cancer cells also promotes ATP consumption, contributing to the Warburg effect whereby cancer cells exhibit higher rates of the less-efficient anaerobic glycolysis – leading to increased lactate production (Warburg, 1956). Dietary restriction (DR) has been shown to be of benefit to some cancer patients and has anti-tumour effects. However, DR is ineffective in *PTEN*-null tumours, due to hyperactivation of AKT and insensitivity to changes in circulating insulin levels (Kalaany & Sabatini, 2009; Song et al., 2012) .

The association between treatment-related hyperglycemia and poor clinical outcome in ALL makes the connection between aberrant PTEN/PI3K/AKT signalling and glucose metabolism particularly relevant (Pan et al., 2012; Weiser et al., 2004). Patients receiving corticosteroid and asparaginase therapy for T-ALL may develop diabetes mellitus, or glucose intolerance (Howard & Pui, 2002). Management of hyperglycemia with the anti-diabetic drug metformin has recently been evaluated for the first time in children with acute lymphoblastic leukemia to be safe and effective (Bostrom et al., 2013). Furthermore, anti-diabetic drugs, for example metformin and rosiglitazone, have been demonstrated *in vitro* to induce apoptosis of acute lymphoblastic leukemia cells, and sensitize cells to conventional chemotherapeutic agents (Leclerc, Leclerc, Kuznetsov, DeSalvo, & Barredo, 2013; Pan et al., 2012).

1.3.3.5 PTEN loss-induced cellular senescence

Cellular senescence is an important tumour suppressive mechanism and emerging therapeutic target that can be activated due to oncogene activation (oncogene-induced senescence – OIS), or as a result of the loss of tumour suppressors. While decreased levels of PTEN normally lead to hyperactivation of PI3K/AKT and therefore cellular proliferation, complete loss of PTEN in the acute phase can trigger a specific type of cellular senescence. PTEN loss-induced cellular senescence (PICS) is associated with high levels of p53 and slow disease progression. In PICS, elevated p53 levels are translationally maintained through mTORC1 signalling. When compared to early stage disease, late stage disease is more likely to have a complete loss of *PTEN*, which coincides with the functional loss of the tumour suppressor, p53 (Beverly et al., 2005), which functions as a transcriptional activator of *PTEN* (Stambolic et al., 2001).

Additionally, p53-induced apoptosis depends on the inhibition of the PI3K pathway, and the subsequent silencing of their tumourigenic signals.

1.3.3.6 PTEN regulates the 'stemness' of Leukemic Stem Cells

The cancer stem cell theory first gained traction in the field of haematological malignancies, with the characterization of leukemic stem cells (LSC) (Bonnet & Dick, 1997; Lapidot et al., 1994). LSCs are believed to be responsible for the initiation and propagation of leukemia and are relatively resistant to conventional therapies (Mikkola, Radu, & Witte, 2010). Thus, LSCs are seen as the most crucial target in leukemia treatment, and are a central focus of research in the field (Huntly & Gilliland, 2005). In normal haematopoietic stem cells (HSCs), the loss of PTEN results in the depletion of the normal population of HSCs and an expansion of LSCs. Treatment with the mTOR complex 1 (mTORC1) inhibitor rapamycin restored the normal properties of the HSCs population and blocked the development of leukemia-initiating LSCs, indicating that PTEN loss results in hyperactive mTORC1 signalling and leukemogenesis (Yilmaz et al., 2006). This is consistent with previous findings that PI3K/AKT/mTOR signalling plays an important role in regulating the self-renewal properties of stem cells (Watanabe et al., 2006). PTEN appears to have different roles in HSCs and LSCs, suggesting that it could be possible to disrupt PTEN signalling in LSCs while maintaining the normal pluripotency of HSCs (Song et al., 2012).

1.3.4: THE ROLE OF PI3K AND AKT SIGNALLING IN T-ALL

In normal T-cell precursors, Notch regulates cell growth and development by modulating PI3K/AKT/mTOR signalling directly, and through the inhibition of PTEN via HES1 and c-MYC (see **Figure 1.3.1**) (Koch & Radtke, 2011). The PI3K/AKT/mTOR pathway is important in normal thymocyte development, and is also central to T-ALL pathogenesis (Tzoneva & Ferrando, 2012). In T-ALL, the constitutive activation of the PI3K/AKT signal transduction pathway is commonly observed, and T-ALL appears to be dependent on this the hyperactivation of AKT for growth and survival (Yuan & Cantley, 2008). This section will explore the key proteins in this signalling pathway, their regulation, and involvement in T-ALL pathogenesis.

1.3.4.1 Phosphatidylinositol 3-Kinase

Class I PI3Ks are heterodimeric molecules composed of a regulatory subunit (p85) and a catalytic subunit (p110). There are four unique isoforms for the catalytic subunit – p110α, p110β, p110γ, and p110δ. In normal thymocyte development, both PI3Kγ and PI3Kδ are required to generate functionally mature thymi, and a recently a role has been posited for these isoforms in the malignant transformation of T-cells (Subramaniam et al., 2012).

Several independent pathways can activate PI3K. Ligand binding to receptor tyrosine kinases (RTKs) leads to RTK dimerization and autophosphorylation of tyrosine residues. Phosphorylated RTKs can interact with specific Src homology 2 (SH2)-domain-containing molecules, based on the amino acids that surround the phosphotyrosine. The p85 regulatory subunit contains SH2-domains that are able to bind to phospho-YXXM

motifs (X is any amino acid) on RTKs, leading to the activation of the p110 catalytic subunit. Alternative to this direct interaction with RTKs, PI3K can be activated after growth factor receptor-bound protein 2 (GRB2) adaptor protein binds to phospho-YXN motifs on RTK. GRB2-associated binding protein (GAB) can bind to GRB2 adaptor proteins and p85 leading to activation of p110. The third mechanism of PI3K activation involves GRB2 activation of Ras, which activates p110 (independent of p85 activation). In the fourth mechanism, GRB2 can form a complex with Ras, GAB, and other scaffold proteins such as the insulin receptor substrate (IRS), bringing p110 into proximity of activating proteins. In different physiological contexts, different mechanisms of PI3K activation may occur (Cully et al., 2006).

When mTORC1 is activated, ribosomal protein S6 Kinase (S6K) can transcriptionally and allosterically repress the insulin receptor substrate (IRS) proteins, resulting in a negative feedback regulation of PI3K (Cully et al., 2006). IRS proteins are phosphorylated in response to insulin or insulin like growth factors binding insulin receptor tyrosine kinases. There is a strong link between cellular metabolism, and in particular insulin sensitivity, with the PI3K/AKT/PTEN signalling pathways.

Once PI3K has been activated, it phosphorylates PIP_2, generating the potent lipid messenger PIP_3. PIP_3 recruits PDK1 to the plasma membrane, where it phosphorylates and activates AKT at Thr308.

1.3.4.2 AKT

AKT is activated through phosphorylation at two residues: Thr308 by PDK1, and Ser473 by mTORC2 . mTORC2 is composed of mTOR, DEP domain-containing mTOR-interacting protein (DEPTOR), mammalian lethal with SEC13 protein 8 (mLST8), stress-

activated MAP kinase-interacting protein 1 (mSIN1 or MAPKAP1), Pro-rich protein 5 (PRR5 or PROTOR) and rapamycin insensitive companion of mTOR (RICTOR) (Jacinto et al., 2004). There are three isoforms of AKT that have distinct functions, although there is some overlap. AKT1 promotes cellular proliferation and survival, AKT2 regulates insulin-mediated metabolism, and AKT3 is also associated with cellular proliferation and growth (Bellacosa, Testa, Moore, & Larue, 2004; Garofalo et al., 2003; Stiles et al., 2002; Tschopp et al., 2005). Overall, activation of the three AKT isoforms promotes leukemogenesis through phosphorylation of downstream targets that drive cell survival, cell proliferation, and metabolism.

1.3.4.3 Multiple pathways converge on TSC2

AKT phosphorylates the tuberous sclerosis protein 2 (TSC2) on a number of residues. This phosphorylation prevents TSC2 from forming a complex with TSC1, blocking the GTP-ase activating protein (GAP) activity, and therefore blocking the inhibition of RAS-related small GTPase RAS homologue enriched in brain (RHEB). Due to AKT phosphorylation of TSC2, RHEB remains active and is able to promote mTORC1 signalling. While TSC1 and TSC2 were originally implicated in the autosomal dominantly inherited tumour syndrome tuberous sclerosis (TSC), inactivation of these genes has now been correlated with a number of neoplastic diseases including acute leukemia (Rosner, Fuchs, Siegel, Valli, & Hengstschläger, 2009). In acute leukemia patient samples, it was found that there are reduced levels of TSC2 mRNA (but normal levels of TSC1 mRNA) (Cully et al., 2006). Several pathways converge on the TSC1-TSC2 complex. Extracellular-regulated kinase (ERK) phosphorylates TSC2 at a distinct site from AKT, also inhibiting the GAP activity of TSC1-TSC2. Both ERK and AKT are

downstream of Ras, suggesting an important role for the AKT-TSC2-mTORC1 axes in Ras-dependent disease (Ma et al., 2005).

The homozygous loss of the *TSC1* or *TSC2* genes results in increased mTORC1 signalling, and through a negative feedback loop may result in inhibition of growth-factor stimulated PI3K signalling (Manning et al., 2005). However, if the tumour suppressor PTEN is lost or if its activity is downregulated, this negative feedback loop would be disrupted. Inhibiting the mTORC1 pathway results in upregulation of the PI3K/AKT pathways, and increases signalling through the Ras-mitogen-activated protein kinase (MAPK) pathway. Ras is able to activate PI3K, leading to increased AKT activity, and therefore inhibition of TSC2. There is significant crosstalk between the Ras signalling pathway and PI3K and PTEN, due to the involvement of TSC2 in these pathways as well as the ability of Ras to activate the p110 subunit of PI3K (Cully et al., 2006; Manning et al., 2005).

1.3.4.4 p53 and the PI3K/AKT/PTEN signalling pathway

The 'guardian of the genome' p53 activates the transcription of *PTEN* and *TSC2*, and therefore, in addition to its transcriptional repression of the gene encoding the catalytic subunit of PI3K, acts as a negative regulator of the PI3K/AKT signalling pathway. p53 is able to block the survival and proliferative signals propagated by the PI3K pathway, and loss of p53 is associated with a broad range of human cancers (Cully et al., 2006). In T-ALL, mutations and deletions in the *p53* are poor prognostic indicators correlated with treatment failure, and in the first relapse of pediatric patients, mutations and deletions correlated with a higher percentage of leukemic cells in S/G2-M phase of the cell cycle (Hof et al., 2011).

The crosstalk between the p53 tumour suppressor and the PI3K/AKT pathway is strengthened by the involvement of the forkhead box transcription factor 3A (FOXO3A). AKT phosphorylates and inactivates numerous proteins that block cell growth and survival, including the FOXOs, as well as p27, TSC2, BAD, PRAS40, and GSK-3 (Sykes et al., 2011). Phosphorylation of the FOXO proteins by AKT is mediated by the mTORC2 phosphorylation of the Ser473 residue of AKT (Sykes et al., 2011). Unphosphorylated FOXO3A is a transcription factor in the nucleus, transcriptionally activating p27, cyclin G2, BIM, and transcriptionally repressing cyclin D1 and p53 (perhaps as a component of a positive feedback loop required for full p53 activation). FOXO transcriptionally promotes quiescence, and apoptosis in a context-dependent manner. p53 activation as well as AKT activation leads to the nuclear expulsion of FOXO3A (Cully et al., 2006).

The role of FOXO transcription factors in leukemogenesis is currently under review. Historically, FOXO transcription factors have been considered tumour suppressors which are silenced by aberrant PI3K/AKT signalling. Interestingly, recent controversial roles have been identified for the FOXO pathway in the maintenance of leukemic stem cells (LSCs or leukemia initiating cells LICs) in AML. In AML, cell fractions enriched for LSCs in both AML cell lines and primary patient samples were found to have inactive AKT and activated FOXO proteins. Activation of AKT or suppression of FOXO proteins resulted in diminished leukemic growth and promoted apoptosis. This paradoxical finding indicates that FOXOs are required to maintain the LSC population in AML (Downing, 2011; Sykes et al., 2011). Future studies will help to dissect the role of the FOXO transcription factors in T-ALL, and specifically their role in

LSC maintenance. These results may hold relevance for understanding drug resistance and disease remission in T-ALL.

1.3.5 THE mTOR SIGNALLING PATHWAY

The mammalian target of rapamycin (mTOR) is a serine/threonine kinase which forms two complexes: mTOR complex 1 (mTORC1, containing raptor) and mTOR complex 2 (mTORC2, containing rictor). The mTOR signalling pathway plays a central role in integrating various signals and transducing the information to effectors that modulate protein synthesis, cell growth, and cell cycle progression. AKT phosphorylates and inactivates proline-rich AKT substrate 40kDa (PRAS40), which prevents PRAS40 from inactivating mTORC1, leading to its activation. mTORC1 can also be activated by Rheb, through AKT phosphorylation of TSC2, and inhibition of the GAP activity of TSC2-TSC1.

In T-ALL, the mTOR pathway is an important target of both the PI3K/AKT pathway and the Notch pathway. Notch signalling in T-ALL appears to activate the mTOR pathway. In one study, inhibition of Notch by Compound E in GSI-sensitive T-ALL cell lines produced the same phosphorylation changes as inhibition of mTORC1 with rapamycin. Upon treatment with Compound E, the primary downstream effectors of mTORC1, eukaryotic translation-initiation factor 4E (eIF4E)-binding protein 1 (4E-BP1) and S6K, were dephosphorylated, followed by cell cycle arrest. Introduction of the activated NICD into T-ALL cell lines resulted in rephosphorylation of S6K, and promoted cell cycle progression. This study postulated that Notch interacts with the mTOR pathway independent of AKT, but dependent on c-Myc (Chan, Weng, Tibshirani, Aster, & Utz, 2007a). The crosstalk between the Notch and PI3K signalling pathways has

been experimentally validated. Notch is able to promote PI3K signalling through HES1-mediated inhibition of PTEN, upregulation of the PI3K stimulating IL-7 receptor (encoded by *Il7r*) and insulin-like growth factor 1 receptor (encoded by *Igf1r*), and through activation of mTOR (Gladys W Wong et al., 2012)

Other groups have shown that mTOR is able to regulate Notch signalling. In one study, dual inhibition of PI3K and mTOR in GSI-sensitive T-ALL cell lines resulted in feedback activation of the Notch-c-Myc pathway (Shepherd et al., 2012). c-Myc has been shown to repress PTEN through the upregulation of microRNA miR-19, and activation of c-Myc resulted in resistance to the cytotoxic effects of PI3K/mTOR signalling (Song et al., 2012). This resistance can be overcome by using Notch or c-Myc inhibitors in tandem with PI3K/mTOR inhibitors.

1.4: T-ALL TREATMENT

1.4.1: OVERVIEW OF CURRENT THERAPY FOR T-ALL

T-ALL is an aggressive hematological malignancy, and treatment of childhood ALL typically lasts for 2 to 3 years. Pediatric T-ALL patients are treated similarly to high-risk precursor-B-ALL pediatric patients (Vrooman & Silverman, 2009), and treatment protocols in Canada and the United States are typically guided by the Children's Oncology Group (COG). The COG is a National Cancer Institute supported collaborative clinical trials research group, which has transformed the treatment of pediatric cancers and vastly improved patient outcomes. In the 1960s, the 5-year survival rate for ALL was less than 10% but in part through the efforts of the COG, this rate has steadily improved. In 2005, the five-year survival rates for ALL patients had reached 90% (Hunger et al., 2012). Most hospitals that treat childhood cancers in Canada and the United States are affiliated with the COG, and there are over 200 member institutions worldwide overseeing clinical trials and translational research.

Initial treatment for T-ALL is called induction therapy, which includes a four to six course of aggressive chemotherapeutic agents including steroids and anthracyclines. This intensive therapy regimen aims to target 99.9% of ALL blast cells and induce complete remission (CR). If this is achieved, induction therapy is followed by consolidation or intensification therapy, and finally maintenance or continuation therapy. Event free survival (EFS) and overall survival for pediatric T-ALL has improved over the past decades through the use of intensified combination therapy and targeted therapies.

Historically, T-ALL has been associated with worse outcomes when compared to non-T lineage ALL. With the introduction of intensive, high-dose, multi-agent

chemotherapy, the EFS for children with T-ALL has gone from 15-20% to around 85% with the most intensive multi-drug regimes, which approximates the EFS rates of precursor-B-ALL (Amylon et al., 1999; Gaynon et al., 1988; Pullen et al., 1999; Steinherz et al., 1986). However, despite these dramatic improvements, relapses in the central nervous system (the CNS, consisting of the brain and the spinal cord) and BM continue to be a common cause of treatment failure. Additional intensification of chemotherapy appears to provide little additional benefit, and unfortunately leads to acute and chronic life-threatening toxicities, including hyperglycemia, low resistance to infection, fatigue, nausea, infertility, secondary malignancies, changes in normal growth and cardiotoxicity (discussed in detail in **1.6: Treatment related cardiotoxicity**) (Barrett et al., 1994; Cancer Research UK, 2013).

1.4.2: INDUCTION THERAPY

The aim of induction chemotherapy for pediatric T-ALL is to achieve remission through the administration of high doses of multiple chemotherapeutic agents, typically over four to six weeks. Complete remission (CR) has traditionally been defined by the COG as less than 5% of blasts in the BM (1 in 20 cells, as determined via light microscopy) with no extramedullary disease by approximately day 40 from initiation of treatment (Asselin et al., 2011). However, as the detection of minimal residual disease (MRD) becomes increasingly more sophisticated, this definition is changing. Polymerase chain reaction (PCR)-based and flow cytometric techniques permit the detection of as few as one leukemic blast per every 10,000 cells (National Cancer Institute, 2014).

Typically, during induction therapy children with T-ALL will receive L-asparaginase or pegylated-asparaginase, vincristine, a steroid (such as dexamethasone or

prednisone) and an anthracycline (such as doxorubicin or daunorubicin). Intrathecal (IT) chemotherapy is given through a lumbar puncture to administer chemotherapy to the cerebral spinal fluid (CSF) to treat or prevent leukemia infiltration into the CNS. IT chemotherapy is normally given when the diagnostic lumbar puncture is performed, prior to commencement of induction therapy, due to the high risk of CNS infiltration at diagnosis associated with T-ALL. IT chemotherapy initially consists of cytarabine, but some protocols will include methotrexate with a steroid. Patients may also require radiation therapy to the brain and spinal cord and treatment with high-doses of intravenous (IV) chemotherapy such as methotrexate or cytarabine to help treat leukemia cells that have spread to the CNS. CNS-directed therapy is especially important for patients with T-ALL as they are at a higher risk of having primary disease in the CNS, and of relapsing in the CNS then patients with the precursor-B-ALL. Male patients with testicular involvement may receive additional therapy including testicular radiation if they fail to respond to induction chemotherapy. Upon achieving a CR, blood counts can begin to recover to normal levels, and patients proceed to consolidation therapy.

In a retrospective analysis of 125 patients with T-ALL treated between 1981 and 1995 on Dana-Farber protocols, 88% of patients achieved CR after induction therapy. Of the patients with persistent disease after one month of induction therapy, only one survived (Goldberg et al., 2003). Patients with induction failure have a poor prognosis, and are candidates for more intensive therapy, provided in the hopes of achieving remission, which can then be consolidated with an allogeneic stem cell transplantation (Pui et al., 2010; Silverman et al., 2010; Vrooman & Silverman, 2009). For patients that do respond to induction therapy, their rate of response and minimal residual disease

(MRD) levels are important prognostic markers (discussed in detail in **1.5 Risk stratification for T-ALL**).

Furthermore, from the Dana-Farber retrospective study, it is apparent that T-ALL patients are more likely (4.5 times more likely) to have toxicity-related induction deaths that patients with precursor-B ALL (Goldberg et al., 2003). In this study, T-ALL patients were more likely to die from infection or complications of severe infection following induction. This highlights the need for more effective therapies for T-ALL patients, especially for those patients at a high risk of induction failure.

1.4.3: CONSOLIDATION THERAPY

Once CR has been achieved, patients proceed to consolidation therapy, also called intensification therapy, which lasts approximately 1 to 2 months and uses many of the same drugs used during the induction phase of chemotherapy. Introduced by the Berlin-Frankfurt-Münster (BFM) clinical trials group, the COG uses the *BFM* therapeutic regime to treat patients during this phase (Möricke et al., 2010). Consolidation is divided into several phases. The first consolidation phase includes cyclophosphamide, low-dose cytarabine and a thiopurine. The second (interim) consolidation phase includes intermediate or high-dose methotrexate with the adjuvant leucovorin (folinic acid), or escalating methotrexate without leucovorin. This phase is followed by a third phase, which includes the same drugs used during induction, and the first phase of consolidation. The final and fourth phase of the *BFM* regime consists of mercaptopurine, low-dose methotrexate, and a steroid.

For high-risk ALL patients (including patients with the T-cell immunophenotype), additional agents are added to intensify the *BFM* regime, such as vincristine and L-

asparaginase. CNS treatment may continue during this period of treatment if this is required, which is typical for patients with T-ALL.

1.4.4: MAINTENANCE THERAPY

Maintenance therapy is administered until patients have achieved 2 to 3 years of continuous CR, and CNS treatment may continue depending on the particular patient and their risk assessment. Maintenance therapy consists of daily oral mercaptopurine and weekly methotrexate treatments. However, non-compliance is a serious obstacle to preventing disease relapse during this phase (Vaitkevičienė et al., 2011). Furthermore, patients must be carefully monitored for toxicity during this extended phase of treatment. Some treatment protocols may also include short courses of vincristine and corticosteroids, which may offer an event free survival advantage (Bleyer et al., 1991; Eden, Pieters, & Richards, 2010).

1.5: RISK STRATIFICATION FOR T-ALL

1.5.1: CURRENT PROGNOSTIC MARKERS FOR T-ALL

The efficient identification of children who are unlikely to respond to induction therapy or are likely to relapse (high-risk patients), from those that are likely to quickly achieve complete remission (low-risk patients), would allow physicians to stratify treatment based on the patient's risk status. Risk-directed therapy would allow high-risk patients to receive the most intensive chemotherapy, but eliminate unnecessary toxicity for low-risk patients. Until recently, good predictive clinical or laboratory based indicators were unavailable to inform risk and therapy stratification. However, there are now emerging clinical features and biomarkers that can inform physicians on the prognoses of their patients. Clinical features with prognostic significance for childhood ALL include presenting age, leukocyte count at diagnosis, initial response to treatment, immunophenotype, chromosomal abnormalities, and MRD (M. Smith et al., 1996). These features are currently used to stratify therapy but it has been suggested by Vrooman and Silverman that the lack of improvement in survival rates over the past decade may indicate that these risk factors are insufficient to accurately identify all high-risk patients (Vrooman & Silverman, 2009).

1.5.2: T-ALL IS A GENETICALLY HETEROGENEOUS DISEASE

T-ALL was initially considered a homogenous disease, however, through molecular profiling it has become clear that T-ALL has a high degree of genetic and molecular heterogeneity (Gorello et al., 2010). The genetic heterogeneity of T-ALL helps to explain differences in therapeutic response (La Starza et al., 2013; Vrooman & Silverman, 2009).

The further identification of T-ALL subgroups through molecular, cytogenetic, and gene expression profiling will provide insight into more prognostically relevant factors for T-ALL. Ultimately, a better understanding of T-ALL can be used to stratify therapeutic regimes for patients, making sure that patients presenting with aggressive 'high-risk' disease are given aggressive treatment appropriate to their specific cytogenetic and molecular features (Vrooman & Silverman, 2009). See sections **1.3.2.3 Activating *NOTCH1* mutations in T-ALL**, **1.3.3.3 Loss of PTEN is a mechanism of resistance to Notch-inhibition** and **1.5.4 Molecular-cytogenetic subgroups as emerging prognostic indicators for T-ALL.**

1.5.3: MINIMAL RESIDUAL DISEASE AS A PROGNOSTIC MARKER FOR T-ALL

Minimal residual disease (MRD) following induction therapy has emerged as a relevant prognostic indicator, and is a measure of the patient's response to therapy. Traditionally, the Children's Oncology Group (COG) has set a cutoff at 5% of lymphoblasts in BM as indicative of whether a patient has achieved CR. For instance, on treatment day 29, MRD levels above 1% have been correlated with a very high risk of relapse (Krampera et al., 2003; Willemse et al., 2002).

Indeed, to date MRD is the most informative independent predictor of relapse in childhood T-ALL (La Starza et al., 2013). In the AEIOP-BFM ALL 200 trial, MRD status at 12 weeks post treatment was the most predictive factor of relapse for patients. Patients with MRD at the end of induction therapy but with no MRD at 12 weeks post treatment performed as well as patients who achieved complete remission at the end of

induction therapy (i.e. end-induction MRD levels were irrelevant if there was no residual disease at 12 weeks (Schrappe et al., 2011).

However, while MRD is currently the most informative predictor of relapse, there still is significant variation in patient outcomes when MRD is the only prognostic marker taken into account. Linking MRD with genomic lesions has been proposed as a method to better assess patient risk and stratify treatment in pediatric T-ALL (La Starza et al., 2013).

1.5.4: MOLECULAR-CYTOGENETIC SUBGROUPS AS EMERGING PROGNOSTIC INDICATORS FOR T-ALL

Cytogenetic subgroups of T-ALL patients have different responses to specific therapies, and therefore the cytogenetic signature of a patient's leukemia is an important prognostic biomarker (La Starza et al., 2013). About half of pediatric T-ALL patients present with recurrent chromosomal translocations, observable via conventional cytogenetics (Beverloo, Langerak, Poulsen, Kamps, & Noesel, 2006). Type "A" genetic lesions are mutually exclusive genomic rearrangements that are drivers in leukemogenesis. Type "B" genetic lesions cooperate with Type A lesions and are represented by genomic imbalances, chromosomal translocations and gene mutations.

Most commonly (in 35% of cases) translocations in T-ALL result in transcription factor genes driven by strong promoters being placed next to the T-cell receptor (TCR) genes TCRB (7q34) or TCRA-D (14q11) (Hagemeijer & Graux, 2010). T-ALL oncogenic transcription factors include basic helix-loop-helix (bHLH) genes such as T-cell acute lymphocytic leukemia 1 and 2 (*TAL1* and *TAL2*), basic domain helix-loop-helix protein class B (*BHLHB1*) and lymphoblastic leukemia derived sequence 1 (*LYL1*);

cytsteine-rich domain (LIM-only domain or LMO) containing genes such as *LMO1* and *LMO2;* homeodomain genes such as T-cell leukemia homeobox 1 and 3 (*TLX1/HOX11* and *TLX3/HOX11L2*), NK2 homeobox 1 and 5 (*NKX2-1* and *NKX2-5*), and human hox genes on chromosome 7 (*HOXA*); *MYC*; and myeloblastosis viral oncogene homolog (*MYB*). Other key T-ALL cytogenetic abnormalities also include rearrangements of genes encoding epigenic modifiers such as the lysine methyltransferase mixed lineage leukemia gene (*MLL*) and the formation of specific fusion gene products with kinases that drive oncogenic signalling, for instance *NUP214-ABL1* (discussed in detail below in **1.5.5: *NUP214-ABL1* Chromosomal Fusion**) (Paganin & Ferrando, 2011).

Chromosomal rearrangements are frequently correlated with the expression of specific immunophenotypic markers. The immunophenotype of a T-cell refers to the specific cell surface receptors expressed, and these change during T-cell development in the thymus. Therefore, the immunophenotype of a T-ALL would reflect the distinct stage of arrest due to oncogenic transformation during T-cell development. Early immature T-ALLs are double-negative thymocytes; early cortical T-ALLs are associated with activation of the homeodomain genes *TLX1*, *TLX3*, *NKX2.1*, and *NKX2.2* resulting in CD1a, CD4, and CD8 positive T-ALLs; late-cortical thymocytes are associated with the rearrangement of the *TAL1* gene, which encodes the bHLH transcription factor T-ALL protein 1, leading to the proliferation of T-cells bearing mature CD3 cell surface markers and α/β T-cell receptors (Beverloo et al., 2006; Vlierberghe & Ferrando, 2012).

1.5.5: *NUP214-ABL1* CHROMOSOMAL FUSION

ABL1 gene rearrangements occur in 8% of T-ALL patients, most commonly manifesting as the complex *NUP214-ABL1* fusion, reported to occur in 4-6% of T-ALL

patients (Hagemeijer & Graux, 2010; Vlierberghe & Ferrando, 2012). The *BCR-ABL1* and *ETV6-ABL1* rearrangements are rare in T-ALL, but common in other leukemias such as chronic myeloid leukemia (CML) or B-precursor ALL. The V-abl Abelson murine leukemia viral oncogene homolog 1 protein is encoded by the proto-oncogene *ABL1*, and the Nuclear pore complex protein Nup214 is a protein encoded by the *NUP214* gene, both located on chromosome 9q34. The gene fusion occurs on episomes and is not detectable by conventional cytogenetics (Hagemeijer & Graux, 2010).

The *NUP214-ABL1* fusion gene was first reported in 2004 by Graux and colleagues, after fluorescent *in situ* hybridization (FISH) was performed on T-lymphoblasts using an *ABL1* probe (Graux et al., 2004; Hagemeijer & Graux, 2010). The *NUP214-ABL1* rearrangement is almost always found in the context of overexpression of homeodomain genes *TLX1* and *TLX3*, due to rearrangement of these genes and juxtaposition with a strong T-cell receptor promoter. This suggest that there is a functional activation between ABL1 signalling and TLX1 and TLX3 expression, though this has not yet been described (Vlierberghe & Ferrando, 2012). *NUP214-ABL1* fusion gene is located on episomes in the majority of patients, but it also may be present in homogenously staining regions (HSRs) on chromosome 2q, 6q, 9q, and 10q in some patients. Patients positive for *NUP214-ABL1* HSR have poorer outcome and tend to relapse (Hagemeijer & Graux, 2010).

The *NUP214-ABL1* fusion gene encodes a constitutively active tyrosine kinase, similar to the gene product of *BCR-ABL1*, commonly found in chronic myelogenous leukemia. The presence of the *NUP214-ABL1* fusion gene is prognostically relevant, as these patients respond well to small-molecule tyrosine kinase inhibitors, such as imatinib,

and *NUP214-ABL1*-positive T-ALL cell lines show better response *in vitro* to the second generation inhibitors nilotinib and dasatinib (Vrooman & Silverman, 2009). Due to the clinical importance of this cytogenic change, proper detection and diagnosis is critical.

1.6: TREATMENT RELATED TOXICITIES

1.6.1: TREATMENT RELATED CARDIOTOXICITY

Many chemotherapeutic agents used to treat pediatric cancer are associated with adverse off-target effects, which negatively impact on patient outcome, quality of life and overall survival. Treatment related complications may be acute, or may become clinically evident decades after treatment initiation. Data from the Childhood Cancer Survivor study suggests that 30 years after receiving chemotherapy, approximately three-quarters of all pediatric cancer survivors have at least one chronic physical health condition, and just under one-half will have a severe or life-threatening condition, or die from a chronic condition (Deffinger et al., 2006). In particular, several therapies used to treat T-ALL cause severe cardiotoxicity. For example, anthracyclines (e.g. doxorubicin), alkylating agents (e.g. cyclophosphamide), and even targeted agents like small tyrosine kinase inhibitors (e.g. dasatinib and imatinib) cause cardiotoxicity in a proportion of patients (Yeh et al., 2004). In the next section, anthracyclines will be discussed in more detail, as well as the current treatments for mitigating therapy-related toxicity from this class of chemotherapeutics.

1.6.2: ANTHRACYCLINES

Anthracyclines are a highly effective and widely used class of chemotherapy given during the induction and consolidation phase T-ALL treatment. Anthracyclines approved for the treatment of T-ALL include doxorubicin (Adriamycin) and danorubicin (Cerubidine) (Salzer et al., 2010). Doxorubicin is a commonly used antineoplastic agent employed to treat a range of solid and hematological malignancies, but in the pediatric context of intensified treatment for T-ALL, the cardiotoxic effects of anthracyclines are

particularly devastating (Lipshultz et al., 2010; Lipshultz, Cochran, Franco, & Miller, 2013).

Doxorubicin (and related anthracyclines) exerts its anticancer effects through the inhibition of the topoisomerase-II enzyme, induction of DNA damage (particularly in actively dividing cells), and inhibition of DNA repair (Monsuez, Charniot, Vignat, & Artigou, 2010). Doxorubicin penetrates cells and enters the nucleus via proteasomal-mediated transport. Due to its planar multi-ringed structure, doxorubicin intercalates DNA and interferes with transcription and cell replication. Doxorubicin causes an iron-mediated generation of reactive oxygen species (ROS), leading to additional DNA damage, which is inefficiently repaired due to the inhibition of topoisomerase-II (top-II), leading to activation of p53 and the pro-apoptotic BAX, and ultimately apoptosis of cells (Van Dyke, 2007). However, the utility of anthracyclines is diminished by a lifetime cumulative dose-dependent cardiotoxicity. Even when used at "safe" doses, there is a risk of severe heart failure (Monsuez et al., 2010). At lifetime dosages above 300mg/m^2 the risk of heart failure increases exponentially (Suter & Ewer, 2013), and thus the maximum lifetime dose is 400 to 550 mg/m^2 (Wouters, Kremer, Miller, Herman, & Lipshultz, 2005). It is believed that the chemotherapeutic and cardiotoxic mechanisms of anthacyclines are separate and distinct. With this in mind, it is possible that anthacyclines could be combined with a cardioprotectant agent that permits therapeutic efficacy but prevents cardiotoxicity (Liu et al., 2014).

1.6.3: ANTHRACYCLINE-INDUCED CARDIOMYOPATHY

Doxorubicin is well documented to cause dose-dependent cardiotoxicity in a proportion of patients. At the maximum lifetime dose (550 mg/m^2) one quarter of all

patients develop cardiotoxicity (S. Zhang et al., 2012). Acute cardiotoxicity, which occurs during treatment, is observed in less than 1% of patients and presents as an acute decline in myocardial contractility. Acute cardiotoxicity can be reversible, but may also be permanent and life-threatening (Wouters et al., 2005). Early/late-onset chronic progressive cardiotoxicity occurs in 1.6 to 5% of patients, manifests as dilated cardiomyopathy, and can occur as long as 20 years after therapy has been concluded (Deffinger et al., 2006; Lipshultz, Alvarez, & Scully, 2008; Wouters et al., 2005). Doxorubicin-induced cardiomyopathy is caused by cardiomyocyte apoptosis, leading to a spectrum of cardiovascular complications such as decreased contractility, arrhythmias, left ventricular dysfunction, and heart failure. Risk factors for cardiomyopathy include cumulative dose, history of irradiation, use of other agents with cardiotoxic effects (such as cyclophosphamide which may be a part of T-ALL treatment protocols), pre-existing cardiac conditions, female gender, and the age of patient at time of treatment (both young and old patients have a higher chance of developing cardiomyopathy) (Ichikawa et al., 2014; Monsuez et al., 2010; Yeh et al., 2004). Correlative gene expression studies have demonstrated that single nucleotide polymorphisms in carbonyl reductase genes are predictive of cardiotoxicity in response to anthracycline treatment. These studies suggest that patients may be identified who should receive lower dose anthracyclines in conjunction with cardioprotective agents (Blanco et al., 2012).

The exact mechanism for doxorubicin-induced cardiomyopathy is controversial, but the prevailing theory is referred to as the "ROS and iron hypothesis" (Berthiaume & Wallace, 2007; Myers, 1998). Doxorubicin is hypothesized to cause an iron-mediated increase in ROS through futile redox cycling, or by interacting with iron directly causing

iron to cycle between Fe(II) and Fe(III) which again increases cellular ROS levels. Both mechanisms lead to cellular damage (Keizer, Pinedo, Schuurhuis, & Joenje, 1990; X. Xu, Persson, & Richardson, 2005).

This hypothesis is supported by several lines of evidence. In a murine model of human hereditary hemochromatosis with a deficiency in human hemochromatosis protein (Hfe, leading to increased iron absorption and cellular iron concentrations) mice have a greater sensitivity to doxorubicin cardiac-damage (Miranda et al., 2003). Furthermore, iron accumulation in a rat model of dietary carbonyl iron loading also demonstrates increased doxorubicin-induced damage (Panjrath et al., 2007).

Dexrazoxane (Zinecard) is the only currently Food and Drug Administration (FDA)-approved drug for the prevention of doxorubicin-induced cardiotoxicity (Hasinoff & Herman, 2007; Swain & Vici, 2004). Dexrazoxane is an Ethylenediaminetetraacetic acid (EDTA)-derived iron chelator, which further strengthens the "ROS and iron hypothesis" of doxorubicin cardiomyopathy. However, a more potent iron chelator, deferoxamine (DFO), a drug used to treat thalassemia (Neufeld, 2010), has failed to protect against doxorubicin-induced cardiac damage in animal models and in clinical trials (Elihu, Anandasbapathy, & Frishman, 1998). To resolve this discrepancy, Ichikawa and colleagues have recently demonstrated that doxorubicin-induced cardiotoxicity is mediated specifically through mitochondrial iron accumulation, rather than through total cellular iron accumulation (Ichikawa et al., 2014). Furthermore, a reversal of mitochondrial iron accumulation was demonstrated to ameliorate doxorubicin-induced cardiac damage, specifically through the overexpression of the ATP-binding cassette (ABC) protein-B8 (ABCB8) (Ichikawa et al., 2014).

ABCB8 is a mitochondrial inner membrane protein involved in the export of iron from the mitochondria (Ichikawa et al., 2012). Cardiac ABCB8 deletion in a murine model resulted in mitochondrial iron accumulation and iron-dependent cardiomyopathy. In wild-type mice, treatment with doxorubicin significantly reduced the transcription and translation of ABCB8 in the mitochondria, but did not alter the mRNA or protein levels of mitoferrin-2 (Mfrn-2, a mitochondrial iron import protein). Treatment with doxorubicin resulted in the preferential accumulation of iron in cardiomyocyte mitochondria, suggesting that the decrease in ABCB8 is responsible for the accumulation of iron in the mitochondria. Furthermore, it has been demonstrated that the doxorubicin-induced decrease in ABCB8 and mitochondrial iron is independent from the cytotoxic effects of doxorubicin (Ichikawa et al., 2014).

Indeed, when Ichikawa and colleagues overexpressed ABCB8, there was a decrease in mitochondrial iron levels in their murine model, but mitochondrial concentrations of doxorubicin were unaltered. Dexrazoxane is able to selectively reduce mitochondrial iron levels, with no accompanying change in the nuclear and cytosolic iron concentrations, contributing to its protective effects against doxorubicin cardiomyopathy. In contrast, DFO chelated nuclear and cytosolic iron, but was unable to lower mitochondrial iron concentrations (Ichikawa et al., 2014). Therefore, dexrazoxane is hypothesized to protect against doxorubicin-induced cardiotoxicity through a selective chelation of mitochondrial iron.

Additionally, it is hypothesized that dexrazoxane may protect cardiac cells through an inhibition of top-IIβ (S. Zhang et al., 2012). Zhang and colleagues demonstrated that top-IIβ (a known target of doxorubicin) induces cardiac damage

through activation of DNA damage and by triggering cardiomyocyte apoptosis. In their study, deletion of top-IIβ was sufficient to protect against doxorubicin-induced heart failure. Interestingly, the regulation of doxorubicin toxicity through mitochondrial iron concentrations proposed by Ichikawa is independent of the Top-2β pathway (Ichikawa et al., 2014). A link between mitochondrial iron regulation and topoisomerases is highly probable, though not yet established, as both doxorubicin and dexrazoxane are known to affect both iron homeostasis and the activity of top-IIα and top-IIβ (Rao, 2013). Regardless of the mechanism, the iron chelator dexrazoxane has shown promise as a cardioprotectant agent, particularly in the treatment of pediatric ALL (Lipshultz et al., 2010).

1.6.4: DEXRAZOXANE

While dexrazoxane currently is the only FDA-approved drug administered to protect against doxorubicin-induced cardiac damage, its use is limited due to several concerns. Dexrazoxane inhibits top-IIα, which may reduce doxorubicin's capacity to efficiently kill malignant cells (Swain et al., 1997). Dexrazoxane use has also been associated with the development of hematological abnormalities such as acute myeloid leukemia (AML) and myelodysplastic syndrome (Salzer et al., 2010; Tebbi et al., 2007). These concerns have led to an effective end to the use of dexrazoxane in Europe for patients with malignancies other than breast cancer, on the recommendation of the European Medicines Agency (Medicines and Healthcare products Regulatory Agency (MHRA), www.mhra.gov.uk, 2011). Specifically, the Medicines and Healthcare products Regulatory Agency has strongly contraindicated the use of dexrazoxane with doxorubicin for use in children and adolescents up to 18 years. While the FDA is not banned the use

of dexrazoxane, new approaches to protect against the cardiac side effects of doxorubicin are needed, as well as better ways to efficiently screen and evaluate new drug candidates.

1.7 NOVEL THERAPIES BASED ON KNOWN GENETIC PATHWAYS IN T-ALL

As the additional intensification of standard chemotherapy agents is associated with unacceptable toxicity, there is a need for more targeted molecular agents for the treatment of T-ALL. Numerous PI3K/AKT/mTOR inhibitors are currently being tested preclinically *in vitro* and *in vivo*, and several have entered into clinical trials for T-ALL. Below is a summary of the current state of targeted therapy development for T-ALL.

1.7.1: NOTCH AS A DRUG TARGET IN T-ALL

The high frequency of *NOTCH1* mutations in T-ALL has made Notch signalling a target of drug development. Small molecule inhibitors of the γ-secretase complex (γ-secretase inhibitors; GSIs) were initially designed to block the processing of amyloid precursor proteins to treat Alzheimer's disease (Olson & Albright, 2008). GSIs prevent the cleavage of the TM domain of Notch and therefore block the release of the NICD from the plasma membrane. Due to the dependence of Notch1 activation on cleavage by the γ-secretase complex, inhibition of this complex was considered an "Achilles' heel" of aberrant Notch signalling in T-ALL, and GSIs entered into clinical trials for the treatment of T-ALL. While GSIs appeared to hold great therapeutic promise, they ultimately failed to produce any objective clinical response in the Dana-Farber Cancer Institute 04-390 phase I clinical trial of MK-0752 (an oral GSI developed by Merck) (Olson & Albright, 2008). Patients on this trial experienced dose limiting gastrointestinal toxicity, fatigue and did not clinically respond to the GSI treatment (DeAngelo et al., 2006; Tosello & Ferrando, 2013). The toxicities demonstrated in this trial can be attributed to the fact that GSIs not only target Notch signalling in neoplastic tissue, but also target Notch signalling

in normal tissue, leading to fatigue and severe gastrointestinal toxicity, owing in part to the loss of intestinal crypt progenitor cells (Riccio et al., 2008; Sanda et al., 2010).

However, anti-Notch therapies are beginning to show promise for T-ALL, when used in combination with other chemotherapy agents and targeted small molecule inhibitors. For instance, combining GSIs with small molecule inhibitors of the PI3K-AKT-mTOR signalling axis (Chan, Weng, Tibshirani, Aster, & Utz, 2007b; Cullion et al., 2009; Palomero et al., 2007) or with glucocorticoids (Real et al., 2009) has demonstrated a synergistic anti-leukemic effect. Furthermore, intermittent treatment with GSIs and parenteral formulations, as well as co-administration with glucocorticoids has protected against gastrointestinal toxicity (Real et al., 2009). Careful monitoring of patients is imperative to minimize adverse GI effects as additional anti-Notch therapeutics make their way into clinical trials.

1.7.2: PI3K INHIBITORS

The role of the PI3K pathway in numerous cell processes both in normal and diseased states, raises concerns regarding possible side effects of pan-PI3K activity inhibitors, especially because of the importance of PI3K in glucose metabolism and insulin sensitivity (Cho et al., 2001). Not only could PI3K inhibition cause diabetes, but also deregulated PI3K signalling has been associated with schizophrenia and Parkinson disease (Emamian, Hall, Birnbaum, Karayiorgou, & Gogos, 2004). Short-term inhibition of PI3K signalling may be an appropriate therapeutic strategy, but long-term inhibition could have permanent and devastating side effects (Cully et al., 2006).

Isoform-specific inhibitors of PI3K could potentially mitigate the risks of pan-PI3K inhibitors, and minimize toxicities to normal tissue. Recently, a small molecule

inhibitor of the p110γ and p110δ catalytic subunits of PI3K, CAL-130, was shown to block tumour formation and proliferation in a PTEN-null mouse model. This inhibitor did not significantly perturb plasma insulin and glucose concentrations in the mouse model. This provides evidence that specific isoforms of PI3K are critical for T-ALL disease progression, but not for normal homeostasis (Hirsch & Chiarle, 2012; Subramaniam et al., 2012). Several clinical trials (in phases I, II, and III) are currently investigating the efficacy of isoform specific PI3K inhibitors in both solid and liquid malignancies (Weigelt & Downward, 2012).

Alternatively, the PI3K pathway could be inhibited through the use of small molecule HES1 modulators. A recent paper has identified a small molecule inhibitor that down-regulated HES1, providing an antitumourigenic effect in a colorectal cancer cell line (Sail & Hadden, 2013). This may be a potential therapeutic strategy for T-ALL, where HES1 is commonly upregulated through aberrant Notch signalling, leading to decreased PTEN activity, and constitutive activation of the PI3K pathway.

1.7.3: AKT INHIBITORS

Both ATP-competitive and allosteric AKT inhibitors are currently under development and in phase I and phase II clinical trials for leukemias (Weigelt & Downward, 2012). AKT has a wide range of functions in normal tissues; therefore complete inhibition of AKT is not a feasible strategy. However, because T-ALL cells often have hyperactivated AKT, a restoration of normal levels of AKT signalling could be beneficial.

1.7.4 mTOR INHIBITORS

The AKT, TSC2 and mTOR signalling pathways play an important role in both PI3K and Ras mediated cancer, as previously discussed. AKT and TSC2 both converge on mTOR and depend on downstream effectors, such as S6K and 4E-BP1 to promote tumourigenesis. Interestingly, very few activating mutations have been found in the genes encoding S6K and 4E-BP1, suggesting that novel inhibitors against these targets could be successful in resistant and late stage disease. Recently, two activating mutations in mTOR have been discovered, but the frequency of these mutations is relatively low when compared to other tumour suppressors and oncogenic proteins implicated in T-ALL. Additionally, these activating mutations did not confer drug resistance to the classical mTORC1 inhibitor rapamycin (Cully et al., 2006; Sato, Nakashima, Guo, Coffman, & Tamanoi, 2010).

While most mTOR inhibitors are rapamycin analogues, and act as allosteric mTORC1 inhibitors, new dual mTORC1/mTORC2 inhibitors are emerging and entering into clinical trials (Weigelt & Downward, 2012). Recently, a dual mTORC1/mTORC2 inhibitor, OSI-027, was tested pre-clinically in ALL patient samples and in a mouse xenograft model of ALL. OSI-027 produced a more robust anti-proliferative and pro-apoptotic effect than rapamycin. This is the first study of its kind to demonstrate the anti-proliferative and pro-apoptotic activity of a dual mTORC1/mTORC2 inhibitor in primary leukemia samples, and provides a rationale for further drug development and clinical testing (Gupta et al., 2012).

1.8: ANIMAL MODELS FOR T-ALL

Due to the high rate of relapse and primary non-responsive disease, there is a demand for new therapeutic agents for T-ALL. There is a desperate need both for anti-leukemic agents and cardioprotectant agents to help minimize the devastating cardiac side effects of current therapeutics. Both cytotoxic agents such as anthracyclines (e.g. doxorubicin) and targeted agents such as tyrosine kinase inhibitors (e.g. dasatinib) are known to cause cardiotoxicity (Force, Krause, & Van Etten, 2007; Z. Xu, Cang, Yang, & Liu, 2009). These toxicities and the need for more molecularly targeted drugs for T-ALL underscore the need for better and more efficient ways to rapidly screen new small molecules for their therapeutic efficacy. Evaluation of new therapeutic strategies for T-ALL is a lengthy and costly process, which requires validation both in *in vitro* and *in vivo* models of disease before proceeding to clinical trials.

1.8.1: *IN VITRO* MODELS OF T-ALL

Established cell lines have been extensively used to study T-ALL. However, immortalized cell lines may not recapitulate the heterogeneity of a patient's leukemia, and do not help to personalize patient treatment strategies. The evaluation of targeted therapeutics and personalization of patient treatment requires a way to study patient's tumour-drug response *ex vivo*.

To this end, various strategies to culture primary patient derived lymphoblasts *ex vivo* have been developed. These strategies may involve the co-culture of patient cells in suspension, under reduced oxygen conditions, and using stromal feeders, such as BMS2 cells (BM-derived support clone 2; a murine BM stromal cell line) (Martinez Marignac, Smith, Toban, Bazile, & Aloyz, 2013) or the MS5-DL1 (murine BM stromal cells

engineered to express the Notch ligand DL1) (Armstrong et al., 2009). However, co-culture with stromal cells only sustains primary cells for a short period of time, and supports only modest cell proliferation (Yost et al., 2013). To minimize experimental variation, a new serum-free medium (WIT) (Ince et al., 2007) has been described, which permits human breast epithelial cell proliferation for over 70 population doublings. This WIT medium has been modified by Andrew Weng's group through the addition of Stem Cell Factor, interleukin-2, interleukin-7 and insulin-like growth factor-1, referred to as WIT-L (Yost et al., 2013). This medium promotes more robust cell proliferation and expansion than co-culture with MS5-DL1 stromal cells, permitting culture of primary T-lymphoblasts *in vitro* for up to 4 weeks. While *in vitro* culture of primary patient derived lymphoblasts is an important tool in studying T-ALL, it remains technically challenging and expensive.

1.8.2: MURINE MODELS OF T-ALL

Mouse xenograft models of human leukemia are currently widely employed in the characterization of leukemia, and are used to screen and evaluate novel anti-leukemic agents before clinical testing (Dick & Lapidot, 2005). Furthermore, primary T-ALL cells can be engrafted in non-obsese diabetic/severe combined immunodeficient (NOD/SCID) mice) (Chiu, Jiang, & Dick, 2010). Murine models of T-ALL, however, have substantial associated costs and the time in which to complete these studies can be extensive and not compatible with patient-directed interventions in an actionable time frame. Primary human T-ALL biopsy-derived lymphoblasts are not sustainable in culture for extended periods of time and while T-ALL cell lines have shown utility for drug screening, they are unable to inform individual patient treatment decisions. However, the zebrafish

(*Danio rerio*) has recently emerged as a powerful alternative *in vivo* system to study T-ALL with many advantages over *in vitro* cell based assays and murine models of leukemia (Konantz et al., 2012).

1.8.3: ZEBRAFISH AS A MODEL FOR T-ALL

The zebrafish is a powerful and genetically-tractable model organism used to study normal and malignant biological processes. Zebrafish are used extensively to study human malignancies, as important signalling pathways regulating cell proliferation, migration, apoptosis and differentiation are well conserved (Feitsma & Cuppen, 2008; Payne & Look, 2009). Furthermore, many of the signalling pathways important in T-ALL are highly conserved in zebrafish. Of particular significance to this project, the Notch pathway is well-conserved in zebrafish, and our research group has described the importance of Notch signalling in mast cell development (Da'as et al., 2012).

In addition to the high degree of interspecies genetic conservation between zebrafish and mammals, there are technical advantages associated with the use of zebrafish, as compared to *in vitro* models and *in vivo* murine models. For instance, zebrafish reach sexual maturity at three months of age, and externally reproduce large numbers of offspring weekly. Relatively low maintenance costs and short time intervals to complete *in vivo* studies make the zebrafish well suited to a wide range of applications. Additionally, their small size and transparency facilitates high-throughput analyses, making the zebrafish an attractive model for the screening of anti-cancer agents (Ridges et al., 2012). The *casper* double pigment mutant zebrafish line allows enhanced visualization of xenografted tumour cells and their behaviour within the zebrafish (White et al., 2008). Furthermore, zebrafish are permeable to a wide range of small molecules,

facilitating the high-throughput screening of agents able to block tumourigenesis in transgenic lines or proliferation of xenotransplanted human cancer cells (discussed in **1.8.3.1 Small chemical screens in zebrafish)**.

Additionally, zebrafish can be reverse genetically engineered to generate loss-of-function phenotypes, using a variety of techniques such as injection of mRNA to obtain gene overexpression, morpholino oligonucleotides (Nasevicius & Ekker, 2000), zinc-finger nucleases (Doyon et al., 2008), TAL-effector endonucleases (TALENs) (P. Huang et al., 2011) and the new and increasingly used CRISPR-Cas system (Hwang et al., 2013). Due to the relative ease of genetic manipulation, numerous transgenic zebrafish lines have been established that allow the generation of tumours in the fish that recapitulate the features of human tumours both histologically and genetically. As a result, zebrafish have been firmly established as an *in vivo* model for human leukemia. Indeed, the first transgenic cancer model in zebrafish to be established was a *Myc*-induced model of T-cell acute lymphoblastic leukemia (Langenau et al., 2003). In this model, zebrafish express murine c-myc under the control of the zebrafish rag2 promoter, and leukemia cells are tagged with green fluorescent protein (GFP). This model permits excellent visualization of leukemia development and disease progression, and permits screening of drugs that can supress c-myc-induced T-ALL in zebrafish (Langenau et al., 2003).

Despite the generally high conservation of molecular pathways between zebrafish and humans there still are some differences, for example the absence of the *INK4a/ARF* tumour suppressor gene in zebrafish (Sharpless, 2005). Therefore, zebrafish models of leukemia do not fully represent the biological complexity of human leukemia, and this

underscores the importance of human cell lines and primary samples for understanding the molecular pathogenesis of human leukemia and for the evaluation of novel compounds. However, there are significant technical obstacles to performing *in vitro* experiments on primary patient samples, as they are difficult to culture. Recently, zebrafish human xenograft models (termed zebrafish XT) have emerged as important models of human leukemia (discussed in **1.8.3.2 Zebrafish human leukemia xenograft model**) (Corkery et al., 2011; Konantz et al., 2012; Pruvot et al., 2011). The zebrafish human leukemia XT model pioneered by our group permits the study of human leukemia cell lines and primary patient samples in an *in vivo* model which more fully recapitulates the complexity of human disease than *in vitro* systems, but more efficiently than murine models.

1.8.3.1: Small chemical screens in zebrafish

Zebrafish embryos are well suited for large-scale chemical screens, and offer several distinct advantages over conventional drug discovery approaches. For example, by using zebrafish as a whole-organism for phenotype-based screens, the unbiased discoveries of potential therapies and pathways involved in diseases is possible. Normally, drug discovery requires the selection of a hypothetical molecular target, however, the presumed molecular target may not always be the correct target to reverse a particular disease phenotype. For example, it is known that anthracyclines cause cardiac damage in part through iron accumulation and oxidative stress (Simůnek et al., n.d.). However, after extensive *in vitro* and *in vivo* experimentation, it was found that potent iron chelators and antioxidants failed to protect against doxorubicin-cause cardiac damage in clinical settings (Ichikawa et al., 2014; Simůnek et al., n.d.). While iron

accumulation and ROS may be a molecular mechanism of cardiac damage, as drug targets they fail to provide objective benefit.

Organism phenotype-based screens allow the discovery of small molecules that provide anti-leukemic effects or cardioprotection against known chemotherapies even without knowing the desired drug target or pathway contributing to the phenotype (Peterson & Macrae, 2012; Peterson et al., 2004). Promising novel compounds can be rapidly identified from libraries of thousands of drugs, through the observation of phenotypic changes. For example, to evaluate the potency of novel cardioprotectant agents, the development of pericardial edema and decreased circulation can easily be observed in zebrafish embryos (Cheng et al., 2011; Liu et al., 2014). Combinatorial drug treatments with phenotype-inducing drugs and novel compounds can rapidly identify novel compounds with cardioprotective effects. Zebrafish-based screens permit the 'de-risking' of novel compounds before they are moved down the drug development pipeline into rodent models and human clinical trials.

1.8.3.2: Zebrafish human leukemia xenograft model

Xenotransplantation (XT) involves the transplantation of one species-specific tissue into another host species. Specifically, zebrafish XT has gained considerable attention as a system to rapidly study and directly observe tumour cell behaviour and drug response in a live animal model (Corkery et al., 2011; Jung et al., 2012; Konantz et al., 2012; Pruvot et al., 2011; M. P. Smith et al., 2013; Veinotte, Dellaire, & Berman, 2014a). Zebrafish XT was first performed in 2005, with the transplantation of human metastatic melanoma cells into zebrafish (Lee, Seftor, Bonde, Cornell, & Hendrix, 2005). Subsequent studies by Haldi *et al*, determined that incubation of XT embryos at 35^{o}C

permitted both the growth of injected human cell lines and normal zebrafish embryogenesis. Furthermore, they established the yolk sac as a suitable site for injection of human cells and 48 hours post fertilization (hpf) as an appropriate age for XT (Haldi, Ton, Seng, & McGrath, 2006). Human cells can be grown in zebrafish embryos following XT at this age without a need for immunosuppression, as the zebrafish lacks a fully functional adaptive immune system until 28 days post fertilization (Haldi et al., 2006; Lam, Chua, Gong, Lam, & Sin, 2004). This makes zebrafish XT less technically challenging than XT in immune-compromised and humanized mice. The use of the *casper* double-pigment-mutant zebrafish line (White et al., 2008), together with improvements in imaging technology posits the zebrafish as an important model to evaluate drug-tumour interactions, angiogenesis and migration of tumour cells within the zebrafish (Marques et al., 2009).

A wide range of human cancer types, such as melanoma, breast cancer, leukemia, sarcomas, and prostate cancer, have been successfully transplanted into zebrafish embryos (Konantz et al., 2012). Our group has established assays to quantify human cell proliferation and migration using zebrafish XT, allowing a rapid and quantitative read-out for drug response (Bentley et al., 2013; Corkery et al., 2011; Smithen et al., 2013).

The zebrafish XT protocol established by Corkery *et al,* and the Berman and Dellaire laboratories will be described here (**Figure 1.8.3.2**). Human cells are fluorescently labelled with CM-DiI or stably transfected with a fluorescent marker, and approximately 50 cells are delivered as a single injection into the yolk sac of 48 hpf *casper* embryos, using a pulled glass micropipette connected to a PLI-100A Pico-Liter Injector. Transparent embryos are serially imaged to qualitatively evaluate the

proliferation of fluorescently labelled human cells in the presence of vehicle or in response to small molecules. 24 hours post injection (hpi) a group of embryos was dissociated to determine the average number of leukemia cells per zebrafish, and other groups of embryos received treatment for 48 h, after which they were dissociated and the number of leukemia cells per zebrafish determined. Corkery *et al*, demonstrated that K562 and NB-4 human leukemia engrafted and proliferated in zebrafish embryos and had differential response to the targeted inhibition of *BCR-ABL1* using imatinib mesylate and *PML-RARA* using all-*trans* retinoic acid (Corkery et al., 2011). The technical achievement of this particular assay was the rapid *in silico* quantification of the number of leukemia cells per zebrafish. Corkery *et al*, developed a method to image dissociated fish and enumerate the number of fluorescent cells using Image J. This method is more quantitative than previously described zebrafish XT assays (Haldi et al., 2006; Pruvot et al., 2011), and allows for the accurate detection of changes in human cell proliferation within a short time frame.

In this project, I have expanded upon the zebrafish XT chemotherapy response assay *in vivo* pioneered by the Dellaire and Berman laboratories by extending this technique to the xenotransplantation of clinically relevant primary patient samples, and through the simultaneous evaluation of therapy-related toxicities. Primary patient sample XT promises to better recapitulate the complexity of patient tumours than zebrafish XT with established cell lines, and will be a more rapid and efficient model as compared to murine models of T-ALL.

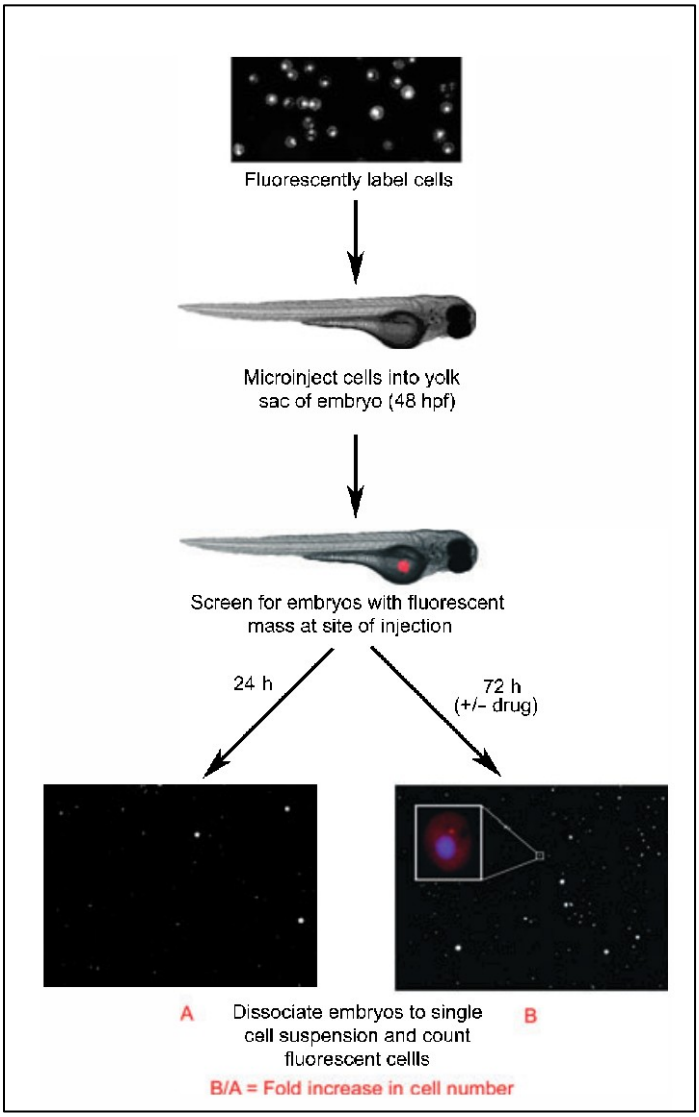

Figure 1.8.3.2: Schematic of *in vivo* human leukemia proliferation assay using zebrafish XT. Human cells are fluorescently labeled using CM-DiI, and microinjected into the yolk sac of 48 hours post fertilization (hpf) *casper* embryos. Embryos are screened for a fluorescent mass at the site of injection, and treatments begin at 24 hours post injection (hpi), and last for 48 h. A group of embryos is dissociated at 24 hpi and groups of embryos either treated with vehicle or drug are dissociated at 72 hpi (48 hours post treatment (hpi)). The average number of human leukemia cells per zebrafish is quantified by imaging fluorescent cells, and fold increase in cell number is calculated by dividing the number of cells at 72 hpi (B) by the number of cells at 24 hpi (A). Adapted with permission from (Corkery et al., 2011).

1.9: RATIONALE

T-ALL is a high risk leukemia associated with primary non-responsive, high MRD, and relapse (Vrooman & Silverman, 2009). Current treatment strategies have reached a point of diminishing returns, as additional intensification of chemotherapy strategies provides minimal therapeutic benefit but is associated with life-threatening toxicities. Taken together, this provides evidence in support of the need for new treatments for pediatric T-ALL patients. A better understanding of the molecular basis of T-ALL will inform the development of new treatments. To facilitate meaningful drug discovery, novel animal models are required to evaluate the benefit of drug candidates, as well as their toxicities, in a timely and economical way. Furthermore, methods to personalize pediatric chemotherapeutic regimes will contribute to the goal of more rapidly achieved complete and long-lasting remission.

1.10: HYPOTHESIS

I hypothesize that a zebrafish human T-ALL XT platform can be used to evaluate the anti-leukemic efficiency and cardiotoxicity of small molecule inhibitors. I also hypothesize that primary patient samples can engraft and proliferate in the zebrafish embryos, allowing patient tumour drug sensitivity to be evaluated. Furthermore, I hypothesize the zebrafish XT platform can be used to evaluate the efficacy of novel cardioprotectant compounds.

CHAPTER 2: MATERIALS AND METHODS

2.1: CELL CULTURE

All T-ALL cell lines were obtained from the Weng laboratory and were confirmed by DNA fingerprinting using the PowerPlex 1.2 system (Promega) in January 2013. T-ALL cell lines were cultured in Roswell Park Memorial Institute (RPMI) 1640 (Gibco) supplemented with 10% fetal bovine serum (FBS; Gibco) and 100 U/mL penicillin and 100 μg/mL streptomycin (Gibco). HeLa cells were cultured in Dulbecco's Modified Eagle Medium (DMEM) supplemented with 10% FBS and 100 U/mL penicillin and 100 μg/mL streptomycin. Mononuclear cells from patient bone marrow aspirate samples performed at the time of diagnosis were obtained by density gradient centrifugation with Lympholyte-H (Cedarlane) and then placed in liquid nitrogen with freezing media until use. Patient lymphocytes were cultured in MarrowMAX bone marrow medium (Gibco) for approximately 12 hours prior to xenotransplantation. Cells were cultured under humidified conditions at 37^{o}C with 5% CO_2.

2.2: CELL VIABILITY ASSAY

T-ALL cells lines were seeded in 96-well plates at a concentration of 5×10^4 viable cells per mL (viable cells counted using Trypan blue (Invitrogen) dye exclusion and a haemocytometer), and cultured in the presence of increasing concentrations of compound E, a γ-secretase inhibitor; triciribine, an AKT inhibitor; and rapamycin, an mTORC complex 1 inhibitor. Cell viability was calculated as a percentage of vehicle (0.01% DMSO) control after 72 hours post-treatment (hpt), using an alamarBlue cell

viability assay (Invitrogen). The alamarBlue assay is designed to quantify the metabolic activity of cells, and can establish the relative viability and cytotoxic effect of drugs on cells. The active component of alamarBlue (resazurin) is a cell permeable compound that is blue and nonfluorescent, but is metabolically converted to resorufin by viable cells, a pink and highly fluorescent compound. Conversion of resazurin to resorufin is quantified using a plate reader (Tecan Infinite M200) set to 560 nm excitation and 590 nm emission (Al-Nasiry, Geusens, Hanssens, Luyten, & Pijnenborg, 2007; Hamalainen-Laanaya & Orloff, 2012).

2.3: DRUGS

Stock solutions of drugs were dissolved in DMSO, except for cAMP which was dissolved in sterile ddH2O: Triciribine (Sigma-Aldrich), rapamycin (Sigma-Aldrich) Compound E (EMD Millipore), doxorubicin (Sigma-Aldrich), visnagin (Sigma-Aldrich), diphenylurea (Sigma-Aldrich), dasatinib (Cayman Chemical company) were dissolved, aliquoted and maintained at -20^{o}C. Drugs were kept protected from light, and freeze-thaw was avoided.

2.4: GENERATION OF CONSTRUCTS AND LUCIFERASE ASSAY

pMig-Notch1, pMig-Notch1ΔPEST and JH23a luciferase reporter plasmid were available in the Weng laboratory. Site-directed mutagenesis was performed by overlap extension PCR (Higuchi, Krummel, & Saiki, 1988). Base substitutions within the Notch1 coding sequence were performed in pMig-Notch1 to create pMig-Notch1-A1696D (GCC to GAC). Plasmids were introduced into HeLa cells with Neon transfection system (Life

Technologies). To assay activation of JH23a-dependent transcription, cells were co-transfected with Notch1 expression constructs, a JH23a firefly luciferase reporter plasmid, and an internal control sea pansy *Renilla* luciferase plasmid (Promega). Normalized firefly luciferase activities were measured in whole-cell extracts prepared 48 h after transfection with the Promega dual luciferase kit. Luciferase was measured using a GloMax 20/20 luminometer (Promega).

2.5: SEQUENCING OF PATIENT EXOMES

Selected regions were amplified from genomic DNA by PCR. Amplified fragments were purified from an agarose gel, and sequenced using Sanger fluorescent sequencing and capillary electrophoresis. Sequencing was performed at the DNA Diagnostic Laboratory at the IWK Health Centre in Halifax, Nova Scotia, Canada. Sequence traces were analyzed using MutationSurveyor V.3.97 (Soft Genetics, Inc.).

2.6: ZEBRAFISH HUSBANDRY, EMBRYO COLLECTION & EMBRYO STAGING

Zebrafish were maintained according to standard protocol (Westerfield, 1995). Double pigment mutant translucent *Casper* (White et al., 2008) (provided by the Zon Laboratory, Children's Hospital, Boston, MA) embryos were employed to permit real-time analysis of tumour cancer cell microenvironment interactions without any auto-fluorescence that might interfere with image quality. Embryos were dechorionated using 10 mg/mL stock solution of Pronase (Roche Applied Science). During the xenotransplantion experiments embryos were housed in a 35°C incubator to permit the

normal growth and development of the zebrafish embryos and the growth of cancer cell lines. Embryos were collected and grown in E3 embryo media (5 mM NaCl, 0.17 mM KCl, 0.4 mM $CaCl_2$, and 0.16 mM $MgSO_4$, pH 7.5, supplemented with 1 x 10-5% Methylene Blue [v/v]) at 28.5^{o}C. Embryos were developmentally staged according to standard protocol (Kimmel, Ballard, Kimmel, Ullmann, & Schilling, 1995).

2.7: XENOTRANSPLANTATION OF HUMAN LEUKEMIA CELLS INTO ZEBRAFISH EMBRYOS, DISSOCIATION, & IMMUNOFLUORESCENCE

2.7.1: LABELING CELLS

Cells in log-phase growth were centrifuged for 5 min at 300xg. Cells were re-suspended in 5 μg/mL CM-DiI (Invitrogen) in Phosphate Buffered Saline (PBS; Gibco). The suspension was incubated for 4 min at 37°C and then for 15 min at 4°C as previously described (Corkery et al., 2011). Cells were washed once in RPMI before being suspended in complete growth media (RPMI with 10% FBS and 1% penicillin/streptomycin) at a concentration of 20 million cells/mL for injection into embryos.

2.7.2 DETERMINATION OF THE MAXIMUM TOLERATED DOSE

Casper zebrafish embryos at 96 hours post fertilization (hpf) were dechorionated, and embryos were placed in 96-well plates. Increasing concentrations of each drug (rapamycin, triciribine and compound E) was added to E3 embryo media, and following 48 h of treatment, embryos were examined for viability. The MTD was defined as the

lowest drug concentration to kill embryos after 48 h of treatment. No drug treatment exceeded half the MTD (termed the MTD50).

2.7.3: OVERVIEW OF XENOTRANSPLANTATION OF HUMAN CELLS

Casper zebrafish embryos at 24 and 48 hours post fertilization (hpf) were dechorionated and anesthetized with 0.090 mg/mL Tricaine (Sigma-Aldrich) and used for cell transplantation using a protocol adapted from Haldi et al. (Corkery et al., 2011; Haldi et al., 2006). Embryos were arrayed in a six lane agarose plate prepared in a medium size (10 cm) Petri dish. Labeled cells were loaded into a pulled glass micropipette and approximately 50 cells were delivered, as a single injection, into the yolk sac of each embryo (injection conditions: 0.1 seconds, 2.5 psi) using a PLI-100A Pico-Liter Injector (Warner instruments) while under observation using a Zeiss SteREO DiscoveryV8 microscope (**Figure 2.7.2**). Following injection, embryos were allowed to recover at 28°C for 1 h before transfer to 35°C where they remained for the duration of the experiment. Experiments were completed at minimum in triplicate.

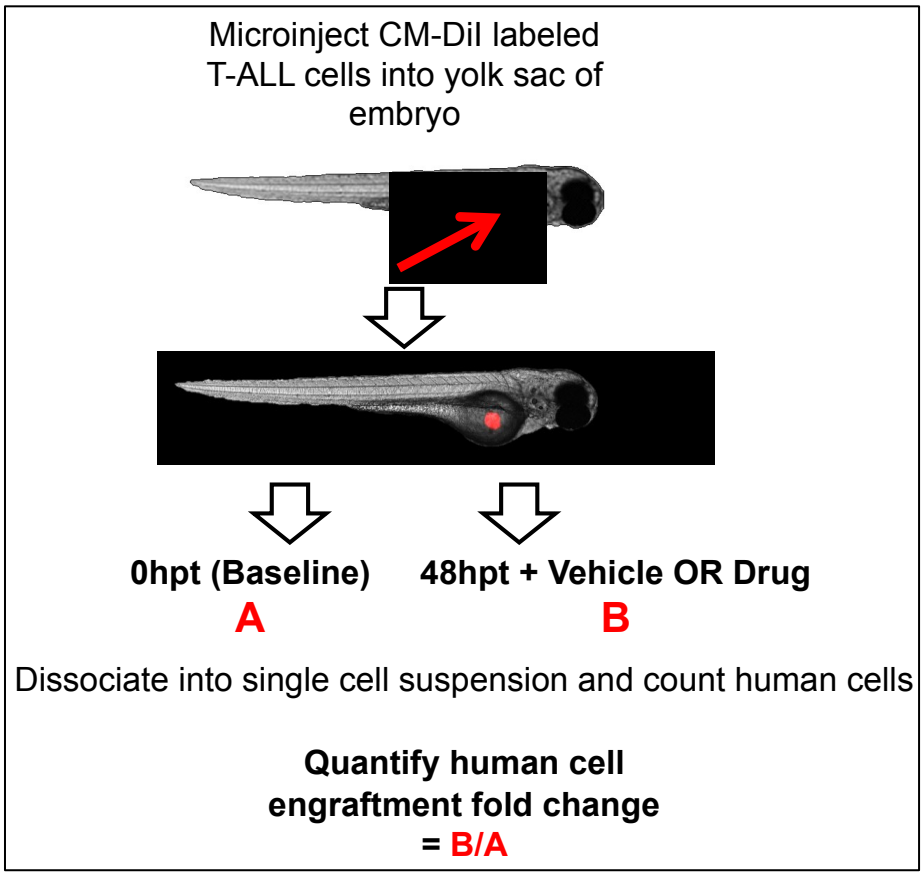

Figure 2.7.3: Schematic of xenotransplantation of human cells. Human cells are fluorescently labeled using CM-DiI, and microinjected into the yolk sac of 24 or 48 hours post fertilization (hpf) *casper* embryos. Embryos are screened for a fluorescent mass at the site of injection. The number of human cells in xenotransplanted (XT) embryos is determined at the commencement of treatment (A; denoted 0 hour post treatment (hpt) or baseline) and at the end of 48 hours of treatment either with vehicle or drug (B; 48 hpt). The average number of human leukemia cells per zebrafish is qualitatively determined by fluorescent imaging of XT embryos, and fold increase in cell number is quantified by dividing the number of cells at the end of treatment (B) by the number of cells at the start of treatment (A). The number of human cells per zebrafish is determined either by counting the number of CM-DiI labeled cells, or by using immunohistochemical approaches to label human cells. Adapted with permission from (Corkery et al., 2011).

2.7.4: XENOTRANSPLANTATION WITH T-ALL CELL LINES

Embryos were xenotransplanted with T-ALL cell lines at 48hpf. At 48 hours post-injection (hpi), only embryos with a uniform fluorescent cell mass at the site of injection were used for proliferation studies. Embryos xenotransplanted with human cancer cells were then maintained in groups of 15-20 within individual Petri dishes prior to drug treatment. At 48 hpi, drugs were added at concentrations that did not adversely affect the embryos (i.e. at or below 50% of the maximum tolerated dose (MTD50) for 48 hpf embryos treated for 48 h) directly to the fish water, at indicated concentrations, and embryos were incubated for 48 hours until 96 hpi. Embryos treated with 0.1% (v/v) DMSO served as a negative control for drug efficacy. For the fluorescence imaging, a filter with excitation/emission wavelengths of 550/605 nm was used and all embryos were photographed under the same settings. Groups of 15-20 xenografted fish were euthanized by a Tricaine overdose and dissociated into a single cell suspension and leukemia cells were enumerated (Corkery et al., 2011). Embryos were place in a microtube of 1 mL of PBS. To this mix, 27 µL of collagenase (Sigma-Aldrich, Oakville, ON, Canada) at 100mg/ml was added. Embryos were incubated and undisturbed for 15 minutes. From 15 minutes onward, the embryo-dissociation mix was homogenized using a Pasteur pipette by passing the dissociating embryos through the pipette and then quickly forcing them out against the bottom of the microtube. This step was repeated as necessary until visual inspection of the microtube revealed fully dissociated embryos. A complete dissociation was confirmed, through inspection, by no detectable whole embryo bodies or tissues remaining intact in the cell suspension, with the exception of the spines and eyes of embryos. The duration of the dissociations was approximately 45 minutes.

Upon completion, 200 μL of FBS was added to the microtubes to end the enzymatic reaction occurring between the dissociation mix and the embryo suspension. The suspension was than centrifuged at 400 X *g* for 5 minutes and the supernatant removed, leaving approximately 100 μl of liquid containing the pelleted suspension content containing the single cells produced by the dissociation assay. These cells were washed once in chilled 1X PBS and finally re-suspended in 10ul per embryo of PBS-FBS solution. The dissociations were analyzed using the inverted Axio Observer Z1 microscope. One 10 μL drop of the suspension at a time was added to a microscope slide, and six boli were imaged per experimental condition. Boli were analyzed as a mosaic 4 X 5 grid, using a 5X objective that captured the entire circumference of the bolus. The mosaic capture program complied equally sized square composite images that represented the entire circular bolus. Following capture, all individual images from the mosaic were analyzed using a semi-automated macro (Image J computer software, NIH, Bethesda, MD, USA) where relative fluorescent cell numbers could be determined per embryo. Of the 20 individual images produced by the mosaic program, 4 out of 6 of the internal/grid images were used to determine cell counts. Exterior grid images were excluded from analysis because they only displayed the circular edge regions of the suspension bolus (Corkery et al., 2011).

2.7.5: XENOTRANSPLANTATION WITH SEPARATED BONE MARROW PATIENT SAMPLES

Embryos were xenotransplanted with separated bone marrow patient samples at 48hpf. At 96 hpi, drugs were added to the fish water at indicated concentrations, and

embryos were incubated for 48 hours until 144 hpi. Fluorescent imaging was performed as indicated above. Groups of fish were dissociated and engraftment fold change enumerated by counting cells positive for PML bodies (expressed in human cells but not zebrafish cells). This was accomplished by performing cytospin (cytospin conditions: 300rpm for 10 minutes, using a Shandon cytospin 3 (Global Medical instrumentation)) of dissociated embryos, and immunohistochemistry for PML bodies (primary antibody: Rabbit Anti-PML (Santa Cruz sc-5621); secondary antibody: DyLight Donkey Anti-Rabbit IgG 649 (Abcam)). Fluorescent images were acquired on a custom built Zeiss Axio Observer Z1 inverted microscope equipped with 405 nm, 488 nm, 561 nm and 633 nm diode-based lasers (Intelligent Imaging Innovations (3i)) and a confocal spinning-disk unit (CSU-X1)(Yokagowa). Cells were observed using a 10X objective and images were recorded using an Evolve 512 electron-multiplying charge-coupled device (EMCCD) camera (Photometrics) and Slidebook 5.1 Software using the mosaic tool (Intelligent Imaging Innovations (3i)).

2.7.6: XENOTRANSPLANTATION WITH DOXORUBICIN-INDUCED CARDIOTOXICITY MODEL

Embryos were xenotransplanted with Jurkat cells at 24 hpf. Embryos were screened at 4hpi, and only embryos with a uniform fluorescent cell mass at the site of injection were used for proliferation studies. A group of embryos was dissociated at 4 hpi (0 hpt, the number of cells here represents the baseline number of cells xenografted), and separate groups of embryos were treated with 100 μM doxorubicin with or without 20 μM visnagin, 20 μM diphenyurea, or 50 μM zinecard and were maintained at 35^{o}C. At 48

hpt groups of xenotransplanted embryos were dissociated, and the number of human cells was quantified using the PML method described above. Zebrafish were screened and imaged to evaluate their cardiac phenotype at both 0 hpt and 48 hpt.

2.8: STUDY APPROVAL

All studies in zebrafish were approved by the Dalhousie University Committee on Laboratory Animals (Protocol 13-132). All studies using human samples were approved by the Research Ethics Board of the IWK Health Centre (File #1007549).

2.9: STATISTICAL ANALYSIS

Analyses were performed with GraphPad Prism 5.0. For parameter comparisons between groups, an unpaired 2-tailed Student's *t* test or 1-way ANOVA followed by Dunnett's multiple comparison test were used when appropriate. *P* values of less than 0.05 were considered significant. Results are reported as mean ± SEM.

CHAPTER 3: RESULTS

3.1: FOCUSED CHEMICAL GENOMICS USING ZEBRAFISH XENOTRANSPLANTATION AS A PRECLINICAL THERAPEUTIC PLATFORM FOR T-CELL ACUTE LYMPHOBLASTIC LEUKEMIA

3.1.1: T-ALL CELL LINES WITH DEFINED MUTATIONS IN *NOTCH* AND *PTEN* HAVE DIFFERENTIAL RESPONSES *IN VITRO* AND *IN VIVO* TO INHIBITION OF NOTCH (COMPOUND E), AKT (TRICIRIBINE) AND mTOR (RAPAMYCIN).

Three T-ALL cell lines, Jurkat, Karpas45 and TALL1, were chosen for evaluation of small molecule inhibitors because they harbour defined mutations in *NOTCH1* and *PTEN* (**Table 3.1.1.1**). Cell lines were evaluated for their *in vitro* sensitivity to inhibitors targeting the PI3K/AKT/mTOR and Notch signalling pathways. Cell lines were treated with increasing concentrations of rapamycin, triciribine, and compound E (**Figure 3.1.1.1**).

Table 3.1.1.1: Mutation profile of T-ALL cell lines

	NOTCH1		PTEN	FBXW7	Drug Response		
Cell Line	HD	PEST			Rapamycin	Triciribine	Compound E
Jurkat	WT	WT	WT Deficient	Mutated 505 R→C	Sensitive	Resistant	Resistant
Karpas45	WT	Mutated 7378 C→T	Mutated 1003 C→T	Mutated 505 R→C	Resistant	Sensitive	Resistant
TALL1	WT	WT	WT Deficient	WT	Resistant	Resistant	Sensitive

Numbers correspond to amino acid residues in *NOTCH1*, *PTEN*, and *FBXW7* respectively.

Summarized from: (Kalender Atak et al., 2012; Medyouf et al., 2010; O'Neil et al., 2007; Palomero et al., 2007; Thompson et al., 2007; Weng et al., 2004)

A 1-way ANOVA followed by Dunnett's multiple comparison test was used to determine statistically significant decreases in cell viability as compared to vehicle control. Of the three cell lines, TALL1 (*NOTCH1* WT) was the only cell line to respond significantly to 2.5 μM of compound E ($P<0.001$). Karpas45 (*PTEN* mutated) cells responded significantly to treatment with 10 μM triciribine ($P<0.001$). Jurkat (*PTEN* mutated) cells responded significantly to treatment with 50 nM rapamycin ($P<0.01$; **Figure 3.1.1.2 A**). The other cell line-drug concentrations did not produce significant decreases in cell viability ($P>0.05$).

Previously, we demonstrated that a zebrafish human cancer xenotransplantation (XT) platform can robustly detect and quantify human leukemia drug response *in vivo*. Corkery and colleagues demonstrated that zebrafish XT platform can be used to quantify the inhibition of leukemia cell proliferation using the targeted agents imatinib mesylate and all-*trans* retinoic acid (Corkery et al., 2011). Building on the zebrafish XT techniques pioneered by the Dellaire and Berman laboratories, I hypothesized that zebrafish XT could be used to recapitulate the *in vitro* results using T-ALL cell lines and small molecule inhibitors *in vivo*.

Determination of the maximum tolerated dose (MTD) for compound E, triciribine, and rapamycin was conducted in non-XT embryos (**Table 3.1.1.2**). Due to poor solubility above 40 μM, the MTD for compound E was not determined (ND). No drug treatment exceeded half the MTD (termed MTD50). Double pigment mutant *casper* zebrafish embryos (White et al., 2008) were injected with approximately 50 CM-DiI

fluorescently labeled T-ALL cells into the yolk sac at 48 h post-fertilization (hpf). Embryos were screened for a uniform fluorescent mass at the site of injection at 48 h post-injection (48 hpi, 96 hpf). A group of 15-20 positively injected embryos was dissociated and the number of leukemia cells per embryo was quantified (referred to as the baseline number of leukemia cells at the start of drug treatment). Groups of 15-20 embryos were treated with an individual drug for 48 h starting at 48 hpi (see **Figure 3.1.1.2 B** for experimental scheme). Leukemia cell number was determined by dissociating groups of xenotransplanted embryos and counting CM-DiI labeled leukemia cells. Previously, we have shown that engrafted CM-DiI labeled leukemia cells are viable and intact using a DRAQ5 viable nuclear stain (Corkery et al., 2011).

Table 3.1.1.2: Maximum tolerated dose

Drug	MTD	MTD50	Treatment concentration
Rapamycin	2.5 μM	1.25 μM	400 nM
Triciribine	200 μM	100 μM	75 μM
Compound E	ND	ND	20 μM

A 1-way ANOVA followed by Dunnett's multiple comparison test was used to determine statistically significant changes in human leukemia cell number as compared to the baseline number of leukemia cells. T-ALL cell lines engrafted and proliferated in zebrafish embryos, indicated by the significant increase ($P<0.05$) in number of leukemia cells from baseline to 48 hpt with vehicle (qualitatively shown in **Figure 3.1.1.2 C** and **Figure 3.1.1.3** and quantitatively shown in **Figure 3.1.1.2 D** and **Figure 3.1.1.4**), and had analogous responses to *in vitro* drug treatments. 20 μM Compound E inhibited TALL1 cell proliferation *in vivo* by 37% compared to vehicle ($P<0.01$), 75 μM triciribine inhibited Karpas45 cell proliferation *in vivo* by 19% ($P<0.05$), 400 nM rapamycin

inhibited Jurkat cell proliferation *in vivo* by 59% ($P<0.01$). Significant inhibition of T-ALL cell line proliferation was not observed with other cell line-drug combinations ($P>0.05$).

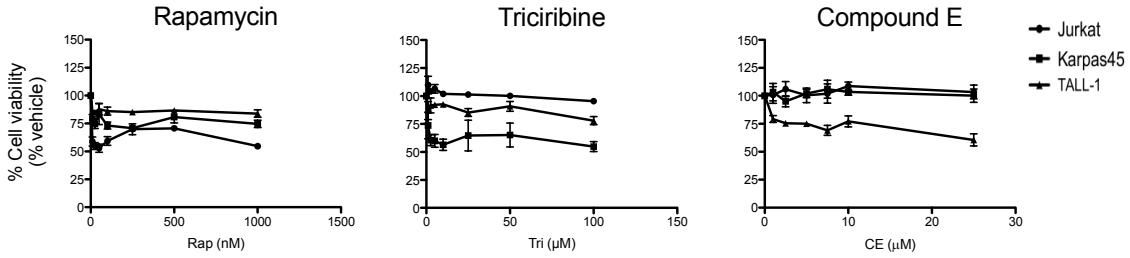

Figure 3.1.1.1: T-ALL cell lines harbouring defined mutation in *NOTCH* and *PTEN* have differential responses *in vitro* to inhibition of Notch (Compound E), AKT (triciribine), and mTOR (rapamycin). *In vitro* cell viability assay. Cell lines were treated with drug or vehicle (0.01% DMSO) for 72 hours, and Cell viability determined (via alamarBlue) as a percentage of vehicle control.

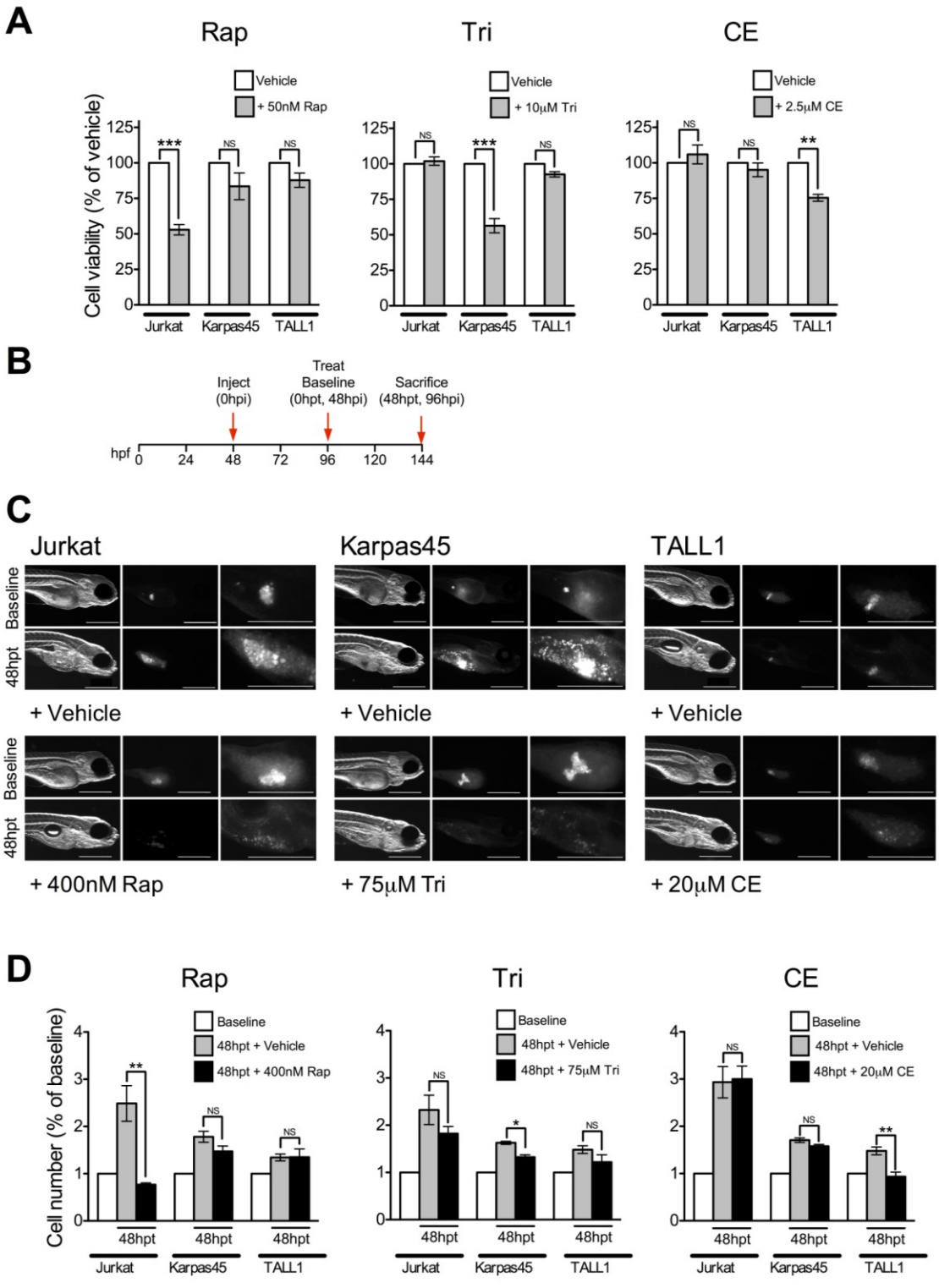
A
Rap
Tri
CE
Vehicle
+ 50nM Rap
+ 10μM Tri
+ 2.5μM CE
Cell viability (% of vehicle)
125
100
75
50
25
0
***
NS
**
Jurkat
Karpas45
TALL1
B
Inject
(0hpi)
Treat
Baseline
(0hpt, 48hpi)
Sacrifice
(48hpt, 96hpi)
hpf 0 24 48 72 96 120 144
C
Jurkat
Karpas45
TALL1
Baseline
48hpt
+ Vehicle
+ 400nM Rap
+ 75μM Tri
+ 20μM CE
D
Rap
Tri
CE
Baseline
48hpt + Vehicle
48hpt + 400nM Rap
48hpt + 75μM Tri
48hpt + 20μM CE
Cell number (% of baseline)
4
3
2
1
0
**
NS
*
48hpt
Jurkat
Karpas45
TALL1

Figure 3.1.1.2: T-ALL cell lines harbouring defined mutation in *NOTCH* and *PTEN* have differential responses *in vitro* and *in vivo* to inhibition of Notch (Compound E), AKT (triciribine), and mTOR (rapamycin). A. *In vitro* cell viability assay. Cell lines were treated with drug or vehicle (0.01% DMSO) for 72 hours, and Cell viability determined (via alamarBlue) as a percentage of vehicle control. B. Schematic of the *in vivo* zebrafish XT cell proliferation assay. C. Representative brightfield and fluorescent and magnified fluorescent images (from left to right) of zebrafish embryos transplanted with CM-DiI-labeled T-ALL cell lines at 0 hpt (baseline, = 48 hpi = 96 hpf) and 48 hpt (96 hpi = 144 hpf) with or without drug. D. *In vivo* proliferation of T-ALL cell lines in the zebrafish XT model. Groups of 15-20 embryos were used for each time point and treatment, 50-100 cells were injected per fish, and the number of fluorescent cells was enumerated as described in Corkery et al. (Corkery et al., 2011). Baseline number of cells was determined at 0 hpt and all drug treatments (at 48 hpt) are shown as a fold change of the baseline. All cell lines engrafted and proliferated in the zebrafish, as represented by the significant increase in number of leukemia cells from baseline to 48hpt with vehicle. Means +/- SEM; N=3; P*<0.05, P**<0.01, P***<0.001 for significant decrease in cell viability and the number of cells was determined using 1-way ANOVA followed by Dunnett's multiple comparison test. N = the number of independent experiments, with 15-20 embryos per group per experiment. hpt = hours post-treatment, hpi = hours post-injection. Scale bars are 500 μM.

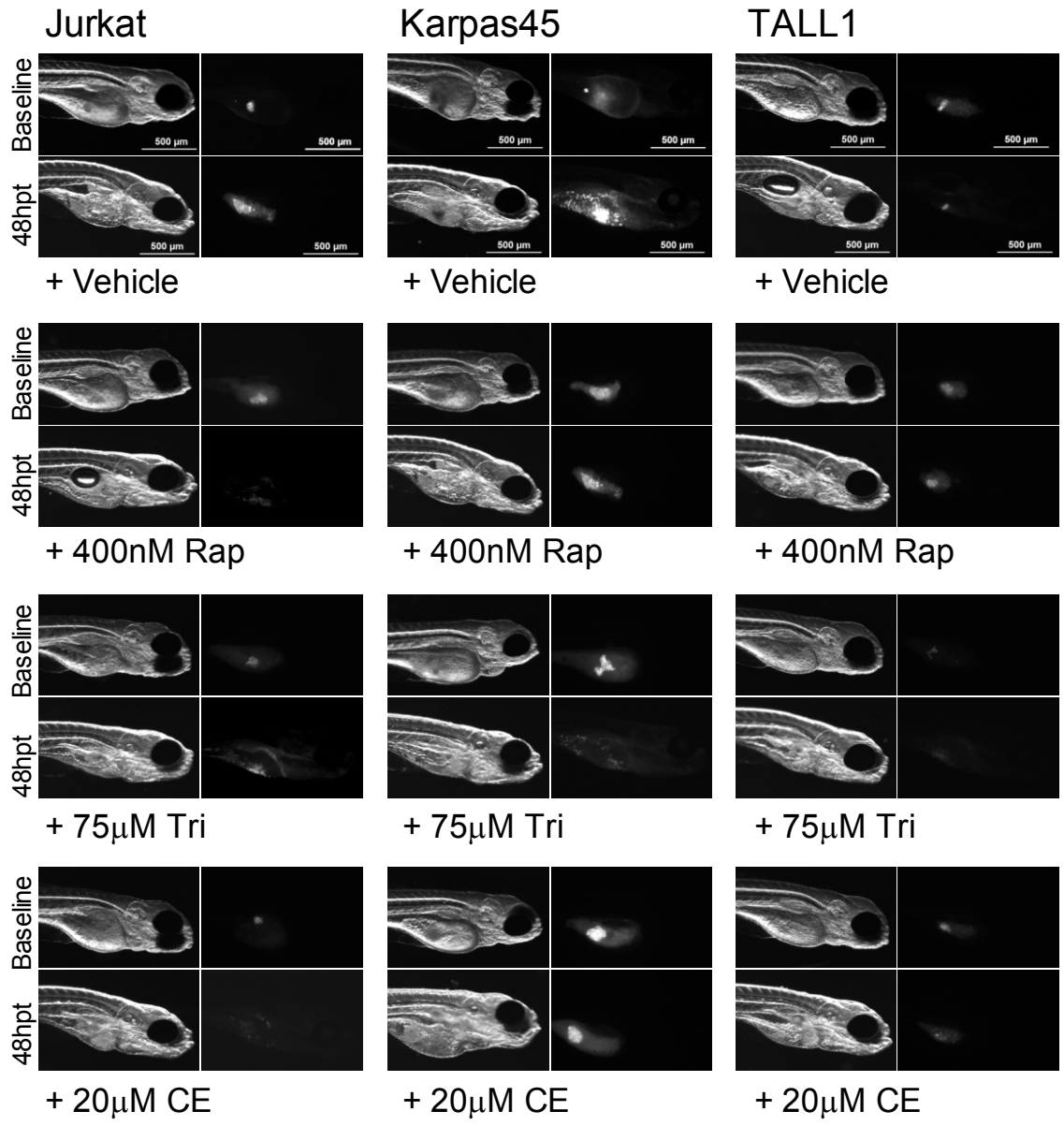

Figure 3.1.1.3: Representative brightfield and fluorescent images of zebrafish embryos transplanted with T-ALL cell lines at Baseline (0hpt, 48hpi) and 48hpt (96hpi) with or without drug. Zebrafish embryos were xenotransplanted with CmDiI-labelled T-ALL cell lines at 48hpf. Cells were given 48h to engraft in zebrafish embryos, embryos were screened for fluorescent masses (48hpi, 0hpt is referred to as 'baseline'), and then were treated with indicated drug for 48h. Embryos were imaged at baseline and 48hpt, and groups of embryos were dissociated at fluorescent cells enumerated at each time point. Drug doses: compound E 20 µM; triciribine 75 µM; rapamycin 200 nM. hpt = hours post treatment; hpi = hours post injection.

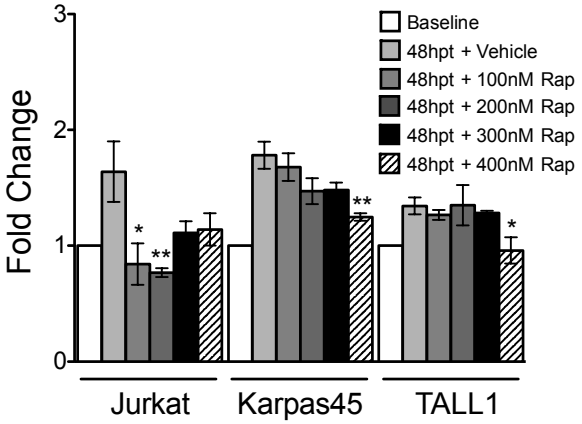

Triciribine

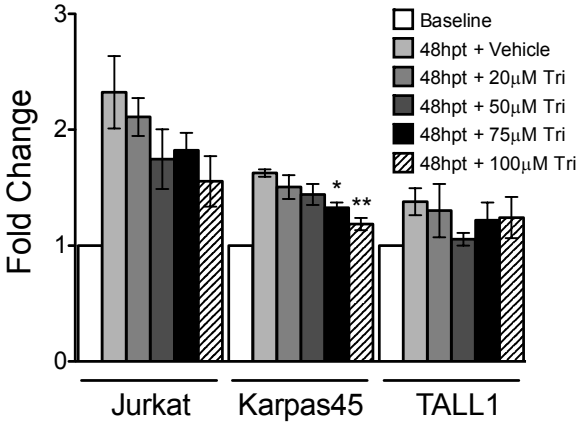

Compound E

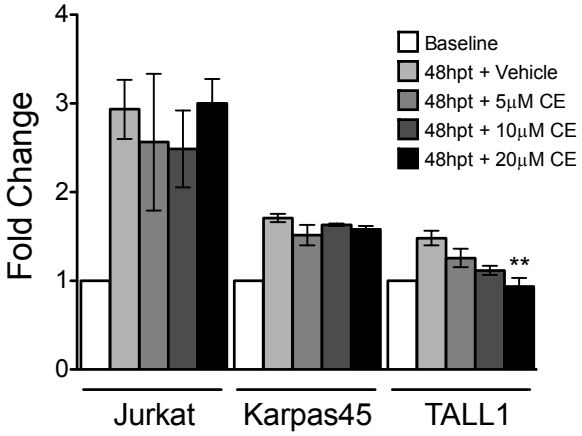

Figure 3.1.1.4: *In vivo* proliferation of T-ALL cell lines in the zebrafish xenograft (XT) model. Quantification of cell proliferation was performed by dissociating groups of xenografted fish at baseline and 48hpt and enumerating fluorescently labeled cells as previously described (Corkery et al., 2011). All drug treatments are shown as a fold change of the number of leukemia cells when treatments were initiated (baseline). Means +/- SEM; N = 1; P*<0.05, P**<0.01, P***<0.001 for significant decrease in number of cells determined using 1-way ANOVA followed by Dunnett's multiple comparison test. Groups of 15-20 embryos were used for each time point and drug treatment. Baseline = Untreated fish at 0hpt; all other treatments are at 48hpt; hpt = hours post-treatment.

3.1.2: ZEBRAFISH XT MODEL UNCOVERS SENSITIVITY TO *IN VIVO* INHIBITION OF NOTCH IN A CHILD WITH T-ALL

I hypothesize that the zebrafish XT model is well suited to determine a patient's drug sensitivity, and could be employed to personalize patient treatment. Bone marrow aspirate samples from two children with T-ALL treated at the IWK health center were obtained at the time of diagnostic bone marrow sample collection. These two patient samples had unknown genotypes but confirmed diagnosis of T-ALL. Lymphoblasts were obtained by density gradient centrifugation with Lympholyte-H, which separates viable lymphocytes and monocytes from dead cells, erythrocytes and granulocytes. Patient lymphoblasts were labeled with CM-DiI and injected into zebrafish embryos to facilitate direct screening of targeted drugs. Primary bone marrow samples engrafted (indicated by a uniform fluorescent mass at the site of injection) at 96 hpi (referred to as baseline) and proliferated within the embryo, as indicated by the increase in number of leukemia cells from baseline to 48 hpt with vehicle. Initial qualitative fluorescent imaging of engrafted embryos showed that neither patient sample 1 or 2, derived from two independent children with T-ALL, responded to treatment with rapamycin in zebrafish xenografts, as evidenced by sustained cell proliferation in the presence of drug (**Figure 3.1.2.2 A)** However, patient sample 1 responded dramatically to treatment with compound E (**Figure 3.1.2.2 A and C)**, which inhibited cell proliferation *in vivo* by 84% (Injection and treatment scheme shown in **Figure 3.1.2.2 B**)

Primary patient samples were grown in the zebrafish XT model over 6 days and proliferate rapidly, and therefore there was concern that the patient cells would out proliferate the CM-DiI labeling. This made quantification based on retention of CM-DiI

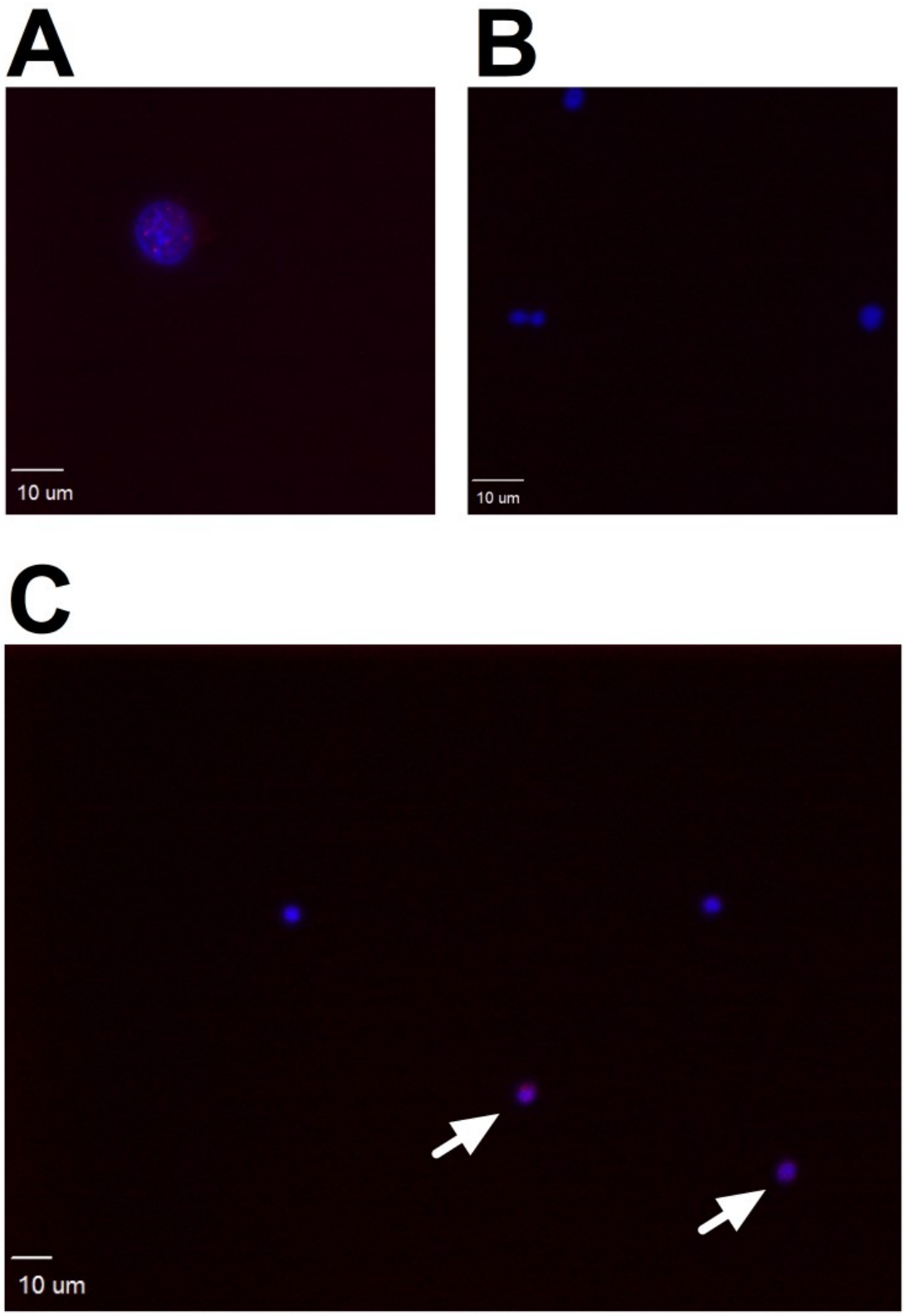
A
10 um
B
10 um
C
10 um

Figure 3.1.2.1: Human cancer cells can be differentiated from zebrafish cells by immunohistochemistry for promyelocytic leukemia (PML) bodies. Cytospins showing that A. Human Jurkat cell are positive for PML bodies (shown in red). B. Zebrafish do not contain PML bodies. C. Dissociated zebrafish engrafted with human Jurkat cells. White arrows indicate human cells (positive for PML bodies). Fluorescent images were acquired on a custom built Zeiss Axio Observer Z1 inverted microscope equipped with 405 nm, 488 nm, 561 nm and 633 nm diode-based lasers (Intelligent Imaging Innovations (3i)) and a confocal spinning-disk unit (CSU-X1)(Yokagowa). Panel A was taken using a 60X objective and panels B and C were taken using a 40X objective. Images were recorded using an Evolve 512 electron-multiplying charge-coupled device (EMCCD) camera (Photometrics) and Slidebook 5.1 Software.

dye an inadequate method. Therefore, I developed a novel way to distinguish human cells from host zebrafish cells to permit the quantification of human cell proliferation in the XT model. Groups of zebrafish XT with patient samples and treated with drug were sacrificed at 0 hpt and 48 hpt and dissociated into a single cell suspension, cytospins were preformed, and samples fixed. Fluorescent immunocytochemistry was employed to label promyelocytic leukemia (PML) nuclear bodies, which are not present in zebrafish cells but are present in human leukemia cells (**Figure 3.1.2.1**) Patient tumour-drug response was quantified by imaging dissociated fish and counting the number of cells positive for PML bodies. This quantification revealed that Patient 1 was very sensitive to NOTCH inhibition by compound E, shown by a significant inhibition of cell proliferation in the compound E treated group, as compared to the vehicle treated group.

Thus, this *in vivo* chemical genomic approach resulted in the identification of sensitivity to γ-secretase inhibition. This sensitivity strongly suggested a targetable mutation in the NOTCH pathway underlying the leukemia of patient 1. In agreement with this hypothesis, Sanger exome sequencing confirmed a heterozygous somatic missense mutation in *NOTCH1* (NM_017617.3) at position c.5087C>A, leading to amino acid change p.A1696D in the C-terminal heterodimerization (HD) domain (**Figure 3.1.2.3 A**). This mutation was previously reported in separate studies in two different patient samples (Kalender Atak et al., 2012; Mansour, Linch, Foroni, Goldstone, & Gale, 2006), however this is the first time that sensitivity to inhibition of γ-secretase has been directly correlated with this mutation. The biopsy sample from patient 1 did not have mutations in the *FBXW7* or *PTEN* gene. This mutational status (WT *FBXW7* and WT *PTEN* with p.A1696D *NOTCH1* mutation) was identified in an separate patient sample reported by

Kalender et al., suggesting that this mutation alone may be sufficient to drive T-ALL pathogenesis (Kalender Atak et al., 2012). Sequencing did not reveal mutations in *NOTCH1* in patient sample 2, consistent with the zebrafish XT results which demonstrated an insensitivity to compound E.

Mutations in the HD domain of *NOTCH1* are reported in nearly half of all T-ALLs and have been associated with *NOTCH1* activation that remains dependent on γ-secretase complex activity (Malecki et al., 2006). To determine the effect of p.A1696D *NOTCH1* mutation on Notch signalling, HeLa cells were transfected with JH23a luciferase reporter plasmid with a Notch plasmid, and luciferase expression was normalized to the internal control sea pansy (*Renilla*) expression. pMig-Notch1 (WT Notch1), pMig-Notch1ΔPEST (Notch1 with a PEST domain deletion which renders Notch constitutively active), and pMig-Notch1-A1696D plasmids were used to evaluate the effect of WT and mutated Notch1 expression on JH23a-dependent luciferase transcription.

Ectopic expression of *NOTCH* carrying the A1696A/D mutation enhanced luciferase expression to a similar extent as a well known activated NOTCH mutant carrying a PEST domain deletion, validating the patient mutation as a gain-of-function mutation in *NOTCH1* (**Figure 3.1.2.3 B**) (Das et al., 2004).

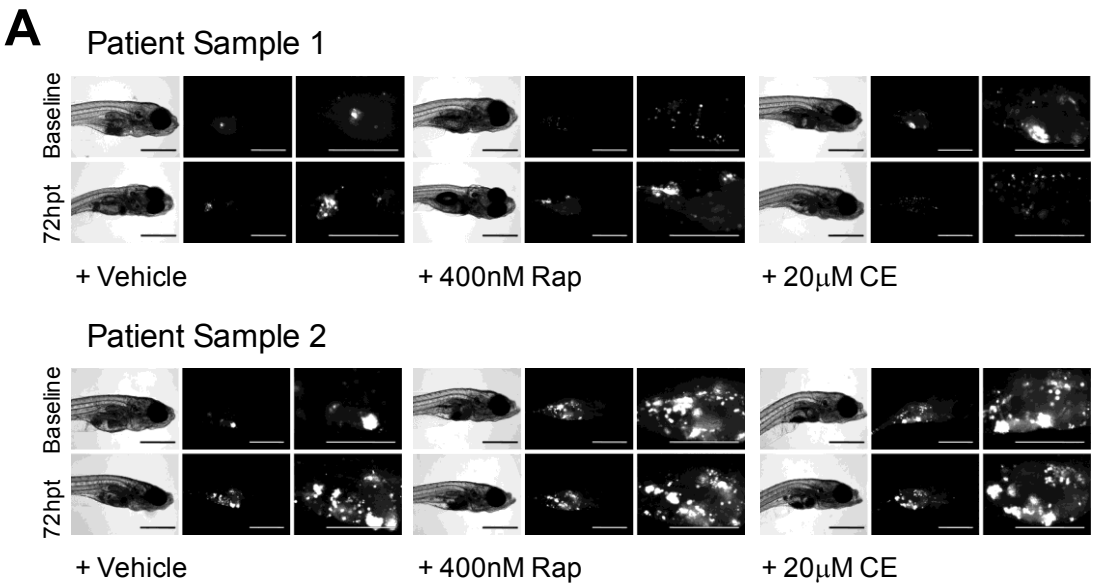
A
Patient Sample 1
Baseline
72hpt
+ Vehicle
+ 400nM Rap
+ 20μM CE
Patient Sample 2
Baseline
72hpt
+ Vehicle
+ 400nM Rap
+ 20μM CE

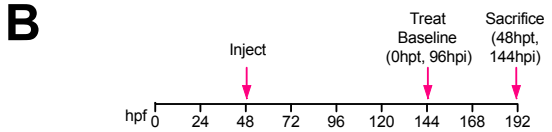
B
Inject
Treat
Baseline
(0hpt, 96hpi)
Sacrifice
(48hpt,
144hpi)
hpf
0
24
48
72
96
120
144
168
192

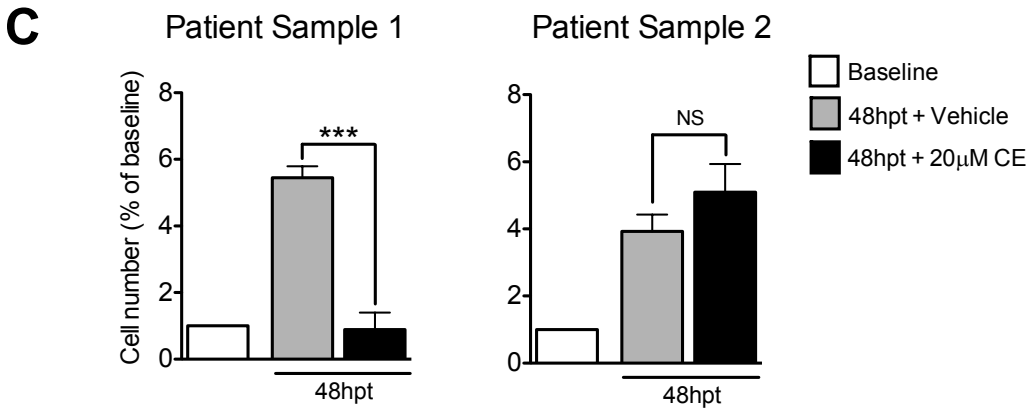
C
Patient Sample 1
Patient Sample 2
Cell number (% of baseline)
8
6
4
2
0
***
NS
48hpt
48hpt
Baseline
48hpt + Vehicle
48hpt + 20μM CE

Figure 3.1.2.2: T-ALL patient sample 1 responds *in vivo* to Notch inhibition with compound E, but not to mTOR inhibition with rapamycin. A. Representative brightfield and fluorescent images of zebrafish embryos transplanted with patient samples 1 and 2 at 0 hpt (baseline) and 72 hpt with or without drug. B. Schematic of *in vivo* zebrafish XT cell proliferation assay. C. Quantification of patient sample engraftment fold change with or without compound E treatment. Patient sample 1 and 2 engrafted and proliferated in the zebrafish XT model (indicated by the significant increase in number of leukemia cells from baseline to 48 hpt with vehicle). Patient sample 1 responded significantly to compound E treatment. Engraftment fold change was determined by sacrificing embryos at 0 hpt and 48 hpt and performing cytospins with dissociated embryos and immunohistochemistry for PML bodies (only present in human cells, not in zebrafish cells). Means +/- SEM; N = 1; P*<0.05, P**<0.01, P***<0.001 for significant decrease in number of cells determined using unpaired 2-tailed student's *t* test. Groups of 15-20 embryos were used for each time point and drug treatment. Scale bars are 500 μM. hpt = h post treatment.

A

	Gene sequenced			
	FBXW7	***IL7-R***	***NOTCH1***	***PTEN***
PS 1	**WT**	**WT**	**c.5087c>CA p.A1696A/D**	**WT**
PS 2	**WT**	**WT**	**WT**	**WT**

B

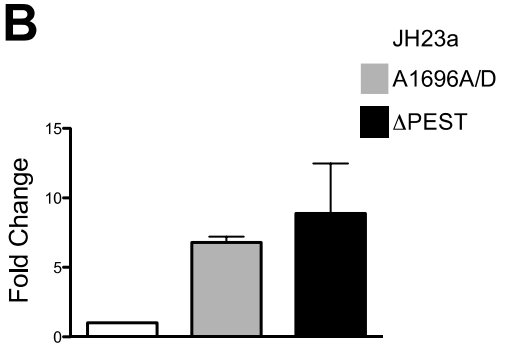

Figure 3.1.2.3: Patient Sample 1 harbours a rare *NOTCH1* mutation. A. Results from Sanger sequencing of patient exomes. Patient sample 1 (PS 1) had a heterozygous mutation in the heterodimerization (HD) domain of the *NOTCH1* gene (p.A1696D). Patient sample 2 (PS 2) did not have any mutations in the genes sequenced. B. p.A1696D mutated *NOTCH1* upregulates luciferase reporter activity. HeLa cells transfected with JH23a Notch reporter plasmid, Renilla, and +/- Notch with A1696A/D or the PEST mutation. P.A1696D mutated Notch plasmid upregulated luciferase reporter activity to a similar degree as constitutively active Notch (with PEST mutation). Means +/- SEM; N=3.

3.1.3: SUMMARY

Zebrafish human leukemia XT is a robust pre-clinical model of human malignancies, and in particular, leukemia. Here we employed the paradigm of T-ALL, a disease with well-defined molecular underpinnings, to demonstrate the suitability of zebrafish XT to evaluate novel drugs. Furthermore, primary human lymphoblasts rapidly engraft and proliferate in the zebrafish XT model, and had differential responses to small molecule inhibitors. This posits zebrafish XT as an efficient model to uncover novel drug-tumour interactions in a clinically relevant time frame, allowing for the personalization of patient treatment for T-ALL and the reduction of treatment-related toxicities.

While zebrafish XT can be used to evaluate novel inhibitors that target molecular pathways important in T-ALL, I hypothesize that zebrafish XT can also be used to improve current standard-of-care treatment strategies. Several drugs used to treat T-ALL have significant and life-threatening off-target side effects. For example, the widely used and effective anthracycline class of cytotoxic drugs is associated with dose-limiting cardiotoxicity. Novel cardioprotectant agents able to minimize cardiac damage while permitting the anti-leukemic effects of anthracyclines would improve patient outcomes and survival by minimizing toxicity.

3.2: ZEBRAFISH XENOTRANSPLANTATION AS A PRECLINICAL THERAPEUTIC PLATFORM TO EVALUATE NOVEL CARDIOPROTECTANT COMPOUNDS

3.2.1: ESTABLISHMENT OF A ZEBRAFISH MODEL OF DOXORUBICIN-INDUCED CARDIAC DAMAGE

It is hypothesized that the chemotherapeutic and cardiotoxic mechanisms of doxorubicin are separate (Liu et al., 2014). Therefore, it may be possible to combine doxorubicin with a compound that prevents cardiac damage while permitting the anti-leukemic effects of doxorubicin. A zebrafish model of doxorubicin-induced cardiac damage is needed to facilitate efficient phenotype-based screening of novel cardioprotective compounds. 24 hpf *casper* zebrafish embryos were treated with 100 μM doxorubicin, and were assessed for phenotypic changes at 48 hpt (72 hpf). By 24 hpf the zebrafish heart has formed and the circulatory system is functional, and therefore doxorubicin treatment beginning at 24 hpf does not interfere with early cardiogenic processes (Wilkinson, Jopling, & van Eeden, 2014). After 48 h of treatment with doxorubicin, zebrafish had extensive pericardial edema, impaired heart contraction leading to an absence of blood cells in tail blood vessels, and the atrium was elongated and the ventricle had collapsed (**Figure 3.2.1**). Furthermore, the number of atrial and ventrical cardiomyocyte number were reduced in doxorubicin-treated embryos, and TUNEL staining demonstrated increased apoptosis of cardiomyocytes (Liu et al., 2014). This model resembles anthracycline-induced cardiac damage in patients, in particular through decreased contractility and apoptosis of cardiomyocytes (Yeh et al., 2004).

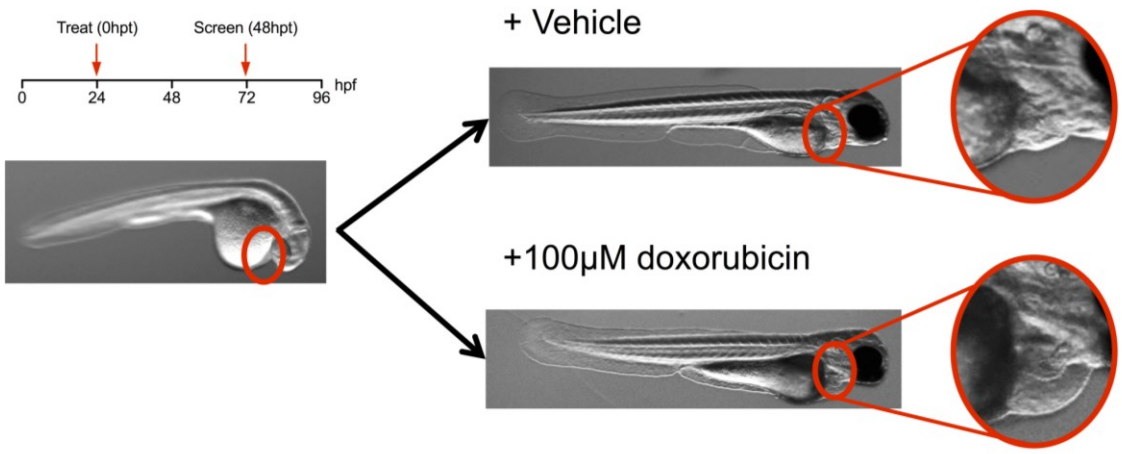

Figure 3.2.1: Doxorubicin treatment induces cardiac damage in zebrafish embryos. 24 hpf *casper* zebrafish embryos were treated with 100 μM doxorubicin, and were assessed for phenotypic changes at 48 hpt (72 hpf). After 48 h of treatment with doxorubicin, zebrafish had extensive pericardial edema, impaired heart contraction leading to an absence of blood cells in tail blood vessels, and the atrium was elongated and the ventricle had collapsed, as compared to vehicle-treated embryos. This phenotypic change formed the basis for a screen for novel cardioprotective agents.

3.2.2: ZEBRAFISH SCREEN IDENTIFIES TWO COMPOUNDS THAT PREVENT DOXORUBICIN-INDUCED CARDIAC DAMAGE

The zebrafish model of doxorubicin-induced cardiotoxicity produces a clear and easily visualized phenotype of pericardial edema and impaired cardiac function. This formed the basis of a high throughput phenotype-based screen, undertaken by Dr. Randall Peterson's group, to discover novel compounds that can protect against doxorubicin-induced cardiotoxicity (**Figure 3.2.2**). Zebrafish embryos were treated with 100 μM doxorubicin from 24 hpf to 72 hpf in combination with a panel of 3,000 small molecules. Eight compounds were found to prevent the doxorubicin-induced cardiotoxic phenotype, and two of these compounds, visnagin (VIS) and diphenylurea (DPU) were found to be effective at protecting embryo hearts at concentrations below 1 μM. VIS and DPU were moved into *in vitro* experiments and the *in vivo* zebrafish human leukemia xenograft (XT) model.

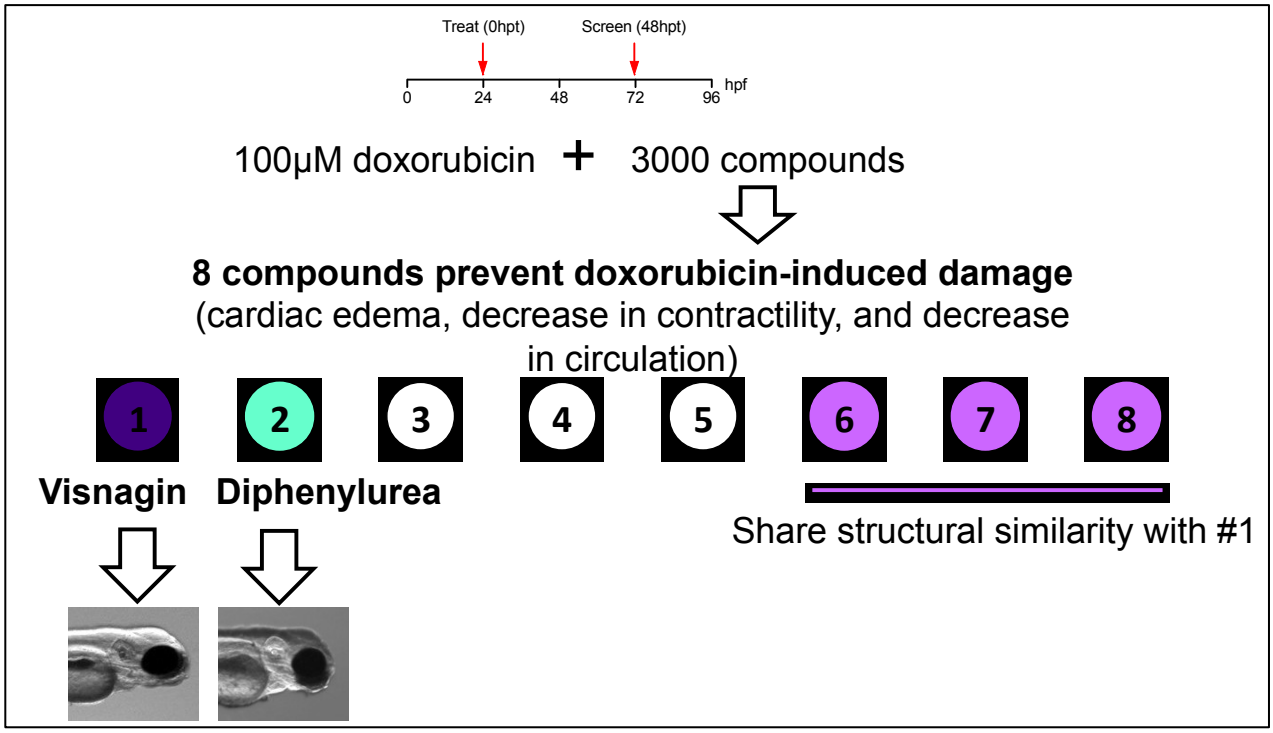

Figure 3.2.2: Whole-organism phenotype-based screen using a doxorubicin-induced model of cardiac damage identifies two novel cardioprotectant compounds, Visnagin (VIS) and diphenylurea (DPU). Zebrafish embryos were treated with 100 μM doxorubicin from 24 hpf to 72 hpf in combination with a panel of 3,000 small molecules. Eight compounds were found to prevent the doxorubicin-induced cardiac edema, contracitilty decrease and circulation impairment. Two of compounds, visnagin (VIS) and diphenylurea (DPU) were found to be effective at preventing doxorubicin-induced cardiac damage embryo hearts at concentrations below 1 μM.

3.2.3: VISNAGIN AND DIPHENYLUREA PROTECT AGAINST DOXORUBICIN-INDUCED CARDIAC DAMAGE, BUT DO NOT PROTECT TUMOUR CELLS *IN VITRO* OR *IN VIVO*

The phenotype-based zebrafish screen uncovered two novel agents able to protect against doxorubicin-induced cardiac damage. For these compounds to be effective cardioprotectant agents, however, they should not interfere with the anti-tumour effects of doxorubicin. The effect of VIS and DPU on cell viability was determined *in vitro.* Jurkat cells were seeded in 96-well plates, and treated with increasing does of VIS, DPU and the FDA-approved cardioprotectant Dexrazoxane (Dxz). Cell viability was calculated as a percentage of vehicle control after 48 hours post-treatment (hpt), using an alamarBlue cell viability assay. There was no statistically significant increase in cell viability after 48 h of treatment with VIS, DPU, or Dxz (**Figure 3.2.3.1 B**).

Doxorubicin potently reduces cell viability, in a dose and time-dependent manner. Jurkat cells were cultured in the presence of increasing dose of doxorubicin (**Figure 3.2.3.1 A**). Jurkat cells were then cultured in the presence of 500 nM doxorubicin in combination with vehicle or increasing dose of VIS, DPU, and Dxz. Neither cardioprotectant compound decreased the ability of 500 nM doxorubicin to kill Jurkat cells. These *in vitro* results demonstrate that neither VIS nor DPU causes an increase in the metabolic activity of Jurkat T-ALL cells, and that the novel cardioprotectant agents do not interfere with the cell killing effects of doxorubicin.

Doxorubicin is a fluorescent drug, and microscopic imaging of zebrafish treated with doxorubicin indicates whether the drug is being absorbed by the *casper* embryos. Zebrafish treated with 100 μM doxorubicin with vehicle or with 20 μM VIS and 20 μM

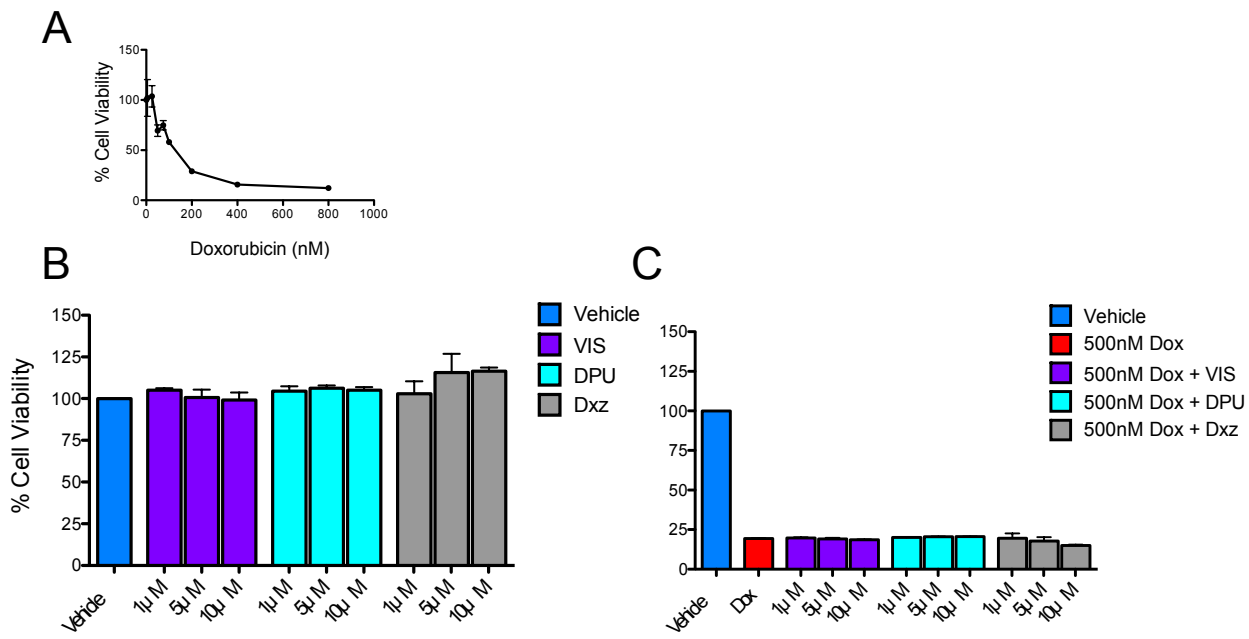

Figure 3.2.3.1: VIS and DPU do not protect leukemia cells *in vitro* from doxorubicin treatment. A. Jurkat T-ALL cells were cultured in increasing dose of doxorubicin for 48 hours, and cell viability was determined using the alamarBlue cell viability assay. Doxorubicin produced a dose-dependent decrease in cell viability. B. VIS, DPU, and Dxz did not increase the cell viability of Jurkat cells after 48 hours of treatment, as determined by alamarBlue assay. C. VIS, DPU, and Dxz do not protect Jurkat cells from doxorubicin-induced decrease in cell viability, as determined by alamarBlue assay. Means +/- SEM; N=3.

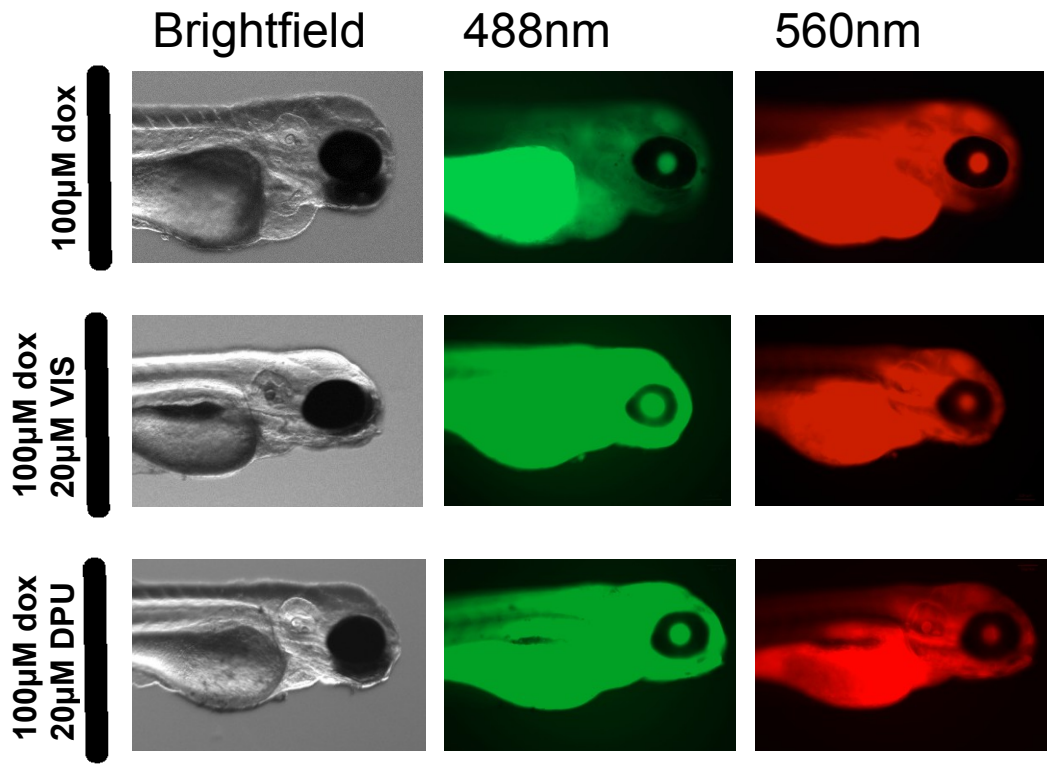

Figure 3.2.3.2: VIS and DPU do not block zebrafish uptake of doxorubicin. Representative fluorescent imaging of zebrafish embryos treated with 100 µM doxorubicin from 24 hpf to 72 hpf in combination with 20 µM VIS or 20 µM DPU demonstrates that doxorubicin is still readily absorbed by embryos.

DPU were imaged to assess if cardioprotectant compounds interfere with the uptake of doxorubicin. Neither VIS nor DPU prevented the uptake of doxorubicin *in vivo* (**Figure 3.2.3.2)**.

Using the human leukemia XT model, I assessed the effect of VIS and DPU on the proliferation of T-ALL cells *in vivo*. Zebrafish were injected with CM-DiI-labelled Jurkat cells at 24 hpf, were screened 4 hpi for a uniform fluorescent mass at the site of injection. A group of 15-20 XT embryos were sacrificed and dissociated at 0 hpt or treated with VIS, DPU or Dzx for 48 h, and then sacrificed and dissociated. The number of human leukemia cells was determined per treatment group by performing cytospins and fluorescent immunohistochemistry was performed for PML bodies. Jurkat cells engrafted and proliferated in zebrafish embryos, indicated by a very significant increase in the number of leukemia cells from 0 hpt (referred to as the baseline number of cells) to 48 hpt. Treatment with 20 μM VIS and 20 μM DPU did not cause leukemia cells to proliferate at a faster rate than vehicle. However, treatment with 50 μM Dxz did cause Jurkat cells to proliferate at a faster rate than vehicle (Shown qualitatively in **Figure 3.2.3.3 A** and quantified in **Figure 3.2.3.3 B**).

Next, XT embryos were treated with doxorubicin with vehicle, or with the novel cardioprotectant agents. Doxorubicin significantly reduced the number of Jurkat cells in the zebrafish and caused a cardiotoxic phenotype. Thus, the zebrafish XT model allowed for the simultaneous screening of therapeutic efficiency and drug toxicity. In agreement with *in vitro* results, neither novel cardioprotectant agent decreased the cell killing effect of doxorubicin *in vivo* (**Figure 3.2.3.4**).

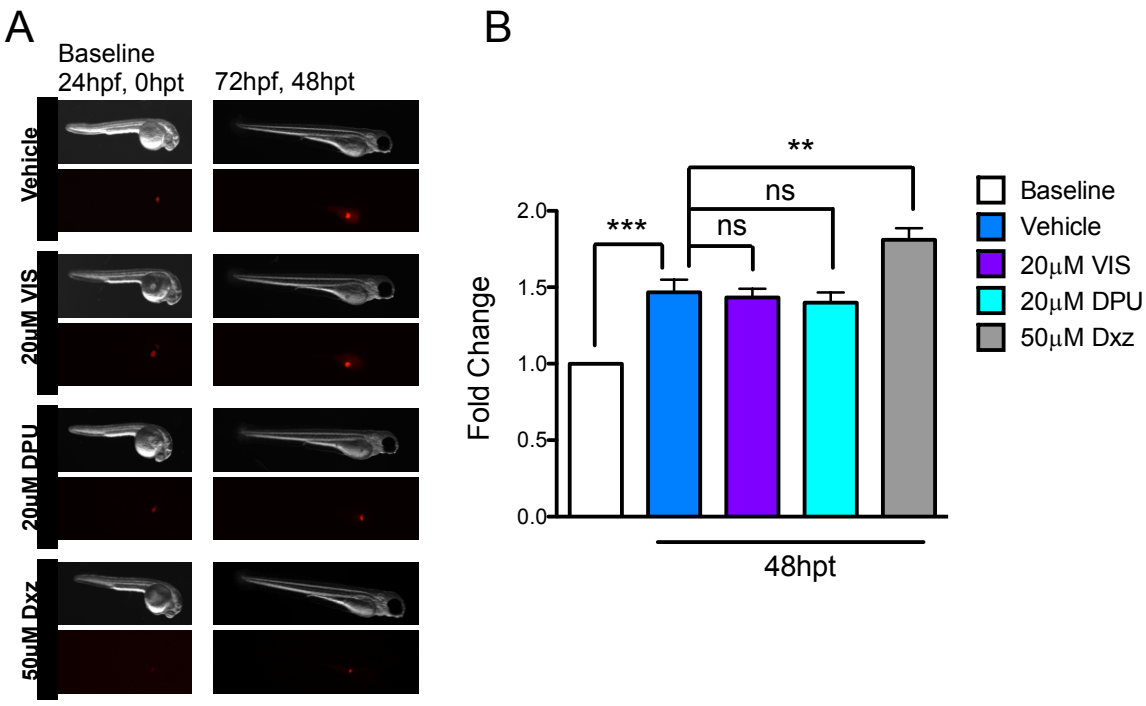

Figure 3.2.3.3: Zebrafish XT demonstrates that VIS and DPU do not increase leukemia cell line viability *in vivo*. Jurkat T-ALL cells were labelled with CM-DiI and injected into 24 hpf embyros, and embryos were treated with VIS, DPU, or Dzx. At 48 hpt embryos were sacrificed and the number of human leukemia cells determined. A. Representative fluorescent images of XT embryos at 0 hpt and 48 hpt. B. VIS and DPU do not cause Jurkat cells to proliferate faster *in vivo* than vehicle-treated XT embryos. However, Jurkat cells in Dxz-treated embryos proliferated significantly faster. Means +/- SEM; N=3, P*<0.05, P**<0.01, P***<0.001 for significant decrease in number of cells determined using 1-way ANOVA followed by Dunnett's multiple comparison test; hpf = hours post fertilization; hpt = hours post treatment. Groups of 15-20 embryos were used for each time point and drug treatment.

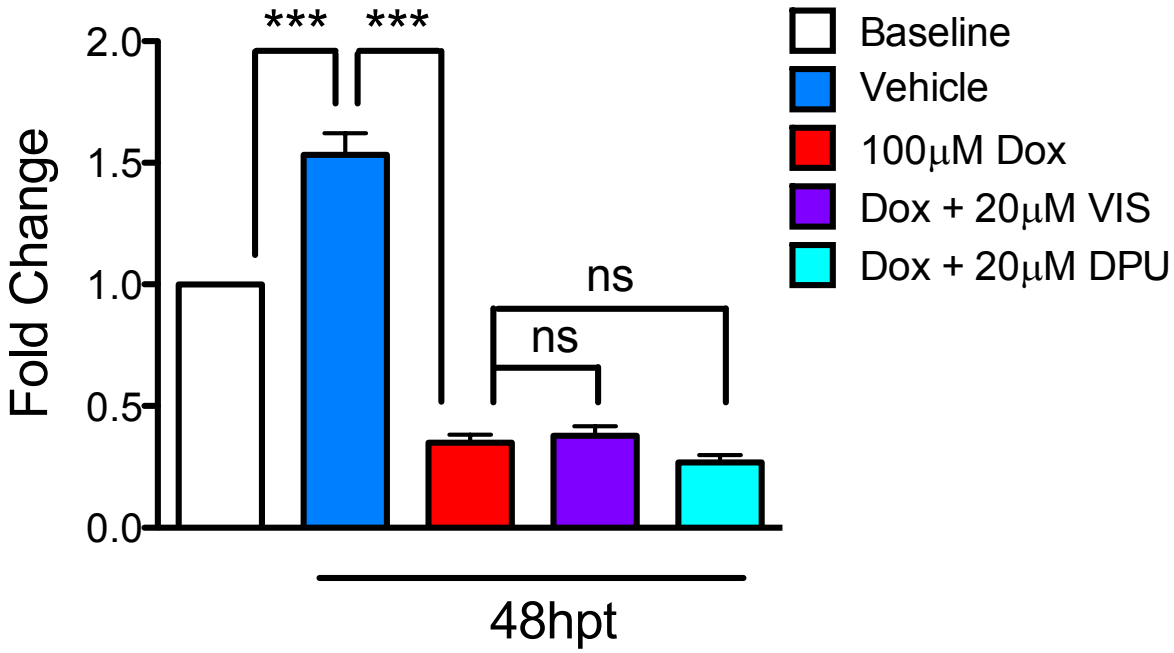

Figure 3.2.3.4 VIS and DPU do not protect leukemia cells from doxorubicin *in vivo*. Jurkat T-ALL cells were labelled with CM-DiI and injected into 24 hpf embyros, and embryos were treated with 100 μM doxorubicin in combination with vehicle, 20 μM VIS or 20 μM DPU. At 48 hpt embryos were sacrificed and the number of human leukemia cells determined VIS and DPU did not protect Jurkat cells from the cell killing effect of doxorubicin. Means +/- SEM; N=3, P*<0.05, P**<0.01, P***<0.001 for significant decrease in number of cells determined using 1-way ANOVA followed by Dunnett's multiple comparison test; hpf = hours post fertilization; hpt = hours post treatment. Groups of 15-20 embryos were used for each time point and drug treatment.

3.2.4: SUMMARY

A doxorubicin-induced cardiotoxicity model was established in zebrafish, and used to conduct a phenotype-based screen for cardioprotective agents. Eight compounds were discovered that could block doxorubicin-induced pericardial edema, decreased contractility, and increased cardiomyocyte apoptosis. Two of these compounds, VIS and DPU were very effective at low concentrations.

Using a combination of *in vitro* and *in vivo* cell viability and proliferation assays, it was determined that neither VIS nor DPU protected leukemia cells from the anti-leukemic effects of doxorubicin. Using the model of doxorubicin-induced cardiotoxicity that discovered the two novel compounds, in combination with our zebrafish XT model, I was able to rapidly evaluate the effect of combinatorial treatment of doxorubicin with cardioprotective agents on T-ALL cell proliferation, while evaluating cardiac function.

CHAPTER 4: DISCUSSION

4.1: FOCUSED CHEMICAL GENOMICS USING ZEBRAFISH XENOTRANSPLANTATION AS A PRECLINICAL THERAPEUTIC PLATFORM FOR T-CELL ACUTE LYMPHOBLASTIC LEUKEMIA

The zebrafish is a powerful vertebrate model of cancer biology. My project set out to build upon the zebrafish xenotransplantation model pioneered by the Dellaire and Berman laboratories (Corkery et al., 2011). In this study, I have demonstrated the feasibility of the zebrafish as a human cancer xenotransplantation (XT) model using both T-ALL cell lines and patient biopsy material. I have also established zebrafish XT as a novel tool for the rapid identification of underlying targetable gene mutations in primary patient samples, as well as a preclinical model well suited to the assessment of known and novel therapeutics for T-ALL. Furthermore, I have demonstrated the utility of the zebrafish XT model to rapidly screen for drug toxicities and to evaluate novel protective compounds using a target-naïve phenotype-based approach.

The paradigm of T-ALL was chosen to evaluate zebrafish XT, as the molecular pathways driving this disease are well characterized and targetable using novel small molecule inhibitors (Paganin & Ferrando, 2011). Zebrafish embryos are an immunopermissive host for human cells, and T-ALL cell lines rapidly engraft and proliferate in the zebrafish. Zebrafish XT recapitulated the *in vitro* responses of three-well characterized T-ALL cell lines to small molecule inhibitors targeting pathways important in T-ALL pathogenesis. Growth in the presence of vehicle or drug was rapidly

quantified using a previously-described method based on the quantification of CM-DiI-labelled human cells (Corkery et al., 2011).

More importantly, biopsy material from two children with T-ALL was successfully engrafted in zebrafish embryos without need of immunosuppression, and primary patient leukemia cells robustly proliferated throughout the experiment. This represents an unprecedented technological advancement over challenging *in vitro* methods for culturing primary patient samples and the costly and time-intensive method of growing primary patient xenografts in highly immunosuppressed and humanized mice. The ability to engraft sorted human acute myeloid leukemia cells in zebrafish embryos has been previously reported by one group, however drug-sensitivity was not evaluated nor prolonged engraftment demonstrated (Pruvot et al., 2011). Here we have built upon previous zebrafish XT efforts by xenografting diagnostic bone marrow samples from children with T-ALL.

Additionally, for the first time, the proliferation of primary T-ALL samples was quantified using the zebrafish XT model. I developed a technique to distinguish human leukemia cells from zebrafish host cell populations, by using fluorescent immunohistochemistry for promyelocytic leukemia (PML) nuclear bodies, which are only present in human cells, and absent from zebrafish cells. I have demonstrated that the response of a patient's leukemia to targeted therapeutics can be accurately and rapidly determined, and that the molecular underpinnings of an individual patient's leukemia can be evaluated using a focused chemical genomics approach.

Specifically, we evaluated the response of the patient-derived lymphoblasts to compound E using zebrafish XT. Using this approach, a mutation that conferred

sensitivity to NOTCH1 inhibition using the γ-secretase inhibitor compound E was identified in patient sample 1. This mutation (p.A1696D) in the C-terminal heterodimerization (HD) domain of patient sample 1 was confirmed by exome sequencing, and was validated as an activating mutation using luciferase assays. This is a therapeutically relevant mutation, as mutations in the HD domain of *NOTCH1* are reported in approximately half of all T-ALLs and confer NOTCH1 activation that is dependent on γ-secretase complex cleavage (Malecki et al., 2006). While these results did not inform patient treatment in this particular case, it was possible to obtain definitive and actionable mutation status to support the potential efficacy of treatment with a γ-secretase inhibitor within just one week following biopsy.

Zebrafish XT can be applied early in the drug developmental pipeline to evaluate and prioritize prospective compounds, and can be used to select candidate compounds to move forward into murine models and human trials. We have demonstrated an *in vivo* method for uncovering patient tumour-drug response using T-ALL biopsy material in an actionable time frame that can inform clinical decision-making. This is aligned with current efforts to provide more personalized and precise cancer therapies, which promise fewer toxicities and shorter times to complete remission.

4.2: ZEBRAFISH XENOTRANSPLANTATION AS A PRECLINICAL THERAPEUTIC PLATFORM TO EVALUATE NOVEL CARDIOPROTECTANT COMPOUNDS

T-ALL is an aggressive disease treated with intensified chemotherapeutic protocols that are associated with significant and life-threatening toxicities. By uncovering novel strategies to minimize these toxicities, zebrafish XT can be used to improve current standard-of-care treatments. Of particular relevance to pediatric T-ALL, zebrafish XT can be used to evaluate cardioprotectants that can block anthracycline-induced cardiac damage. A doxorubicin-induced model of cardiotoxicity in zebrafish formed the basis of a phenotype-based screen undertaken by Dr. Randall Peterson's group, which uncovered two novel cardioprotectant compounds. These compounds, visnagin (VIS) and diphenylurea (DPU), prevent doxorubicin-induced pericardial edema, decreased contractility and apoptosis of cardiomyocytes.

This phenotype-based screen for compounds able to protect against doxorubicin-induced cardiac damage is particularly effective as it is target-naïve. This is important because previous *in vitro* and *in vivo* attempts to discover cardioprotectant agents depended on a thorough understanding of the mechanisms of doxorubicin-induced cardiac damage, which remains controversial. For example, despite the consensus that reactive oxygen species (ROS) produced in part through iron plays an important role in cardiomyocyte apoptosis during doxorubicin treatment (Ichikawa et al., 2014; Simůnek et al., n.d.), antioxidants (e.g. N-acetylcysteine and alpha-tocopherol) and potent iron

chelators (e.g. Deferoxamine) have failed in *in vivo* experiments and clinical trials (Legha et al., 1982; Myers et al., 1983; Neufeld, 2010).

I evaluated the effect of VIS and DPU on doxorubicin-induced leukemia cell death using both an *in vitro* cell viability assay, and the *in vivo* zebrafish human leukemia XT assay. Neither compound prevented doxorubicin-induced cell killing, indicating that it may indeed be possible to separate the chemotherapeutic effects from the cardiotoxic effects of doxorubicin. Using zebrafish XT it was possible to rapidly quantify human drug response to treatment with combinations of doxorubicin and cardioprotectant compounds. This represents the first time that zebrafish human cancer XT has been used to simultaneously screen for toxicities and therapeutic efficiency of combinations of drugs. In summary, Zebrafish XT offers a more realistic setting to evaluate cardioprotectant compounds than *in vitro* systems, and is more rapid and cost-effective than murine models.

4.3: LIMITATIONS AND POTENTIAL PITFALLS

While there are many advantages to performing human XT experiments in zebrafish, there remain limitations to this animal model of human malignancy. Some of these limitations will be overcome in the foreseeable future with advancements in zebrafish XT techniques, while other limitations are inherent to the use of zebrafish (Konantz et al., 2012).

4.3.1 LACK OF ADULT IMMUNE-PERMISSIVE ZEBRAFISH LINES

Zebrafish XT is performed in zebrafish embryos, due to their transparency and immune-permissiveness to human cells. Human cells can be grown in zebrafish embryos without the need for immunosuppression, as the zebrafish lacks a fully functional adaptive immune system until 28 days post fertilization (Haldi et al., 2006; Lam et al., 2004). In particular, the lack of an adaptive immune system may become a limitation to the translation of knowledge from zebrafish XT models to humans, as immune cells likely play important roles in promoting or inhibiting human cancer (Spano, Heck, De Antonellis, Christofori, & Zollo, 2012).

Furthermore, the developing zebrafish represents a fundamentally different environment as compared to adult zebrafish. Differences in vasculature, immune system and growth factors between embryo and adult fish may prove to be relevant to XT models of human disease, and in particular models of adult malignancy. Currently, XT into adult fish requires irradiation of zebrafish or treatment with dexamethasone (Konantz et al., 2012). However, the development of immune-permissive zebrafish lines will permit the XT of human cells into adult fish, and will help to overcome this limitation.

Recently, a *rag2* mutant fish has been developed by Langenau's group, allowing for the engraftment of transgenic T-ALL zebrafish cancer cells into an adult recipient fish (Tang et al., 2014). While XT into adult *rag2* mutant fish remains to be optimized, it is thought that these fish will be an immunopermissive recipient for human cells. Agreement between XT experiments performed in adult fish and embryos could help to determine the relevance of findings in a developing organism.

Furthermore, the relative size of zebrafish cells, vasculature, and organs as compared to larger human cells may also present a technical challenge (Konantz et al., 2012). However, despite theses differences in size, leukemia and sarcoma cells have been able to proliferate, metastasize, and circulate throughout the embryonic vasculature (Corkery et al., 2011; Konantz et al., 2012; Veinotte, Dellaire, & Berman, 2014b).

4.3.2 LIMITATIONS OF ORTHOTOPIC TRANSPLANTATION

Another limitation of the zebrafish XT model is the lack of analogous organs between zebrafish and humans, and therefore a lack of sites to perform othotopic transplantation experiments in. While the experiments in this project used the yolk sac as the site of injection for human cells, increasingly sophisticated XT experiments may desire a higher degree of similarity between the site of injection and the normal location of human disease.

While the zebrafish lack human organs such as the lungs, prostate and breast, it may be possible to overcome these technical limitations through the use of analogous structures. For instance, the zebrafish gills could be used to study lung cancer due to similar degrees of vascularization. Furthermore, humanization of zebrafish embryos

through the co-injection of human cytokines and accessory cells could better recapitulate the human tumour microenvironment. This is an approach that has been successfully been used in mice (Dialynas, Shao, Billman, & Yu, 2001).

4.3.3 DURATION OF EXPERIMENTS

An advantage of zebrafish XT experiments is the short time frame to completion of studies, and rapid readouts. However, the expediency of this model may limit the relevance of certain experiments. Below I will discuss the limitations of the short-term nature of zebrafish XT experiments in the context of the cardioprotective studies.

While there are several significant advantages to the zebrafish model of doxorubicin-induced cardiac damage established by Dr. Peterson's group, this approach ultimately is a model of short-term and high-dose exposure to doxorubicin and acute cardiac-toxicity (Liu et al., 2014). In this model, 24 hpf embryos are treated with high dose doxorubicin for 48 h, which causes a dramatic cardiac phenotype of heart failure. 24 hpf embryos are young and while early cardiogenic processes have occurred by this time point, the embryos still are developing. Both the age of the embryos and acute nature of the doxorubicin treatment represents a limitation to this study.

In the clinic, while some patients do develop acute cardiotoxicity during induction therapy, the majority of patients who experience cardiac toxicity have early/late-onset chronic progressive cardiotoxicity which occurs after longer exposure to doxorubicin, and can occur decades after therapy has been concluded (Deffinger et al., 2006; Lipshultz et al., 2008; Wouters et al., 2005).

This limitation can be overcome through the adoption of longer treatment protocols, as well as the use of murine models. Zebrafish could be treated with lower doses of doxorubicin over a longer period of time, and hearts evaluated phenotypically for pericardial edema, changes in ventricle and atrial structure, decreased contractility, and decreased circulation. While long-term exposure to low-dose doxorubicin likely would not cause as dramatic a phenotype as the acute exposure to high-dose doxorubicin, we hypothesize that changes to cardiac structure will be present. Histological analysis of cardiac structure using hematocylin and eosin stain and immunohistochemistry for markers of apoptosis will help to evaluate cardiac damage.

Furthermore, murine models of cardiac toxicity caused by chronic exposure to doxorubicin can be employed to compliment zebrafish models of cardiotoxicity. Indeed, Liu et al. employed a murine model of chronic doxorubicin exposure to validate the cardiotoxic protectant effects of visnagin and diphenylurea(Liu et al., 2014). Interestingly, this chronic model phenocopied the zebrafish acute model, lending credibility to the use of zebrafish for short-term cardiac-phenotype based screens.

4.4: FUTURE DIRECTIONS

This project provides a compelling rationale for future zebrafish leukemia XT experiments. Below I will outline some of the future directions of this project.

4.4.1 ZEBRAFISH XT TO EVALUATE NOVEL COMBINATION THERAPIES

We have demonstrated that zebrafish XT can be used to evaluate the efficacy of small molecule inhibitors using the paradigm of T-ALL (Bentley et al., 2013). However, while small molecule inhibitors may produce dramatic results in short-term XT studies using established cell lines and even patient samples, they may fail to provide the same benefit in a clinical setting. Indeed, there has been a lack of durable responses to single-agent targeted therapies in many malignancies, due to the development of resistance (Kwong, Heffernan, & Chin, 2013).

We propose that zebrafish XT could be used to evaluate the effect of combination treatment using targeted small molecule inhibitors with standard-of-care chemotherapy drugs, or novel combinations of small molecule inhibitors. Novel combinations of drugs may make therapies more efficient by sensitizing cells to chemotherapy, or by creating synthetic lethalities. Ultimately this could permit lower doses of drugs to be used, and may minimize therapy-related toxicities. Furthermore, combinatorial treatment strategies may also help to circumvent acquired resistance by staying ahead of the tumours ability to adapt to selective drug pressures.

4.4.2: ZEBRAFISH XT TO EVALUATE CARDIOPROTECTANT COMPOUNDS FOR TREATMENT-RELATED CARDIOTOXICITY

To our knowledge, combinatorial treatment with doxorubicin and cardioprotectant compounds in our zebrafish T-ALL XT model is the first instance of combination therapies being used in an zebrafish XT model, and certainly the first application of zebrafish XT in the context of cardioprotection (Liu et al., 2014). While anthracyclines are well documented to cause cardiotoxicity, several commonly used chemotherapeutic agents are also known to cause cardiac damage, and there is a lack of relevant animal models of therapy-induced cardiac damage. For instance, even targeted agents such as tyrosine kinase inhibitors (e.g. dasatinib) may cause off-target damage to normal tissue, resulting in heart failure in a proportion of patients (Force et al., 2007).

We propose that zebrafish screens of chemotherapeutic agents could identify compounds that produce cardiac damage, and could be employed to screen novel cardioprotectant agents, using the paradigm established by Dr. Randall Peterson's group (Liu et al., 2014). Furthermore, zebrafish XT could be used to evaluate the combination of chemotherapeutic agent with cardioprotectant agent. Zebrafish XT offers the ability to ensure that cardioprotectant agents do not diminish the cell killing effect of chemotherapeutic agents, while simultaneously evaluating cardiac toxicities.

4.4.3 ZEBRAFISH XT TO EVALUATE PATIENT DRUG-TUMOUR INTERACTIONS

This study has demonstrated the feasibility of injecting patient biopsy material into zebrafish embryos and screening for drug sensitivities specific to that patient's

particular leukemia. We have shown that zebrafish XT can rapidly uncover sensitivities to small molecule inhibitors, and targetable mutations, specifically in the *NOTCH1* gene. We propose that zebrafish XT could be used in the future to tailor patient therapy in real time, by rapidly evaluating patient tumour-drug interactions in a clinically relevant time frame.

As a proof of principle, we would like to correlate primary patient sample XT responses to conventional chemotherapeutic agents with clinical outcome data from the patients the biopsies were obtained from. Correlations could be made between responses to chemotherapy in the zebrafish XT model with prognostically relevant clinical features of the patient's disease, such as time to complete response (CR) and minimal residual disease (MRD) levels.

Furthermore, we would like to characterize patient samples using flow cytometry before xenotransplantation, and following xenotransplantation and treatment with therapeutics. It would be valuable to understand how a patient's leukemia responds to the selective pressure of drug treatments and would help predict the composition of a relapsed leukemia. Serial transplantation of treated xenografted patient samples would help predict drug sensitivities of relapsed leukemia.

Additionally, we would like to correlate the rate of proliferation of human cells in the zebrafish with the aggressiveness of patient disease. Dr. John Dick's group has established an assay to correlate the aggressiveness of human disease using a mouse XT model. In their model, the rate of engraftment and proliferation of human cells in mice has been correlated with important clinical parameters and overall prognosis, and samples from patients that had more rapid engraftment and proliferation had more aggressive

disease (Kennedy et al., 2013). However murine models may not produce results in a clinically relevant timeframe, as there is a much longer engraftment time for mouse xenografts. Therefore we propose that zebrafish XT could be a rapid readout for patient prognosis and risk assessment. Furthermore, we would like to evaluate combination therapy with primary patient sample zebrafish XT, as a way to determine clinically effective drug combinations. Indeed, such a "systems biology approach" to personalizing patient therapy has been proposed using murine models (Kwong et al., 2013), however we foresee zebrafish XT as being a more efficient and cost-effective system.

4.5: CONCLUSIONS

In conclusion, this project has employed the paradigm of T-ALL, a molecularly heterogeneous disease with defined and targetable molecular underpinnings, to develop the zebrafish human leukemia XT model pioneered by our laboratories. Human cells engraft and proliferate in the zebrafish embryo, and human tumour-drug response can be rapidly quantified.

I have demonstrated that T-ALL cell lines with defined mutations in *NOTCH1* and *PTEN* have differential *in vitro* responses to targeted inhibition of Notch, mTOR and AKT, and that these responses can be recapitulated *in vivo*. Furthermore, I have successfully engrafted primary T-ALL bone marrow samples from pediatric T-ALL patients in the zebrafish XT model, and through a functional genomics approach have identified a targetable *NOTCH1* mutation that confers sensitivity to Notch inhibition using a GSI. Additionally, for the first time, this particular mutation has been correlated with a gain of function in Notch transcriptional activation.

Finally, in this project, the zebrafish XT model has been applied to the evaluation of therapy-related toxicities. Zebrafish XT with human cells was used to screen for cardiactoxicity caused by doxorubicin, and the effect of novel cardioprotectant agents on cardiac function and the cell killing effect of doxorubicin was determined.

The zebrafish XT model permits a rapid read out of the efficacy and toxicity of both conventional therapeutics and novel compounds. This project has set the stage for subsequent experiments. We hope to employ this robust model to rapidly and efficiently evaluate novel therapeutic agents for T-ALL, and extend this model to the clinic where it

can be used to evaluate patient-drug response and help inform personalized treatment strategies in a clinically actionable timeframe.

REFERENCES

Al-Nasiry, S., Geusens, N., Hanssens, M., Luyten, C., & Pijnenborg, R. (2007). The use of Alamar Blue assay for quantitative analysis of viability, migration and invasion of choriocarcinoma cells. *Human Reproduction (Oxford, England)*, *22*(5), 1304–9. doi:10.1093/humrep/dem011

Amylon, M. D., Shuster, J., Pullen, J., Berard, C., Link, M. P., Wharam, M., … Murphy, S. B. (1999). Intensive high-dose asparaginase consolidation improves survival for pediatric patients with T cell acute lymphoblastic leukemia and advanced stage lymphoblastic lymphoma: a Pediatric Oncology Group study. *Leukemia*, *13*(3), 335–42. Retrieved from http://www.ncbi.nlm.nih.gov/pubmed/10086723

Armstrong, F., Brunet de la Grange, P., Gerby, B., Rouyez, M.-C., Calvo, J., Fontenay, M., … Pflumio, F. (2009). NOTCH is a key regulator of human T-cell acute leukemia initiating cell activity. *Blood*, *113*(8), 1730–40. doi:10.1182/blood-2008-02-138172

Asselin, B. L., Devidas, M., Wang, C., Pullen, J., Borowitz, M. J., Hutchison, R., … Camitta, B. M. (2011). Effectiveness of high-dose methotrexate in T-cell lymphoblastic leukemia and advanced-stage lymphoblastic lymphoma: a randomized study by the Children's Oncology Group (POG 9404). *Blood*, *118*(4), 874–83. doi:10.1182/blood-2010-06-292615

Bailis, W., & Pear, W. S. (2012). Notch and PI3K: how is the road traveled? *Blood*, *120*(7), 1349–1350.

Barrett, A. J., Horowitz, M. M., Pollock, B. H., Zhang, M. J., Bortin, M. M., Buchanan, G. R., … Rowlings, P. A. (1994). Bone marrow transplants from HLA-identical siblings as compared with chemotherapy for children with acute lymphoblastic leukemia in a second remission. *The New England Journal of Medicine*, *331*(19), 1253–8. doi:10.1056/NEJM199411103311902

Bartel, D. P. (2009). MicroRNAs: target recognition and regulatory functions. *Cell*, *136*(2), 215–33. doi:10.1016/j.cell.2009.01.002

Bellacosa, A., Testa, J. R., Moore, R., & Larue, L. (2004). A portrait of AKT kinases: human cancer and animal models depict a family with strong individualities. *Cancer Biology & Therapy*, *3*(3), 268–75. Retrieved from http://www.ncbi.nlm.nih.gov/pubmed/15034304

Bentley, V. L., Veinotte, C. J., Corkery, D., Leblanc, M. A., Bedard, K., Weng, A. P., … Berman, J. N. (2013). Zebrafish Xenotransplantation and Focused Chemical Genomics: A Preclinical Therapeutic Model For T-Cell Acute Lymphoblastic Leukemia. *Blood*, *122*(21), 2670–. Retrieved from http://bloodjournal.hematologylibrary.org/content/122/21/2670

Berthiaume, J. M., & Wallace, K. B. (2007). Adriamycin-induced oxidative mitochondrial cardiotoxicity. *Cell Biology and Toxicology*, *23*(1), 15–25. doi:10.1007/s10565-006-0140-y

Beverloo, H. B., Langerak, A. W., Poulsen, T. S., Kamps, W. A., & Noesel, M. M. Van. (2006). The Outcome of mulecular-cytogenetic subgroups in pediatric T-cell acute

lymphoblastic leukemia: a retrospective study of patients treated according to DCOG or COALL protocols. *Hematologica*, (91), 1212–1221.

Beverly, L. J., Felsher, D. W., & Capobianco, A. J. (2005). Suppression of p53 by Notch in lymphomagenesis: implications for initiation and regression. *Cancer Research*, *65*(16), 7159–68. doi:10.1158/0008-5472.CAN-05-1664

Bigas, A., & Espinosa, L. (2012). Hematopoietic stem cells: to be or Notch to be. *Blood*, *119*(14), 3226–35. doi:10.1182/blood-2011-10-355826

Bigas, A., Guiu, J., & Gama-Norton, L. (2013). Notch and Wnt signaling in the emergence of hematopoietic stem cells. *Blood Cells, Molecules & Diseases*, *51*(4), 264–70. doi:10.1016/j.bcmd.2013.07.005

Blanco, J. G., Sun, C.-L., Landier, W., Chen, L., Esparza-Duran, D., Leisenring, W., … Bhatia, S. (2012). Anthracycline-related cardiomyopathy after childhood cancer: role of polymorphisms in carbonyl reductase genes--a report from the Children's Oncology Group. *Journal of Clinical Oncology : Official Journal of the American Society of Clinical Oncology*, *30*(13), 1415–21. doi:10.1200/JCO.2011.34.8987

Bleyer, W. A., Sather, H. N., Nickerson, H. J., Coccia, P. F., Finklestein, J. Z., Miller, D. R., … Hammond, G. D. (1991). Monthly pulses of vincristine and prednisone prevent bone marrow and testicular relapse in low-risk childhood acute lymphoblastic leukemia: a report of the CCG-161 study by the Childrens Cancer Study Group. *Journal of Clinical Oncology : Official Journal of the American*

Society of Clinical Oncology, *9*(6), 1012–21. Retrieved from http://www.ncbi.nlm.nih.gov/pubmed/2033414

Bonnet, D., & Dick, J. E. (1997). Human acute myeloid leukemia is organized as a hierarchy that originates from a primitive hematopoietic cell. *Nature Medicine*, *3*(7), 730–7. Retrieved from http://www.ncbi.nlm.nih.gov/pubmed/9212098

Bostrom, B., Uppal, P., Chu, J., Messinger, Y., Gandrud, L., & McEvoy, R. (2013). Safety and efficacy of metformin for therapy-induced hyperglycemia in children with acute lymphoblastic leukemia. *Journal of Pediatric Hematology/oncology*, *35*(7), 504–8. doi:10.1097/MPH.0b013e31829cdeba

Bray, S. J. (2006). Notch signalling: a simple pathway becomes complex. *Nature Reviews. Molecular Cell Biology*, *7*(9), 678–89. doi:10.1038/nrm2009

Butler, J. M., Nolan, D. J., Vertes, E. L., Varnum-Finney, B., Kobayashi, H., Hooper, A. T., … Rafii, S. (2010). Endothelial cells are essential for the self-renewal and repopulation of Notch-dependent hematopoietic stem cells. *Cell Stem Cell*, *6*(3), 251–64. doi:10.1016/j.stem.2010.02.001

Cancer Research UK. (2013, May 9). Long term side effects of ALL treatment. Cancer Research UK. Retrieved from http://www.cancerresearchuk.org/cancer-help/type/all/treatment/Sideeffects/long-term-side-effects-of-ALL-treatment#children

Chan, S. M., Weng, A. P., Tibshirani, R., Aster, J. C., & Utz, P. J. (2007a). Notch signals positively regulate activity of the mTOR pathway in T-cell acute lymphoblastic leukemia. *Blood*, *110*(1), 278–86. doi:10.1182/blood-2006-08-039883

Chan, S. M., Weng, A. P., Tibshirani, R., Aster, J. C., & Utz, P. J. (2007b). Notch signals positively regulate activity of the mTOR pathway in T-cell acute lymphoblastic leukemia. *Blood*, *110*(1), 278–86. doi:10.1182/blood-2006-08-039883

Cheng, H., Kari, G., Dicker, A. P., Rodeck, U., Koch, W. J., & Force, T. (2011). A novel preclinical strategy for identifying cardiotoxic kinase inhibitors and mechanisms of cardiotoxicity. *Circulation Research*, *109*(12), 1401–9. doi:10.1161/CIRCRESAHA.111.255695

Chiu, P. P. L., Jiang, H., & Dick, J. E. (2010). Leukemia-initiating cells in human T-lymphoblastic leukemia exhibit glucocorticoid resistance. *Blood*, *116*(24), 5268–79. doi:10.1182/blood-2010-06-292300

Cho, H., Mu, J., Kim, J. K., Thorvaldsen, J. L., Chu, Q., Crenshaw, E. B., … Birnbaum, M. J. (2001). Insulin resistance and a diabetes mellitus-like syndrome in mice lacking the protein kinase Akt2 (PKB beta). *Science (New York, N.Y.)*, *292*(5522), 1728–31. doi:10.1126/science.292.5522.1728

Ciofani, M., & Zúñiga-Pflücker, J. C. (2005). Notch promotes survival of pre-T cells at the beta-selection checkpoint by regulating cellular metabolism. *Nature Immunology*, *6*(9), 881–8. doi:10.1038/ni1234

Clappier, E., Collette, S., Grardel, N., Girard, S., Suarez, L., Brunie, G., … Cavé, H. (2010). NOTCH1 and FBXW7 mutations have a favorable impact on early response to treatment, but not on outcome, in children with T-cell acute lymphoblastic leukemia (T-ALL) treated on EORTC trials 58881 and 58951. *Leukemia*, *24*(12), 2023–31. doi:10.1038/leu.2010.205

Clements, W. K., Kim, A. D., Ong, K. G., Moore, J. C., Lawson, N. D., & Traver, D. (2011). A somitic Wnt16/Notch pathway specifies haematopoietic stem cells. *Nature*, *474*(7350), 220–4. doi:10.1038/nature10107

Corkery, D. P., Dellaire, G., & Berman, J. N. (2011). Leukaemia xenotransplantation in zebrafish--chemotherapy response assay in vivo. *British Journal of Haematology*, *153*(6), 786–9. doi:10.1111/j.1365-2141.2011.08661.x

Cullion, K., Draheim, K. M., Hermance, N., Tammam, J., Sharma, V. M., Ware, C., … Kelliher, M. A. (2009). Targeting the Notch1 and mTOR pathways in a mouse T-ALL model. *Blood*, *113*(24), 6172–81. doi:10.1182/blood-2008-02-136762

Cully, M., You, H., Levine, A. J., & Mak, T. W. (2006). Beyond PTEN mutations: the PI3K pathway as an integrator of multiple inputs during tumorigenesis. *Nature Reviews. Cancer*, *6*(3), 184–192. doi:10.1038/nrc1819

Da'as, S. I., Coombs, A. J., Balci, T. B., Grondin, C. A., Ferrando, A. A., & Berman, J. N. (2012). The zebrafish reveals dependence of the mast cell lineage on Notch signaling in vivo. *Blood*, *119*(15), 3585–94. doi:10.1182/blood-2011-10-385989

Das, I., Craig, C., Funahashi, Y., Jung, K.-M., Kim, T.-W., Byers, R., … Kitajewski, J. (2004). Notch oncoproteins depend on gamma-secretase/presenilin activity for processing and function. *The Journal of Biological Chemistry*, *279*(29), 30771–80. doi:10.1074/jbc.M309252200

DeAngelo, D. J., Stone, R. M., Silverman, L. B., Stock, W., Attar, E. C., Fearen, I., … Aster, J. (2006). A phase I clinical trial of the notch inhibitor MK-0752 in patients with T-cell acute lymphoblastic leukemia/lymphoma (T-ALL) and other leukemias -- Deangelo et al. 24 (18 Supplement): 6585 -- ASCO Meeting Abstracts. *Journal of Clinical Oncology : 2006 ASCO ANnual Meedting Proceedings*, *24*. Retrieved from http://meeting.ascopubs.org/cgi/content/short/24/18_suppl/6585

Deffinger, K., Mertens, A., Sklar, C., Kawashima, T., Hudson, M., Meadows, A., … Robison, L. (2006). Chronic Health Conditions in Adult Survivors of Childhood Cancer — NEJM. *N Engl J Med*. Retrieved June 03, 2014, from http://www.nejm.org/doi/full/10.1056/NEJMsa060185

Delaney, C., Heimfeld, S., Brashem-Stein, C., Voorhies, H., Manger, R. L., & Bernstein, I. D. (2010). Notch-mediated expansion of human cord blood progenitor cells capable of rapid myeloid reconstitution. *Nature Medicine*, *16*(2), 232–6. doi:10.1038/nm.2080

Demarest, R. M., Ratti, F., & Capobianco, A. J. (2008). It's T-ALL about Notch. *Oncogene*, *27*(38), 5082–91. doi:10.1038/onc.2008.222

Dialynas, D. P., Shao, L., Billman, G. F., & Yu, J. (2001). Engraftment of human T-cell acute lymphoblastic leukemia in immunodeficient NOD/SCID mice which have been preconditioned by injection of human cord blood. *Stem Cells (Dayton, Ohio)*, *19*(5), 443–52. doi:10.1634/stemcells.19-5-443

Dick, J. E., & Lapidot, T. (2005). Biology of normal and acute myeloid leukemia stem cells. *International Journal of Hematology*, *82*(5), 389–96. doi:10.1532/IJH97.05144

Downing, J. R. (2011). A New FOXO Pathway Required for Leukemogenesis. *Cell*, *146*(5), 669–670. doi:10.1016/j.cell.2011.08.019

Doyon, Y., McCammon, J. M., Miller, J. C., Faraji, F., Ngo, C., Katibah, G. E., … Amacher, S. L. (2008). Heritable targeted gene disruption in zebrafish using designed zinc-finger nucleases. *Nature Biotechnology*, *26*(6), 702–8. doi:10.1038/nbt1409

Dzierzak, E., & Speck, N. A. (2008). Of lineage and legacy: the development of mammalian hematopoietic stem cells. *Nature Immunology*, *9*(2), 129–36. doi:10.1038/ni1560

Eden, T. O. B., Pieters, R., & Richards, S. (2010). Systematic review of the addition of vincristine plus steroid pulses in maintenance treatment for childhood acute lymphoblastic leukaemia - an individual patient data meta-analysis involving 5,659 children. *British Journal of Haematology*, *149*(5), 722–33. doi:10.1111/j.1365-2141.2010.08148.x

Elihu, N., Anandasbapathy, S., & Frishman, W. H. (1998). Chelation therapy in cardiovascular disease: ethylenediaminetetraacetic acid, deferoxamine, and dexrazoxane. *Journal of Clinical Pharmacology*, *38*(2), 101–5. Retrieved from http://www.ncbi.nlm.nih.gov/pubmed/9549639

Ellisen, L. W., Bird, J., West, D. C., Soreng, A. L., Reynolds, T. C., Smith, S. D., & Sklar, J. (1991). TAN-1, the human homolog of the Drosophila notch gene, is broken by chromosomal translocations in T lymphoblastic neoplasms. *Cell*, *66*(4), 649–61. Retrieved from http://www.ncbi.nlm.nih.gov/pubmed/1831692

Emamian, E. S., Hall, D., Birnbaum, M. J., Karayiorgou, M., & Gogos, J. A. (2004). Convergent evidence for impaired AKT1-GSK3beta signaling in schizophrenia. *Nature Genetics*, *36*(2), 131–7. doi:10.1038/ng1296

Eng, C. (2003). PTEN: one gene, many syndromes. *Human Mutation*, *22*(3), 183–98. doi:10.1002/humu.10257

Escrivà, M., Peiró, S., Herranz, N., Villagrasa, P., Dave, N., Montserrat-Sentís, B., … García de Herreros, A. (2008). Repression of PTEN phosphatase by Snail1 transcriptional factor during gamma radiation-induced apoptosis. *Molecular and Cellular Biology*, *28*(5), 1528–40. doi:10.1128/MCB.02061-07

Feitsma, H., & Cuppen, E. (2008). Zebrafish as a cancer model. *Molecular Cancer Research : MCR*, *6*(5), 685–94. doi:10.1158/1541-7786.MCR-07-2167

Ferrando, A. (2010). NOTCH mutations as prognostic markers in T-ALL. *Leukemia*, *24*(12), 2003–4. doi:10.1038/leu.2010.237

Ferrando, A. A. (2009). The role of NOTCH1 signaling in T-ALL. *Hematology / the Education Program of the American Society of Hematology. American Society of Hematology. Education Program*, 353–61. doi:10.1182/asheducation-2009.1.353

Force, T., Krause, D. S., & Van Etten, R. A. (2007). Molecular mechanisms of cardiotoxicity of tyrosine kinase inhibition. *Nature Reviews. Cancer*, *7*(5), 332–44. doi:10.1038/nrc2106

Fryer, C. J., White, J. B., & Jones, K. A. (2004). Mastermind recruits CycC:CDK8 to phosphorylate the Notch ICD and coordinate activation with turnover. *Molecular Cell*, *16*(4), 509–20. doi:10.1016/j.molcel.2004.10.014

Garofalo, R. S., Orena, S. J., Rafidi, K., Torchia, A. J., Stock, J. L., Hildebrandt, A. L., … Coleman, K. G. (2003). Severe diabetes, age-dependent loss of adipose tissue, and mild growth deficiency in mice lacking Akt2/PKB beta. *The Journal of Clinical Investigation*, *112*(2), 197–208. doi:10.1172/JCI16885

Gaynon, P. S., Bleyer, W. A., Steinherz, P. G., Finklestein, J. Z., Littman, P. S., Miller, D. R., … Hammond, G. D. (1988). Modified BFM therapy for children with previously untreated acute lymphoblastic leukemia and unfavorable prognostic features. Report of Children's Cancer Study Group Study CCG-193P. *The American Journal of Pediatric Hematology/oncology*, *10*(1), 42–50. Retrieved from http://www.ncbi.nlm.nih.gov/pubmed/3056061

Goldberg, J. M., Silverman, L. B., Levy, D. E., Dalton, V. K., Gelber, R. D., Lehmann, L., … Asselin, B. L. (2003). Childhood T-cell acute lymphoblastic leukemia: the Dana-Farber Cancer Institute acute lymphoblastic leukemia consortium experience. *Journal of Clinical Oncology : Official Journal of the American Society of Clinical Oncology*, *21*(19), 3616–22. doi:10.1200/JCO.2003.10.116

Gorello, P., La Starza, R., Varasano, E., Chiaretti, S., Elia, L., Pierini, V., … Mecucci, C. (2010). Combined interphase fluorescence in situ hybridization elucidates the genetic heterogeneity of T-cell acute lymphoblastic leukemia in adults. *Haematologica*, *95*(1), 79–86. doi:10.3324/haematol.2009.010413

Grabher, C., von Boehmer, H., & Look, a T. (2006). Notch 1 activation in the molecular pathogenesis of T-cell acute lymphoblastic leukaemia. *Nature Reviews. Cancer*, *6*(5), 347–59. Retrieved from http://www.ncbi.nlm.nih.gov/pubmed/16612405

Graux, C., Cools, J., Melotte, C., Quentmeier, H., Ferrando, A., Levine, R., … Hagemeijer, A. (2004). Fusion of NUP214 to ABL1 on amplified episomes in T-cell acute lymphoblastic leukemia. *Nature Genetics*, *36*(10), 1084–1089. Retrieved from http://www.ncbi.nlm.nih.gov/pubmed/15361874

Gupta, M., Hendrickson, A. E. W., Yun, S. S., Han, J. J., Schneider, P. A., Koh, B. D., … Kaufmann, S. H. (2012). Dual mTORC1/mTORC2 inhibition diminishes Akt activation and induces Puma-dependent apoptosis in lymphoid malignancies. *Blood*. doi:10.1182/blood-2011-04-346601

Gupta-Rossi, N., Six, E., LeBail, O., Logeat, F., Chastagner, P., Olry, A., … Brou, C. (2004). Monoubiquitination and endocytosis direct gamma-secretase cleavage of activated Notch receptor. *The Journal of Cell Biology*, *166*(1), 73–83. doi:10.1083/jcb.200310098

Gutierrez, A., Grebliunaite, R., Feng, H., Kozakewich, E., Zhu, S., Guo, F., … Look, A. T. (2011). Pten mediates Myc oncogene dependence in a conditional zebrafish model of T cell acute lymphoblastic leukemia. *The Journal of Experimental Medicine*, *208*(8), 1595–1603. Retrieved from http://discovery.ucl.ac.uk/1348789/

Hagemeijer, A., & Graux, C. (2010). ABL1 Rearrangements in T -Cell Acute Lymphoblastic Leukemia, *308*(November 2009), 299–308. doi:10.1002/gcc

Haldi, M., Ton, C., Seng, W. L., & McGrath, P. (2006). Human melanoma cells transplanted into zebrafish proliferate, migrate, produce melanin, form masses and stimulate angiogenesis in zebrafish. *Angiogenesis*, *9*(3), 139–51. doi:10.1007/s10456-006-9040-2

Hamalainen-Laanaya, H. K., & Orloff, M. S. (2012). Analysis of cell viability using time-dependent increase in fluorescence intensity. *Analytical Biochemistry*, *429*(1), 32–8. doi:10.1016/j.ab.2012.07.006

Han, H., Tanigaki, K., Yamamoto, N., Kuroda, K., Yoshimoto, M., Nakahata, T., … Honjo, T. (2002). Inducible gene knockout of transcription factor recombination signal binding protein-J reveals its essential role in T versus B lineage decision.

International Immunology, *14*(6), 637–45. Retrieved from http://www.ncbi.nlm.nih.gov/pubmed/12039915

Hasinoff, B. B., & Herman, E. H. (2007). Dexrazoxane: how it works in cardiac and tumor cells. Is it a prodrug or is it a drug? *Cardiovascular Toxicology*, *7*(2), 140–4. doi:10.1007/s12012-007-0023-3

Higuchi, R., Krummel, B., & Saiki, R. K. (1988). A general method of in vitro preparation and specific mutagenesis of DNA fragments: study of protein and DNA interactions. *Nucleic Acids Research*, *16*(15), 7351–67. Retrieved from http://www.pubmedcentral.nih.gov/articlerender.fcgi?artid=338413&tool=pmcentrez&rendertype=abstract

Hildebrandt, M. A. T., Yang, H., Hung, M.-C., Izzo, J. G., Huang, M., Lin, J., … Wu, X. (2009). Genetic variations in the PI3K/PTEN/AKT/mTOR pathway are associated with clinical outcomes in esophageal cancer patients treated with chemoradiotherapy. *Journal of Clinical Oncology : Official Journal of the American Society of Clinical Oncology*, *27*(6), 857–71. doi:10.1200/JCO.2008.17.6297

Hirsch, E., & Chiarle, R. (2012). CALming Down T Cell Acute Leukemia. *Cancer Cell*. doi:10.1016/j.ccr.2012.03.025

Hof, J., Krentz, S., van Schewick, C., Körner, G., Shalapour, S., Rhein, P., … Kirschner-Schwabe, R. (2011). Mutations and deletions of the TP53 gene predict nonresponse to treatment and poor outcome in first relapse of childhood acute lymphoblastic

leukemia. *Journal of Clinical Oncology : Official Journal of the American Society of Clinical Oncology*, *29*(23), 3185–93. doi:10.1200/JCO.2011.34.8144

Hollander, M. C., Blumenthal, G. M., & Dennis, P. A. (2011). PTEN loss in the continuum of common cancers, rare syndromes and mouse models. *Nature Reviews. Cancer*, *11*(4), 289–301. doi:10.1038/nrc3037

Howard, S. C., & Pui, C.-H. (2002). Endocrine complications in pediatric patients with acute lymphoblastic leukemia. *Blood Reviews*, *16*(4), 225–43. Retrieved from http://www.ncbi.nlm.nih.gov/pubmed/12350366

Huang, P., Xiao, A., Zhou, M., Zhu, Z., Lin, S., & Zhang, B. (2011). Heritable gene targeting in zebrafish using customized TALENs. *Nature Biotechnology*, *29*(8), 699–700. doi:10.1038/nbt.1939

Huang, W.-C., & Hung, M.-C. (2009). Induction of Akt activity by chemotherapy confers acquired resistance. *Journal of the Formosan Medical Association = Taiwan Yi Zhi*, *108*(3), 180–94. doi:10.1016/S0929-6646(09)60051-6

Hunger, S. P., Lu, X., Devidas, M., Camitta, B. M., Gaynon, P. S., Winick, N. J., … Carroll, W. L. (2012). Improved survival for children and adolescents with acute lymphoblastic leukemia between 1990 and 2005: a report from the children's oncology group. *Journal of Clinical Oncology : Official Journal of the American Society of Clinical Oncology*, *30*(14), 1663–9. doi:10.1200/JCO.2011.37.8018

Huntly, B. J. P., & Gilliland, D. G. (2005). Leukaemia stem cells and the evolution of cancer-stem-cell research. *Nature Reviews. Cancer*, *5*(4), 311–21. doi:10.1038/nrc1592

Hutchcroft, S., Clarke, A., & Mao, Y. (1995). *This Battle Which I Must Fight. Cancer in Canada's Children and Teenagers.* Public Health Agency of Canada.

Hwang, W. Y., Fu, Y., Reyon, D., Maeder, M. L., Tsai, S. Q., Sander, J. D., … Joung, J. K. (2013). Efficient genome editing in zebrafish using a CRISPR-Cas system. *Nature Biotechnology*, *31*(3), 227–229. doi:10.1038/nbt.2501

Ichikawa, Y., Bayeva, M., Ghanefar, M., Potini, V., Sun, L., Mutharasan, R. K., … Ardehali, H. (2012). Disruption of ATP-binding cassette B8 in mice leads to cardiomyopathy through a decrease in mitochondrial iron export. *Proceedings of the National Academy of Sciences of the United States of America*, *109*(11), 4152–7. doi:10.1073/pnas.1119338109

Ichikawa, Y., Ghanefar, M., Bayeva, M., Wu, R., Khechaduri, A., Naga Prasad, S. V, … Ardehali, H. (2014). Cardiotoxicity of doxorubicin is mediated through mitochondrial iron accumulation. *The Journal of Clinical Investigation*, *124*(2), 617–30. doi:10.1172/JCI72931

Ince, T. A., Richardson, A. L., Bell, G. W., Saitoh, M., Godar, S., Karnoub, A. E., … Weinberg, R. A. (2007). Transformation of different human breast epithelial cell types leads to distinct tumor phenotypes. *Cancer Cell*, *12*(2), 160–70. doi:10.1016/j.ccr.2007.06.013

Jacinto, E., Loewith, R., Schmidt, A., Lin, S., Rüegg, M. A., Hall, A., & Hall, M. N. (2004). Mammalian TOR complex 2 controls the actin cytoskeleton and is rapamycin insensitive. *Nature Cell Biology*, *6*(11), 1122–8. doi:10.1038/ncb1183

Jotta, P. Y., Ganazza, M. a, Silva, a, Viana, M. B., da Silva, M. J., Zambaldi, L. J. G., … Yunes, J. a. (2010). Negative prognostic impact of PTEN mutation in pediatric T-cell acute lymphoblastic leukemia. *Leukemia*, *24*(1), 239–42. doi:10.1038/leu.2009.209

Jung, D.-W., Oh, E.-S., Park, S.-H., Chang, Y.-T., Kim, C.-H., Choi, S.-Y., & Williams, D. R. (2012). A novel zebrafish human tumor xenograft model validated for anti-cancer drug screening. *Molecular bioSystems*, *8*(7), 1930–9. doi:10.1039/c2mb05501e

Kalaany, N. Y., & Sabatini, D. M. (2009). Tumours with PI3K activation are resistant to dietary restriction. *Nature*, *458*(7239), 725–31. doi:10.1038/nature07782

Kalender Atak, Z., De Keersmaecker, K., Gianfelici, V., Geerdens, E., Vandepoel, R., Pauwels, D., … Aerts, S. (2012). High accuracy mutation detection in leukemia on a selected panel of cancer genes. *PloS One*, *7*(6), e38463. doi:10.1371/journal.pone.0038463

Kao, H. Y., Ordentlich, P., Koyano-Nakagawa, N., Tang, Z., Downes, M., Kintner, C. R., … Kadesch, T. (1998). A histone deacetylase corepressor complex regulates the Notch signal transduction pathway. *Genes & Development*, *12*(15), 2269–77. Retrieved from

http://www.pubmedcentral.nih.gov/articlerender.fcgi?artid=317043&tool=pmcentrez&rendertype=abstract

Keizer, H. G., Pinedo, H. M., Schuurhuis, G. J., & Joenje, H. (1990). Doxorubicin (adriamycin): a critical review of free radical-dependent mechanisms of cytotoxicity. *Pharmacology & Therapeutics*, *47*(2), 219–31. Retrieved from http://www.ncbi.nlm.nih.gov/pubmed/2203071

Kennedy, J. A., Mitchell, A., Chen, W. C., McLeod, J., Popescu, A. C., Arruda, A., … Wang, J. C. Y. (2013). Leukemic Engraftment In NOD.SCID Mice Is Correlated With Clinical Parameters and Predicts Outcome In Human AML. *Blood*, *122*(21), 50–. Retrieved from http://bloodjournal.hematologylibrary.org/content/122/21/50.short

Kimmel, C. B., Ballard, W. W., Kimmel, S. R., Ullmann, B., & Schilling, T. F. (1995). Stages of embryonic development of the zebrafish. *Developmental Dynamics : An Official Publication of the American Association of Anatomists*, *203*(3), 253–310. doi:10.1002/aja.1002030302

Koch, U., & Radtke, F. (2011). Mechanisms of T cell development and transformation. *Annual Review of Cell and Developmental Biology*, *27*, 539–62. doi:10.1146/annurev-cellbio-092910-154008

Konantz, M., Balci, T. B., Hartwig, U. F., Dellaire, G., André, M. C., Berman, J. N., & Lengerke, C. (2012). Zebrafish xenografts as a tool for in vivo studies on human

cancer. *Annals of the New York Academy of Sciences*, *1266*(1), 124–37. doi:10.1111/j.1749-6632.2012.06575.x

Krampera, M., Vitale, A., Vincenzi, C., Perbellini, O., Guarini, A., Annino, L., … Pizzolo, G. (2003). Outcome prediction by immunophenotypic minimal residual disease detection in adult T-cell acute lymphoblastic leukaemia. *British Journal of Haematology*, *120*(1), 74–9. Retrieved from http://www.ncbi.nlm.nih.gov/pubmed/12492579

Kumano, K., Chiba, S., Kunisato, A., Sata, M., Saito, T., Nakagami-Yamaguchi, E., … Hirai, H. (2003). Notch1 but not Notch2 is essential for generating hematopoietic stem cells from endothelial cells. *Immunity*, *18*(5), 699–711. Retrieved from http://www.ncbi.nlm.nih.gov/pubmed/12753746

Kwong, L. N., Heffernan, T. P., & Chin, L. (2013). A systems biology approach to personalizing therapeutic combinations. *Cancer Discovery*, *3*(12), 1339–44. doi:10.1158/2159-8290.CD-13-0394

La Starza, R., Lettieri, A., Pierini, V., Nofrini, V., Gorello, P., Songia, S., … Mecucci, C. (2013). Linking genomic lesions with minimal residual disease improves prognostic stratification in children with T-cell acute lymphoblastic leukaemia. *Leukemia Research*, *37*(8), 928–35. doi:10.1016/j.leukres.2013.04.005

Lam, S. H., Chua, H. L., Gong, Z., Lam, T. J., & Sin, Y. M. (2004). Development and maturation of the immune system in zebrafish, Danio rerio: a gene expression profiling, in situ hybridization and immunological study. *Developmental and*

Comparative Immunology, *28*(1), 9–28. Retrieved from http://www.ncbi.nlm.nih.gov/pubmed/12962979

Langenau, D. M., Traver, D., Ferrando, A. A., Kutok, J. L., Aster, J. C., Kanki, J. P., … Look, A. T. (2003). Myc-induced T cell leukemia in transgenic zebrafish. *Science (New York, N.Y.)*, *299*(5608), 887–90. doi:10.1126/science.1080280

Lapidot, T., Sirard, C., Vormoor, J., Murdoch, B., Hoang, T., Caceres-Cortes, J., … Dick, J. E. (1994). A cell initiating human acute myeloid leukaemia after transplantation into SCID mice. *Nature*, *367*(6464), 645–8. doi:10.1038/367645a0

Leclerc, G. M., Leclerc, G. J., Kuznetsov, J. N., DeSalvo, J., & Barredo, J. C. (2013). Metformin induces apoptosis through AMPK-dependent inhibition of UPR signaling in ALL lymphoblasts. *PloS One*, *8*(8), e74420. doi:10.1371/journal.pone.0074420

Lee, L. M. J., Seftor, E. A., Bonde, G., Cornell, R. A., & Hendrix, M. J. C. (2005). The fate of human malignant melanoma cells transplanted into zebrafish embryos: assessment of migration and cell division in the absence of tumor formation. *Developmental Dynamics : An Official Publication of the American Association of Anatomists*, *233*(4), 1560–70. doi:10.1002/dvdy.20471

Legha, S. S., Wang, Y. M., Mackay, B., Ewer, M., Hortobagyi, G. N., Benjamin, R. S., & Ali, M. K. (1982). Clinical and pharmacologic investigation of the effects of alpha-tocopherol on adriamycin cardiotoxicity. *Annals of the New York Academy of Sciences*, *393*, 411–8. Retrieved from http://www.ncbi.nlm.nih.gov/pubmed/6959564

Lipshultz, S. E., Alvarez, J. A., & Scully, R. E. (2008). Anthracycline associated cardiotoxicity in survivors of childhood cancer. *Heart (British Cardiac Society)*, *94*(4), 525–33. doi:10.1136/hrt.2007.136093

Lipshultz, S. E., Cochran, T. R., Franco, V. I., & Miller, T. L. (2013). Treatment-related cardiotoxicity in survivors of childhood cancer. *Nature Reviews. Clinical Oncology*, *10*(12), 697–710. doi:10.1038/nrclinonc.2013.195

Lipshultz, S. E., Scully, R. E., Lipsitz, S. R., Sallan, S. E., Silverman, L. B., Miller, T. L., … Colan, S. D. (2010). Assessment of dexrazoxane as a cardioprotectant in doxorubicin-treated children with high-risk acute lymphoblastic leukaemia: long-term follow-up of a prospective, randomised, multicentre trial. *The Lancet Oncology*, *11*(10), 950–61. doi:10.1016/S1470-2045(10)70204-7

Liu, Y., Asnani, A., Zou, L., Bentley, V. L., Yu, M., Wang, Y., … Peterson, R. T. (2014). Visnagin protects against doxorubicin-induced cardiomyopathy through inhibtion of mitochondrial malate dehydrogenase. *In Submission*.

Lobry, C., Ntziachristos, P., Ndiaye-Lobry, D., Oh, P., Cimmino, L., Zhu, N., … Aifantis, I. (2013). Notch pathway activation targets AML-initiating cell homeostasis and differentiation. *The Journal of Experimental Medicine*, *210*(2), 301–19. doi:10.1084/jem.20121484

Lobry, C., Oh, P., Mansour, M. R., Look, A. T., & Aifantis, I. (2014). Notch signaling: switching an oncogene to a tumor suppressor. *Blood*, *123*(16), 2451–9. doi:10.1182/blood-2013-08-355818

Locatelli, F., Schrappe, M., Bernardo, M. E., & Rutella, S. (2012). How I treat relapsed childhood acute lymphoblastic leukemia. *Blood*, *120*(14), 2807–16. doi:10.1182/blood-2012-02-265884

Lu, J., Jeong, H.-W., Jeong, H., Kong, N., Yang, Y., Carroll, J., … Chai, L. (2009). Stem cell factor SALL4 represses the transcriptions of PTEN and SALL1 through an epigenetic repressor complex. *PloS One*, *4*(5), e5577. doi:10.1371/journal.pone.0005577

Ma, L., Teruya-Feldstein, J., Behrendt, N., Chen, Z., Noda, T., Hino, O., … Pandolfi, P. P. (2005). Genetic analysis of Pten and Tsc2 functional interactions in the mouse reveals asymmetrical haploinsufficiency in tumor suppression. *Genes & Development*, *19*(15), 1779–86. doi:10.1101/gad.1314405

Malecki, M. J., Sanchez-Irizarry, C., Mitchell, J. L., Histen, G., Xu, M. L., Aster, J. C., & Blacklow, S. C. (2006). Leukemia-associated mutations within the NOTCH1 heterodimerization domain fall into at least two distinct mechanistic classes. *Molecular and Cellular Biology*, *26*(12), 4642–51. doi:10.1128/MCB.01655-05

Manning, B. D., Logsdon, M. N., Lipovsky, A. I., Abbott, D., Kwiatkowski, D. J., & Cantley, L. C. (2005). Feedback inhibition of Akt signaling limits the growth of tumors lacking Tsc2. *Genes & Development*, *19*(15), 1773–8. doi:10.1101/gad.1314605

Mansour, M. R., Linch, D. C., Foroni, L., Goldstone, A. H., & Gale, R. E. (2006). High incidence of Notch-1 mutations in adult patients with T-cell acute lymphoblastic leukemia. *Leukemia*, *20*(3), 537–9. doi:10.1038/sj.leu.2404101

Marques, I. J., Weiss, F. U., Vlecken, D. H., Nitsche, C., Bakkers, J., Lagendijk, A. K., … Bagowski, C. P. (2009). Metastatic behaviour of primary human tumours in a zebrafish xenotransplantation model. *BMC Cancer*, *9*(1), 128. doi:10.1186/1471-2407-9-128

Martinez Marignac, V. L., Smith, S., Toban, N., Bazile, M., & Aloyz, R. (2013). Resistance to Dasatinib in primary chronic lymphocytic leukemia lymphocytes involves AMPK-mediated energetic re-programming. *Oncotarget*, *4*(12), 2550–66. Retrieved from http://www.pubmedcentral.nih.gov/articlerender.fcgi?artid=3926848&tool=pmcentrez&rendertype=abstract

Medicines and Healthcare products Regulatory Agency (MHRA), www.mhra.gov.uk, info@mhra. gsi. gov. u. (2011). Dexrazoxane (Cardioxane): restriction of use to adults with advanced or metastatic breast cancer only. Retrieved from http://www.mhra.gov.uk/Safetyinformation/DrugSafetyUpdate/CON123122

Medyouf, H., Gao, X., Armstrong, F., Gusscott, S., Liu, Q., Gedman, A. L., … Weng, A. P. (2010). Acute T-cell leukemias remain dependent on Notch signaling despite PTEN and INK4A/ARF loss. *Blood*, *115*(6), 1175–84. doi:10.1182/blood-2009-04-214718

Mikkola, H. K. A., Radu, C. G., & Witte, O. N. (2010). Targeting leukemia stem cells. *Nature Biotechnology*, *28*(3), 237–8. doi:10.1038/nbt0310-237

Miranda, C. J., Makui, H., Soares, R. J., Bilodeau, M., Mui, J., Vali, H., … Santos, M. M. (2003). Hfe deficiency increases susceptibility to cardiotoxicity and exacerbates changes in iron metabolism induced by doxorubicin. *Blood*, *102*(7), 2574–80. doi:10.1182/blood-2003-03-0869

Monsuez, J.-J., Charniot, J.-C., Vignat, N., & Artigou, J.-Y. (2010). Cardiac side-effects of cancer chemotherapy. *International Journal of Cardiology*, *144*(1), 3–15. doi:10.1016/j.ijcard.2010.03.003

Möricke, A., Zimmermann, M., Reiter, A., Henze, G., Schrauder, A., Gadner, H., … Schrappe, M. (2010). Long-term results of five consecutive trials in childhood acute lymphoblastic leukemia performed by the ALL-BFM study group from 1981 to 2000. *Leukemia*, *24*(2), 265–84. doi:10.1038/leu.2009.257

Mulligan, P., Yang, F., Di Stefano, L., Ji, J.-Y., Ouyang, J., Nishikawa, J. L., … Näär, A. M. (2011). A SIRT1-LSD1 corepressor complex regulates Notch target gene expression and development. *Molecular Cell*, *42*(5), 689–99. doi:10.1016/j.molcel.2011.04.020

Myers, C. (1998). The role of iron in doxorubicin-induced cardiomyopathy. *Seminars in Oncology*, *25*(4 Suppl 10), 10–4. Retrieved from http://www.ncbi.nlm.nih.gov/pubmed/9768818

Myers, C., Bonow, R., Palmeri, S., Jenkins, J., Corden, B., Locker, G., … Epstein, S. (1983). A randomized controlled trial assessing the prevention of doxorubicin cardiomyopathy by N-acetylcysteine. *Seminars in Oncology*, *10*(1 Suppl 1), 53–5. Retrieved from http://www.ncbi.nlm.nih.gov/pubmed/6340204

Nagel, A. C., Krejci, A., Tenin, G., Bravo-Patiño, A., Bray, S., Maier, D., & Preiss, A. (2005). Hairless-mediated repression of notch target genes requires the combined activity of Groucho and CtBP corepressors. *Molecular and Cellular Biology*, *25*(23), 10433–41. doi:10.1128/MCB.25.23.10433-10441.2005

Nasevicius, a, & Ekker, S. C. (2000). Effective targeted gene "knockdown" in zebrafish. *Nature Genetics*, *26*(2), 216–20. doi:10.1038/79951

National Cancer Institute. (2014). Childhood Acute Lymphoblastic Leukemia Treatment (PDQ®) - National Cancer Institute. *National Institutes of Health*. Retrieved June 04, 2014, from http://www.cancer.gov/cancertopics/pdq/treatment/childALL/HealthProfessional/page1/AllPages#Section_526

Neufeld, E. J. (2010). Update on iron chelators in thalassemia. *Hematology / the Education Program of the American Society of Hematology. American Society of Hematology. Education Program*, *2010*, 451–5. doi:10.1182/asheducation-2010.1.451

O'Neil, J., Grim, J., Strack, P., Rao, S., Tibbitts, D., Winter, C., … Look, A. T. (2007). FBW7 mutations in leukemic cells mediate NOTCH pathway activation and

resistance to gamma-secretase inhibitors. *The Journal of Experimental Medicine*, *204*(8), 1813–24. doi:10.1084/jem.20070876

Ogawara, Y., Kishishita, S., Obata, T., Isazawa, Y., Suzuki, T., Tanaka, K., … Gotoh, Y. (2002). Akt enhances Mdm2-mediated ubiquitination and degradation of p53. *The Journal of Biological Chemistry*, *277*(24), 21843–21850. Retrieved from http://www.ncbi.nlm.nih.gov/pubmed/11923280

Olson, R. E., & Albright, C. F. (2008). Recent progress in the medicinal chemistry of gamma-secretase inhibitors. *Current Topics in Medicinal Chemistry*, *8*(1), 17–33. Retrieved from http://www.ncbi.nlm.nih.gov/pubmed/18220929

Paganin, M., & Ferrando, A. (2011). Molecular pathogenesis and targeted therapies for NOTCH1-induced T-cell acute lymphoblastic leukemia. *Blood Reviews*, *25*(2), 83–90. Retrieved from http://www.pubmedcentral.nih.gov/articlerender.fcgi?artid=3033461&tool=pmcentrez&rendertype=abstract

Palomero, T., Lim, W. K., Odom, D. T., Sulis, M. L., Real, P. J., Margolin, A., … Ferrando, A. A. (2006). NOTCH1 directly regulates c-MYC and activates a feed-forward-loop transcriptional network promoting leukemic cell growth. *Proceedings of the National Academy of Sciences of the United States of America*, *103*(48), 18261–18266. Retrieved from http://www.pubmedcentral.nih.gov/articlerender.fcgi?artid=1838740&tool=pmcentrez&rendertype=abstract

Palomero, T., Sulis, M. L., Cortina, M., Real, P. J., Barnes, K., Ciofani, M., … Ferrando, A. A. (2007). Mutational loss of PTEN induces resistance to NOTCH1 inhibition in T-cell leukemia. *Nature Medicine*, *13*(10), 1203–1210. Retrieved from http://www.pubmedcentral.nih.gov/articlerender.fcgi?artid=2600418&tool=pmcentrez&rendertype=abstract

Pan, J., Chen, C., Jin, Y., Fuentes-Mattei, E., Velazquez-Tores, G., Benito, J. M., … Yeung, S.-C. J. (2012). Differential impact of structurally different anti-diabetic drugs on proliferation and chemosensitivity of acute lymphoblastic leukemia cells. *Cell Cycle*. doi:10.4161/cc.20770

Panjrath, G. S., Patel, V., Valdiviezo, C. I., Narula, N., Narula, J., & Jain, D. (2007). Potentiation of Doxorubicin cardiotoxicity by iron loading in a rodent model. *Journal of the American College of Cardiology*, *49*(25), 2457–64. doi:10.1016/j.jacc.2007.02.060

Payne, E., & Look, T. (2009). Zebrafish modelling of leukaemias. *British Journal of Haematology*, *146*(3), 247–56. doi:10.1111/j.1365-2141.2009.07705.x

Pear, W. S. (2010). Hooked on Hes: a T-ALL of addiction. *Immunity*, *33*(5), 645–647. doi:10.1016/j.immuni.2010.11.018

Peterson, R. T., & Macrae, C. A. (2012). Systematic approaches to toxicology in the zebrafish. *Annual Review of Pharmacology and Toxicology*, *52*, 433–53. doi:10.1146/annurev-pharmtox-010611-134751

Peterson, R. T., Shaw, S. Y., Peterson, T. A., Milan, D. J., Zhong, T. P., Schreiber, S. L., … Fishman, M. C. (2004). Chemical suppression of a genetic mutation in a zebrafish model of aortic coarctation. *Nature Biotechnology*, *22*(5), 595–9. doi:10.1038/nbt963

Pieters, R., den Boer, M. L., Durian, M., Janka, G., Schmiegelow, K., Kaspers, G. J., … Veerman, A. J. (1998). Relation between age, immunophenotype and in vitro drug resistance in 395 children with acute lymphoblastic leukemia--implications for treatment of infants. *Leukemia*, *12*(9), 1344–8. Retrieved from http://www.ncbi.nlm.nih.gov/pubmed/9737681

Pieters, R., Kaspers, G. J., van Wering, E. R., Huismans, D. R., Loonen, A. H., Hählen, K., & Veerman, A. J. (1993). Cellular drug resistance profiles that might explain the prognostic value of immunophenotype and age in childhood acute lymphoblastic leukemia. *Leukemia*, *7*(3), 392–7. Retrieved from http://www.ncbi.nlm.nih.gov/pubmed/8445945

Pitsouli, C., & Delidakis, C. (2005). The interplay between DSL proteins and ubiquitin ligases in Notch signaling. *Development (Cambridge, England)*, *132*(18), 4041–50. doi:10.1242/dev.01979

Pruvot, B., Jacquel, A., Droin, N., Auberger, P., Bouscary, D., Tamburini, J., … Solary, E. (2011). Leukemic cell xenograft in zebrafish embryo for investigating drug efficacy. *Haematologica*, *96*(4), 612–6. doi:10.3324/haematol.2010.031401

Pui, C. H., Pei, D., Sandlund, J. T., Ribeiro, R. C., Rubnitz, J. E., Raimondi, S. C., … Relling, M. V. (2010). Long-term results of St Jude Total Therapy Studies 11, 12, 13A, 13B, and 14 for childhood acute lymphoblastic leukemia. *Leukemia*, *24*(2), 371–82. doi:10.1038/leu.2009.252

Pullen, J., Shuster, J. J., Link, M., Borowitz, M., Amylon, M., Carroll, A. J., … Camitta, B. (1999). Significance of commonly used prognostic factors differs for children with T cell acute lymphocytic leukemia (ALL), as compared to those with B-precursor ALL. A Pediatric Oncology Group (POG) study. *Leukemia*, *13*(11), 1696–707. Retrieved from http://www.ncbi.nlm.nih.gov/pubmed/10557041

Radtke, F., Wilson, A., Stark, G., Bauer, M., van Meerwijk, J., MacDonald, H. R., & Aguet, M. (1999). Deficient T cell fate specification in mice with an induced inactivation of Notch1. *Immunity*, *10*(5), 547–58. Retrieved from http://www.ncbi.nlm.nih.gov/pubmed/10367900

Rao, V. A. (2013). Iron chelators with topoisomerase-inhibitory activity and their anticancer applications. *Antioxidants & Redox Signaling*, *18*(8), 930–55. doi:10.1089/ars.2012.4877

Real, P. J., Tosello, V., Palomero, T., Castillo, M., Hernando, E., de Stanchina, E., … Ferrando, A. (2009). Gamma-secretase inhibitors reverse glucocorticoid resistance in T cell acute lymphoblastic leukemia. *Nature Medicine*, *15*, 50–58. doi:10.1038/nm.1900

Rebay, I., Fleming, R. J., Fehon, R. G., Cherbas, L., Cherbas, P., & Artavanis-Tsakonas, S. (1991). Specific EGF repeats of Notch mediate interactions with Delta and Serrate: implications for Notch as a multifunctional receptor. *Cell*, *67*(4), 687–99. Retrieved from http://www.ncbi.nlm.nih.gov/pubmed/1657403

Riccio, O., van Gijn, M. E., Bezdek, A. C., Pellegrinet, L., van Es, J. H., Zimber-Strobl, U., … Radtke, F. (2008). Loss of intestinal crypt progenitor cells owing to inactivation of both Notch1 and Notch2 is accompanied by derepression of CDK inhibitors p27Kip1 and p57Kip2. *EMBO Reports*, *9*(4), 377–83. doi:10.1038/embor.2008.7

Ridges, S., Heaton, W. L., Joshi, D., Choi, H., Eiring, A., Batchelor, L., … Trede, N. S. (2012). Zebrafish screen identifies novel compound with selective toxicity against leukemia. *Blood*, *119*(24), 5621–31. Retrieved from http://www.ncbi.nlm.nih.gov/pubmed/22490804

Rosner, M., Fuchs, C., Siegel, N., Valli, A., & Hengstschläger, M. (2009). New insights into the role of the tuberous sclerosis genes in leukemia. *Leukemia Research*. doi:10.1016/j.leukres.2009.02.013

Sail, V., & Hadden, M. K. (2013). Identification of small molecule Hes1 modulators as potential anticancer chemotherapeutics. *Chemical Biology & Drug Design*, *81*(3), 334–42. doi:10.1111/cbdd.12059

Salzer, W. L., Devidas, M., Carroll, W. L., Winick, N., Pullen, J., Hunger, S. P., & Camitta, B. A. (2010). Long-term results of the pediatric oncology group studies for

childhood acute lymphoblastic leukemia 1984-2001: a report from the children's oncology group. *Leukemia*, *24*(2), 355–70. doi:10.1038/leu.2009.261

Sanchez-Irizarry, C., Carpenter, A. C., Weng, A. P., Pear, W. S., Aster, J. C., & Blacklow, S. C. (2004). Notch subunit heterodimerization and prevention of ligand-independent proteolytic activation depend, respectively, on a novel domain and the LNR repeats. *Molecular and Cellular Biology*, *24*(21), 9265–73. doi:10.1128/MCB.24.21.9265-9273.2004

Sanda, T., Li, X., Gutierrez, A., Ahn, Y., Neuberg, D. S., O'Neil, J., … Look, A. T. (2010). Interconnecting molecular pathways in the pathogenesis and drug sensitivity of T-cell acute lymphoblastic leukemia. *Blood*, *115*(9), 1735–1745. Retrieved from http://www.pubmedcentral.nih.gov/articlerender.fcgi?artid=2832805&tool=pmcentrez&rendertype=abstract

Sato, T., Nakashima, A., Guo, L., Coffman, K., & Tamanoi, F. (2010). Single amino-acid changes that confer constitutive activation of mTOR are discovered in human cancer. *Oncogene*, *29*(18), 2746–52. doi:10.1038/onc.2010.28

Schrappe, M., Valsecchi, M. G., Bartram, C. R., Schrauder, A., Panzer-Grümayer, R., Möricke, A., … Conter, V. (2011). Late MRD response determines relapse risk overall and in subsets of childhood T-cell ALL: results of the AIEOP-BFM-ALL 2000 study. *Blood*, *118*(8), 2077–84. doi:10.1182/blood-2011-03-338707

Sharpless, N. E. (2005). INK4a/ARF: a multifunctional tumor suppressor locus. *Mutation Research*, *576*(1-2), 22–38. doi:10.1016/j.mrfmmm.2004.08.021

Shepherd, C., Banerjee, L., Cheung, C. W., Mansour, M. R., Jenkinson, S., Gale, R. E., & Khwaja, A. (2012). PI3K/mTOR inhibition upregulates NOTCH-MYC signalling leading to an impaired cytotoxic response. *Leukemia*. doi:10.1038/leu.2012.285

Silva, A., Jotta, P. Y., Silveira, A. B., Ribeiro, D., Brandalise, S. R., Yunes, J. A., & Barata, J. T. (2010). Regulation of PTEN by CK2 and Notch1 in primary T-cell acute lymphoblastic leukemia: rationale for combined use of CK2- and gamma-secretase inhibitors. *Haematologica*, *95*(4), 674–8. doi:10.3324/haematol.2009.011999

Silverman, L. B., Stevenson, K. E., O'Brien, J. E., Asselin, B. L., Barr, R. D., Clavell, L., … Sallan, S. E. (2010). Long-term results of Dana-Farber Cancer Institute ALL Consortium protocols for children with newly diagnosed acute lymphoblastic leukemia (1985-2000). *Leukemia*, *24*(2), 320–34. doi:10.1038/leu.2009.253

Simůnek, T., Stérba, M., Popelová, O., Adamcová, M., Hrdina, R., & Gersl, V. (n.d.). Anthracycline-induced cardiotoxicity: overview of studies examining the roles of oxidative stress and free cellular iron. *Pharmacological Reports : PR*, *61*(1), 154–71. Retrieved from http://www.ncbi.nlm.nih.gov/pubmed/19307704

Smith, M., Arthur, D., Camitta, B., Carroll, A. J., Crist, W., Gaynon, P., … Ungerleider, R. (1996). Uniform approach to risk classification and treatment assignment for children with acute lymphoblastic leukemia. *Journal of Clinical Oncology : Official Journal of the American Society of Clinical Oncology*, *14*(1), 18–24. Retrieved from http://www.ncbi.nlm.nih.gov/pubmed/8558195

Smith, M. P., Ferguson, J., Arozarena, I., Hayward, R., Marais, R., Chapman, A., … Wellbrock, C. (2013). Effect of SMURF2 targeting on susceptibility to MEK inhibitors in melanoma. *Journal of the National Cancer Institute*, *105*(1), 33–46. doi:10.1093/jnci/djs471

Smithen, D. A., Forrester, A. M., Corkery, D. P., Dellaire, G., Colpitts, J., McFarland, S. A., … Thompson, A. (2013). Investigations regarding the utility of prodigiosenes to treat leukemia. *Organic & Biomolecular Chemistry*, *11*(1), 62–8. doi:10.1039/c2ob26535d

Song, M. S., Salmena, L., & Pandolfi, P. P. (2012). The functions and regulation of the PTEN tumour suppressor. *Nature Reviews. Molecular Cell Biology*, *13*(5), 283–96. doi:10.1038/nrm3330

Spano, D., Heck, C., De Antonellis, P., Christofori, G., & Zollo, M. (2012). Molecular networks that regulate cancer metastasis. *Seminars in Cancer Biology*, *22*(3), 234–49. doi:10.1016/j.semcancer.2012.03.006

Stambolic, V., MacPherson, D., Sas, D., Lin, Y., Snow, B., Jang, Y., … Mak, T. W. (2001). Regulation of PTEN transcription by p53. *Molecular Cell*, *8*(2), 317–25. Retrieved from http://www.ncbi.nlm.nih.gov/pubmed/11545734

Steinherz, P. G., Gaynon, P., Miller, D. R., Reaman, G., Bleyer, A., Finklestein, J., … Sather, H. (1986). Improved disease-free survival of children with acute lymphoblastic leukemia at high risk for early relapse with the New York regimen--a new intensive therapy protocol: a report from the Childrens Cancer Study Group.

Journal of Clinical Oncology : Official Journal of the American Society of Clinical Oncology, *4*(5), 744–52. Retrieved from http://www.ncbi.nlm.nih.gov/pubmed/3517244

Stiles, B., Gilman, V., Khanzenzon, N., Lesche, R., Li, A., Qiao, R., … Wu, H. (2002). Essential role of AKT-1/protein kinase B alpha in PTEN-controlled tumorigenesis. *Molecular and Cellular Biology*, *22*(11), 3842–51. Retrieved from http://www.pubmedcentral.nih.gov/articlerender.fcgi?artid=133830&tool=pmcentrez&rendertype=abstract

Subramaniam, P. S., Whye, D. W., Efimenko, E., Chen, J., Tosello, V., De Keersmaecker, K., … Diacovo, T. G. (2012). Targeting Nonclassical Oncogenes for Therapy in T-ALL. *Cancer Cell*. doi:10.1016/j.ccr.2012.02.029

Suter, T. M., & Ewer, M. S. (2013). Cancer drugs and the heart: importance and management. *European Heart Journal*, *34*(15), 1102–11. doi:10.1093/eurheartj/ehs181

Swain, S. M., & Vici, P. (2004). The current and future role of dexrazoxane as a cardioprotectant in anthracycline treatment: expert panel review. *Journal of Cancer Research and Clinical Oncology*, *130*(1), 1–7. doi:10.1007/s00432-003-0498-7

Swain, S. M., Whaley, F. S., Gerber, M. C., Weisberg, S., York, M., Spicer, D., … Gams, R. A. (1997). Cardioprotection with dexrazoxane for doxorubicin-containing therapy in advanced breast cancer. *Journal of Clinical Oncology : Official Journal of the*

American Society of Clinical Oncology, *15*(4), 1318–32. Retrieved from http://www.ncbi.nlm.nih.gov/pubmed/9193323

Sykes, S. M., Lane, S. W., Bullinger, L., Kalaitzidis, D., Yusuf, R., Saez, B., … Scadden, D. T. (2011). AKT/FOXO Signaling Enforces Reversible Differentiation Blockade in Myeloid Leukemias. *Cell*, *146*(5), 697–708. doi:10.1016/j.cell.2011.09.015

Tang, Q., Abdelfattah, N. S., Blackburn, J. S., Moore, J. C., Martinez, S. A., Moore, F. E., … Langenau, D. M. (2014). Optimized cell transplantation using adult rag2 mutant zebrafish. *Nature Methods*, *11*(8), 821–824. doi:10.1038/nmeth.3031

Tebbi, C. K., London, W. B., Friedman, D., Villaluna, D., De Alarcon, P. A., Constine, L. S., … Schwartz, C. L. (2007). Dexrazoxane-associated risk for acute myeloid leukemia/myelodysplastic syndrome and other secondary malignancies in pediatric Hodgkin's disease. *Journal of Clinical Oncology : Official Journal of the American Society of Clinical Oncology*, *25*(5), 493–500. doi:10.1200/JCO.2005.02.3879

Thompson, B. J., Buonamici, S., Sulis, M. L., Palomero, T., Vilimas, T., Basso, G., … Aifantis, I. (2007). The SCFFBW7 ubiquitin ligase complex as a tumor suppressor in T cell leukemia. *The Journal of Experimental Medicine*, *204*, 1825–1835. doi:10.1084/jem.20070872

Tosello, V., & Ferrando, A. A. (2013). The NOTCH signaling pathway: role in the pathogenesis of T-cell acute lymphoblastic leukemia and implication for therapy. *Therapeutic Advances in Hematology*, *4*(3), 199–210. doi:10.1177/2040620712471368

Trotman, L. C., Wang, X., Alimonti, A., Chen, Z., Teruya-Feldstein, J., Yang, H., … Pandolfi, P. P. (2007). Ubiquitination regulates PTEN nuclear import and tumor suppression. *Cell*, *128*(1), 141–56. doi:10.1016/j.cell.2006.11.040

Tschopp, O., Yang, Z.-Z., Brodbeck, D., Dummler, B. A., Hemmings-Mieszczak, M., Watanabe, T., … Hemmings, B. A. (2005). Essential role of protein kinase B gamma (PKB gamma/Akt3) in postnatal brain development but not in glucose homeostasis. *Development (Cambridge, England)*, *132*(13), 2943–54. doi:10.1242/dev.01864

Tzoneva, G., & Ferrando, A. A. (2012). Recent Advances on NOTCH Signaling in T-ALL. *Curr. Top. Microbiol. Immunol.*, *360*, 163–182. doi:10.1007/82

Uren, A. G., Kool, J., Matentzoglu, K., de Ridder, J., Mattison, J., van Uitert, M., … Berns, A. (2008). Large-scale mutagenesis in p19(ARF)- and p53-deficient mice identifies cancer genes and their collaborative networks. *Cell*, *133*(4), 727–41. doi:10.1016/j.cell.2008.03.021

Vaitkevičienė, G., Forestier, E., Hellebostad, M., Heyman, M., Jonsson, O. G., Lähteenmäki, P. M., … Schmiegelow, K. (2011). High white blood cell count at diagnosis of childhood acute lymphoblastic leukaemia: biological background and prognostic impact. Results from the NOPHO ALL-92 and ALL-2000 studies. *European Journal of Haematology*, *86*(1), 38–46. doi:10.1111/j.1600-0609.2010.01522.x

Van Dyke, T. (2007). p53 and tumor suppression. *The New England Journal of Medicine*, *356*(1), 79–81. doi:10.1056/NEJMcibr066301

Veinotte, C. J., Dellaire, G., & Berman, J. N. (2014a). Hooking the big one: the potential of zebrafish xenotransplantation to reform cancer drug screening in the genomic era. *Disease Models and Mechanisms*.

Veinotte, C. J., Dellaire, G., & Berman, J. N. (2014b). Hooking the big one: the potential of zebrafish xenotransplantation to reform cancer drug screening in the genomic era. *Disease Models & Mechanisms*, *7*(7), 745–754. doi:10.1242/dmm.015784

Vlierberghe, P. Van, & Ferrando, A. (2012). The molecular basis of T cell acute lymphoblastic leukemia, *122*(10). doi:10.1172/JCI61269.3398

Vrooman, L. M., & Silverman, L. B. (2009). Childhood acute lymphoblastic leukemia: update on prognostic factors. *Current Opinion in Pediatrics*, *21*(1), 1–8. Retrieved from http://www.ncbi.nlm.nih.gov/pubmed/19242236

Warburg, O. (1956). On the origin of cancer cells. *Science (New York, N.Y.)*, *123*(3191), 309–14. Retrieved from http://www.ncbi.nlm.nih.gov/pubmed/13298683

Watanabe, S., Umehara, H., Murayama, K., Okabe, M., Kimura, T., & Nakano, T. (2006). Activation of Akt signaling is sufficient to maintain pluripotency in mouse and primate embryonic stem cells. *Oncogene*, *25*(19), 2697–2707. doi:10.1038/sj.onc.1209307

Weigelt, B., & Downward, J. (2012). Genomic Determinants of PI3K Pathway Inhibitor Response in Cancer. *Frontiers in Oncology*. doi:10.3389/fonc.2012.00109

Weiser, M. A., Cabanillas, M. E., Konopleva, M., Thomas, D. A., Pierce, S. A., Escalante, C. P., … O'Brien, S. M. (2004). Relation between the duration of remission and hyperglycemia during induction chemotherapy for acute lymphocytic leukemia with a hyperfractionated cyclophosphamide, vincristine, doxorubicin, and dexamethasone/methotrexate-cytarabine regimen. *Cancer*, *100*(6), 1179–85. doi:10.1002/cncr.20071

Wendorff, A. A., Koch, U., Wunderlich, F. T., Wirth, S., Dubey, C., Brüning, J. C., … Radtke, F. (2010). Hes1 is a critical but context-dependent mediator of canonical Notch signaling in lymphocyte development and transformation. *Immunity*, *33*(5), 671–84. doi:10.1016/j.immuni.2010.11.014

Weng, A. P., Ferrando, A. A., Lee, W., Morris, J. P., Silverman, L. B., Sanchez-Irizarry, C., … Aster, J. C. (2004). Activating mutations of NOTCH1 in human T cell acute lymphoblastic leukemia. *Science (New York, N.Y.)*, *306*(5694), 269–271.

Weng, A. P., Millholland, J. M., Yashiro-Ohtani, Y., Arcangeli, M. L., Lau, A., Wai, C., … Aster, J. C. (2006). c-Myc is an important direct target of Notch1 in T-cell acute lymphoblastic leukemia/lymphoma. *Genes & Development*, *20*(15), 2096–109. doi:10.1101/gad.1450406

Westerfield, M. (1995). *The zebrafish book. A guide for the laboratory use of zebrafish (Danio rerio)*. Eugene: University of Oregon Press.

Westhoff, B., Colaluca, I. N., D'Ario, G., Donzelli, M., Tosoni, D., Volorio, S., … Di Fiore, P. P. (2009). Alterations of the Notch pathway in lung cancer. *Proceedings of the National Academy of Sciences of the United States of America*, *106*(52), 22293–8. doi:10.1073/pnas.0907781106

White, R. M., Sessa, A., Burke, C., Bowman, T., LeBlanc, J., Ceol, C., … Zon, L. I. (2008). Transparent adult zebrafish as a tool for in vivo transplantation analysis. *Cell Stem Cell*, *2*(2), 183–9. doi:10.1016/j.stem.2007.11.002

Wilkinson, R. N., Jopling, C., & van Eeden, F. J. M. (2014). Zebrafish as a model of cardiac disease. *Progress in Molecular Biology and Translational Science*, *124*, 65–91. doi:10.1016/B978-0-12-386930-2.00004-5

Willemse, M. J., Seriu, T., Hettinger, K., d'Aniello, E., Hop, W. C. J., Panzer-Grümayer, E. R., … van Dongen, J. J. M. (2002). Detection of minimal residual disease identifies differences in treatment response between T-ALL and precursor B-ALL. *Blood*, *99*(12), 4386–93. Retrieved from http://www.ncbi.nlm.nih.gov/pubmed/12036866

Wong, G. W., Knowles, G. C., Mak, T. W., Ferrando, A. A., & Zu, J. C. (2012). HES1 opposes a PTEN-dependent check on survival , differentiation , and proliferation of TCR $_{NL}$ -selected mouse thymocytes, *120*(7), 1439–1448. doi:10.1182/blood-2011-12-395319.There

Wong, G. W., Knowles, G. C., Mak, T. W., Ferrando, A. A., & Zuniga-Pflucker, J. C. (2012). HES1 opposes a PTEN-dependent check on survival, differentiation, and

proliferation of TCR -selected mouse thymocytes. *Blood*. doi:10.1182/blood-2011-12-395319

Wouters, K. A., Kremer, L. C. M., Miller, T. L., Herman, E. H., & Lipshultz, S. E. (2005). Protecting against anthracycline-induced myocardial damage: a review of the most promising strategies. *British Journal of Haematology*, *131*(5), 561–78. doi:10.1111/j.1365-2141.2005.05759.x

Xu, X., Persson, H. L., & Richardson, D. R. (2005). Molecular pharmacology of the interaction of anthracyclines with iron. *Molecular Pharmacology*, *68*(2), 261–71. doi:10.1124/mol.105.013383

Xu, Z., Cang, S., Yang, T., & Liu, D. (2009). Cardiotoxicity of tyrosine kinase inhibitors in chronic myelogenous leukemia therapy. *Hematology Reports (formerly Hematology Reviews)*, *1*. doi:10.4081/hr.2009.e4

Yatim, A., Benne, C., Sobhian, B., Laurent-Chabalier, S., Deas, O., Judde, J.-G., … Benkirane, M. (2012). NOTCH1 nuclear interactome reveals key regulators of its transcriptional activity and oncogenic function. *Molecular Cell*, *48*(3), 445–58. doi:10.1016/j.molcel.2012.08.022

Yeh, E. T. H., Tong, A. T., Lenihan, D. J., Yusuf, S. W., Swafford, J., Champion, C., … Ewer, M. S. (2004). Cardiovascular complications of cancer therapy: diagnosis, pathogenesis, and management. *Circulation*, *109*(25), 3122–31. doi:10.1161/01.CIR.0000133187.74800.B9

Yilmaz, O. H., Valdez, R., Theisen, B. K., Guo, W., Ferguson, D. O., Wu, H., & Morrison, S. J. (2006). Pten dependence distinguishes haematopoietic stem cells from leukaemia-initiating cells. *Nature*, *441*(7092), 475–82. doi:10.1038/nature04703

Yost, A. J., Shevchuk, O. O., Gooch, R., Gusscott, S., You, M. J., Ince, T. A., … Weng, A. P. (2013). Defined, serum-free conditions for in vitro culture of primary human T-ALL blasts. *Leukemia*, *27*(6), 1437–40. doi:10.1038/leu.2012.337

Yuan, T. L., & Cantley, L. C. (2008). PI3K pathway alterations in cancer: variations on a theme. *Oncogene*, *27*(41), 5497–5510. doi:10.1038/onc.2008.245

Zhang, J., Ding, L., Holmfeldt, L., Wu, G., Heatley, S. L., Payne-Turner, D., … Mullighan, C. G. (2012). The genetic basis of early T-cell precursor acute lymphoblastic leukaemia. *Nature*.

Zhang, S., Liu, X., Bawa-Khalfe, T., Lu, L.-S., Lyu, Y. L., Liu, L. F., & Yeh, E. T. H. (2012). Identification of the molecular basis of doxorubicin-induced cardiotoxicity. *Nature Medicine*, *18*(11), 1639–42. doi:10.1038/nm.2919